THE UNIVERSITY *of* EDINBURGH

Genetic Dissection of Nitric Oxide Signalling Network In Plant Defence Response

Minghui Yin

Doctor of Philosophy

Institute of Molecular Plant Sciences

The University of Edinburgh

Oct 2014

Contents

Abstract

Following pathogen recognition, nitric oxide (NO) is rapidly produced in plants, this small molecule has emerged as a key signal in plant defence responses. S-nitrosylation is the major route of NO signal transduction in plants, a redox-based modification by addition of an NO moiety on cysteine thiol to form an S-nitrosothiol (SNO). S-nitrosoglutathione reductase (GSNOR) regulates cellular levels of S-nitrosylation and displays a key role in regulating the plant defence response. In this context, NO is important to orchestrate both defence gene expression and the hypersensitive response (HR) during attempted microbial infection. However, how the plant immune system recognizes NO and how NO level could elicit plant defence responses are poorly understood.

The *Arabidopsis thaliana* (*Arabidopsis*) mutant *NO overproducing 1* (*nox1*) was employed to characterize how NO level elicits defence dynamics. In response to microbial infection, resistance (*R*) gene-mediated defence and basal resistance were found to be compromised in the *nox1* mutant relative to wild type Col-0 plants. Interestingly, *nox1* mutant exhibit similar levels of HR and pathogen susceptibility to the GSNOR loss-of-function mutant *atgsnor1-3*. This phenomenon suggests that NO might regulate defence responses via GSNOR-mediated S-nitrosylation. Therefore, the *nox1 atgsnor1-3* double mutant was generated and characterized to clarify this hypothesis. Accelerated HR and increased pathogen susceptibility are shown in the double mutant, which implies that increased NO mediated by *nox1* and elevated SNOs resulting from *atgsnor1-3*, are additive with respect to the plant defence response.

To identify genes responsible for NO perception, forward genetic screens were developed to identify *Arabidopsis* mutants with abnormal NO recognition. NO marker genes for genetic screens were identified from both lab and open source microarray data. Two genes, *At3g28740* and *At1g76600* were selected and experimentally confirmed to be strongly induced by NO. Transgenic *Arabidopsis* plants were generated carrying a NO reporter cassette, which consist of a luciferase reporter gene (*LUC*) driven by the promoter of NO marker gene. This forward

genetic approach might be a powerful tool to identify genes integral to NO signal transduction.

Three C2H2 zinc finger transcription factors (ZnTFs) *ZAT7, ZAT8* and *ZAT12* were identified as being rapidly and strongly induced by NO donors, which could be modulators of redox/NO-dependent signalling pathway. T-DNA insertion mutants within these ZnTFs have been identified. Basal resistance against *Pseudomonas syringae* pv tomato (*Pst*) DC3000 is compromised in all single knockout lines. Therefore, the full characterisation of defence phenotype of these mutants would be necessary to explore the role of these TFs in the plant defence. Furthermore, *zat8* mutant is more sensitive to nitrosative stress when compared to wild type Col-0. This suggests that ZAT8 may be involved in protecting plants against nitrosative stress. However, the molecular mechanisms that underpin this function remain to be determined.

In conclusion, NO and SNOs might regulate plant disease resistance via distinct pathways. Our work has also established NO-reporter lines to identify genes responsible for NO perception. In addition, three NO-induced ZnTFs have been identified that participate in regulation of basal resistance, which might unveil aspects of NO signalling related to the regulation of transcription.

Declaration

I hereby declare that the work presented here is my own and has not been submitted in any form for any degree at this or other university.

Minghui Yin

- Remark: I would like to acknowledge Dr. Byung-Wook Yun for his help in Figure 3-1, Figure 3-2 and Figure 3-3.
- I would like to acknowledge Dr. Yvette Wilson for her help in Figure 5-4.
- I would like to thank you Dr. Xin Tian for his help in Figure 6-9.

Acknowledgments

Firstly, I would like to express my deepest gratitude to the following people who made my thesis possible:

Professor Gary Loake, My supervisor, who supported me since my PhD application, who has been providing valuable advice and direction since, thank you for always pushing me;

Dr. Byung-Wook Yun and Dr. Yiqin Wang, the experienced biologists and teachers who taught me experimental techniques;

Dr. Zejun Yan, Dr. Debra Frederickson Matika and Dr. Manda Yu, who dedicated their time and attention to proofread my thesis.

A sincere “thank you” to all my lab mates who shared happiness and bitterness over the years: Adil, Carols, Corin, Debbie, Edurado, Eunjung, James, John, Kerstin, Kirsti, Krieng, Michael, Noor, Priya, Rabia, Rafael, Rumana, Saad, Steven, Suzy, Thomas, Usman, Yan and Yuan;

And all my friends in Scotland.

I would like to express my sincere thanks to the Torrance Bequest Studentship for financial support during my PhD.

I would like to dedicate this work to my parents, for their unfailing love and support even during their difficult time, without whom, I would be unable to complete my studies.

Abbreviations

µg	Microgram
µl	Microlitre
35S	Cauliflower mosaic virus 35S promoter
AFLP	Amplification Fragment Length Polymorphism
At	*Arabidopsis thaliana*
Avr	Avirulent
ATP	Adenosine Triphosphate
Bp	Base Pair
bZIP	Basic Leucine Zipper
Bgh	*Blumeria graminis* f. sp. *hordei*
Bgt	*Blumeria graminis* f. sp. *tritici*
CaMV	Cauliflower Mosaic Virus
CaM	Calmodulin
CC	Coiled-Coil
CDHR	Cell Death by Hypersensitive Response
CEBiP	Chitin Elicitor Binding Protein
CERK	Chitin Elicitor Receptor Kinase
CNGC	Cyclic Nucleotide Gated Channel
CNL	CC-NBS-LRR
cGMP	Guanosine cyclic Monophosphate
Col-0	*Arabidopsis* ecotype Columbia
CTAB	Cetyltrimethylammonium Bromide
CUL3	Cullin3 Ubiquitin E3 ligase
Cys	Cysteine
Cys-NO	S-nitrosocysteine
DAMP	Damage-Associated Molecular Patterns
DNA	Deoxyribonucleic Acid
DTT	Dithiothreitol
EAR	ERF- Associated Amphiphile Repression
E. coli	*Escherichia coli*
ECD	Extracellular Domain
EMS	Ethane-Methyl-Sulphonate
ERF	Ethylene-Responsive Element-Binding Factor
ETS	Effector-Triggered Susceptibility
ETI	Effector Triggered Immunity
FAD	Flavin Adenine Dinucleotide

FMN	Flavin Mononucleotide
GAPDH	Glyceraldehyde 3-Phosphate Dehydrogenase
GDC	Glycine Decarboxylase
GFP	Green Fluorescent Protein
GSH	Glutathione
GSNO	S-nitrosoglutathione
GSNOR	GSNO Reductase
GSSG	Glutathione Disulphide
GST	Glutathione-S-Transferase
GTP	Guanosine Triphosphate
Hb	Haemoglobin
His	Histidine
H_2O_2	Hydrogen peroxide
HR	Hypersensitive Response
Kan	Kanamycin
Lb	leghemoglobin
L-NNA	L-N-Nitroarginine
L-NAME	L-N-Nitroarginine Methylester
LPS	Lipopolysaccharides
LUC	Luciferase
MAPK	Mitogen Activated Protein Kinase
MeSA	Methylsalicylic Acid
NB-LRR	Nucleotide Binding Leucine-Rich Repeat
NADPH	Nicotinamide Adenine Dinucleotide Phosphate H
NBS	Nucleotide Binding Site
NO	Nitric Oxide
NOS	Nitric Oxide Synthase
NR	Nitrate Reductase
PAMP	Pathogen-associated Molecular Pattern
PCD	Programmed Cell Death
PDE	Phosphodiesterases
PGN	Peptidoglycan
PM	Plasma membrane
PMSF	Phenylmethanesulfonyl Fluoride
PR	Pathogen Related
PRR	Pattern recognition receptor
Pst DC3000 (*avrB*)	*Pseudomonas syringae* pv tomato DC3000 carrying *avrB*
Pst DC3000 (*avrRps4*)	*Pseudomonas syringae* pv tomato DC3000 carrying *avrRps4*
Pst DC3000	*Pseudomonas syringae* pv tomato DC3000

PTI	PAMP-Triggered Immunity
R	Resistance
Rboh	Respiratory Burst Oxidase Homologues
RCCD	Red Chlorophyll Catabolite Reductase
RCD	Runway Cell Death
RLK	Receptor-Like Kinase
RLP	Receptor-Like Protein
RNAi	RNA interference
RNS	Reactive Nitrogen Species
ROS	Reactive Oxygen Species
RT	Reverse Transcription
SA	Salicylic Acid
SAR	Systemic Acquired Resistance
sGC	Soluble guanylate cyclase
SNO	S-nitrosothiol
SNP	Sodium Nitroprusside
SOD	Superoxide Dismutase
STAND	Signal transduction ATPases with numerous domains
TAIR	The *Arabidopsis* Information Resource
TB	Trypan blue
TIR	Toll/Interleukin-1 Receptor
TF	Transcription Factor
TNL	TIR-NBS-LRR
TM	Transmembrane Domain
TMV	Tobacco Mosaic Virus
T3SS	Type Three Secretion System
TRXs	Thioredoxins
Tyr	Tyrosine
vir	Virulent
ZnTF	Zinc Finger Transcription Factor

Index of Figures

Index of Table

Chapter 1 Introduction

1.1 Plant immunity

Immunity is a mechanism to prevent disease development through sufficient defence responses. It is a critical necessity of all living organisms to survive from unwanted biological invasions. In mammals, immunity consists of both an innate and adaptive immune system (Lydyard *et al.* 2004). To be the early line of defence, innate immunity confers the cellular and biochemical defence mechanisms that are always present and ready to provide immediate defence against the infection from harmful species (Abbas and Lichtman 2009). In contrast, adaptive immune system only becomes activated against particular pathogens, which are able to overcome the innate immune system. When activated, it fights against the present pathogens through the lymphocyte-mediated mechanisms (T cell and B cell, the multipotent hematopoietic stem cells), and develops the memory upon re-exposure to each pathogen (Abbas and Lichtman 2009). Adaptive immunity is considered to be complementary to innate immunity. Their function cooperative strategy offers systemic defence responses to provide integrated protection. Plants immune responses are classified as innate immunity (Ausubel 2005).

Plants have evolved a multi-layered defence mechanism to defend against potential pathogens. The first layer consists of the waxy cuticle layers, pre-formed anti-microbial compounds and cell walls, passively impedes the growth and spread of potential pathogens (Chassot *et al.* 2007). The second layer is activated upon the perception of pathogens. This recognition is then translated into subsequent responses, including defence signal transduction, production of anti-microbial compounds or the hypersensitive response (HR) (Fig 1-1). This efficient perception system contains both extra and intra-cellular detection (Jones and Dangl 2006). The initial perception is the recognition of pathogen-associated molecular patterns (PAMPs) by cell surface-localized pattern recognition receptors (PRRs), which is known as PAMP-triggered immunity (PTI). However, the effectors secreted by adapted pathogens can overcome PTI, which leads to effector-triggered susceptibility

(ETS). In response to ETS, plants have evolved to recognize pathogen effectors through resistance (R) proteins. This perception contributes to effector-triggered immunity (ETI). Because R proteins can only mediate resistance to specific pathogens, this R protein derived immunity is also termed *R*-gene specific resistance or gene-for-gene disease resistance (Ingle *et al.* 2006). Although plants are not mobile and do not have a circulatory system to defend external attacks, their responses to pathogen attack rely on the innate immunity activities of each cell and transduction of signalling from the infection site to distant tissues (Spoel and Dong 2012).

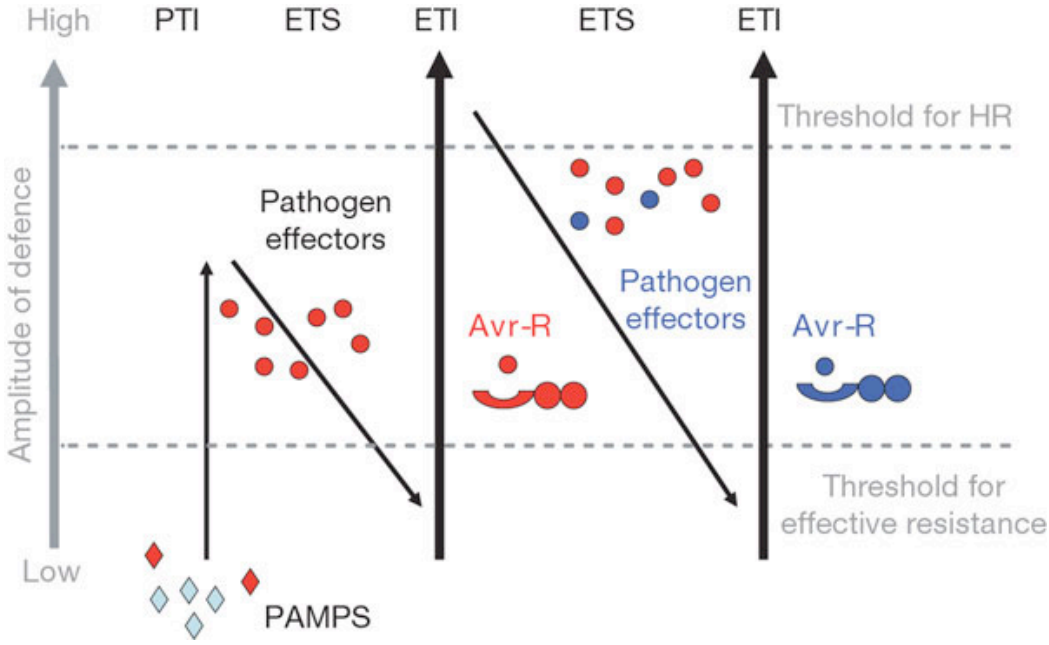

Figure 1-1 Disease resistance or susceptibility is dictated by the interaction between plants and pathogens (Jones and Dangl 2006).

Plants recognize PAMPs (red diamonds) via PRRs to trigger PTI. Secondly, in order to enable pathogen nutrition and dispersal, pathogens deliver effectors into the plant cell to interfere with PTI, which results in ETS. In response to EST, plants recognize pathogen effectors (indicated in red circle) through nucleotide binding – leucine rich repeat (NB-LRR) proteins, which subsequently activates ETI. That often passes a threshold leads to the induction of HR. However, pathogens have evolved to produce new effectors perhaps through horizontal gene flow (in blue), which cannot be recognized by existing R proteins. This helps pathogens to suppress ETI. Therefore, natural selection favours newly evolved plants that have NB-LRR alleles that can recognize the newly acquired effectors, and ultimately triggers ETI (Jones and Dangl 2006).

1.1.1 Host extracellular matrix responses

Plants establish an unwelcome environment to the attempted pathogen challenge by secreting cutin and waxes onto the outer surface of cells, which form the cuticle of the leaf epidermis (Nawrath 2006). This waxy layer is a natural barrier, and it is specially evolved in plants. It not only prevents water loss, but also restricts growth and spread of pathogens. As a result, the invading pathogens are segregated from the plant apoplast (Aharoni *et al.* 2004).

Stomata are the natural surface opening in the leaf epidermis, through which, the external environment is connected with internal tissues. However, this also allows the pathogens to enter into the plant apoplast at certain favourable environmental conditions, e.g. high humidity and moderate temperature (Zeng *et al.* 2010). In response to this, stomata are forced to close through the activity of guard cells. So, the regulation of stomata closure is considered as an important defence mechanism in plant innate immunity (Zeng *et al.* 2010). In addition, the plant cell wall offers another physical barrier to protect plants against pathogens. Upon pathogen attacks, further reinforcement of the plant cell wall by callose deposition can increase the strength and elasticity of the cell wall. As a result, it enhances the capability to resist pathogen entry (Senthil-Kumar and Mysore 2013). However, pathogens, such as bacteria, fungi and oomycetes, have evolved to confer the ability to break down these primary defence barriers through different mechanisms. For example, pathogens secrete cell wall degrading enzymes (e.g. pectinase, cellulases and xylanases) that break down the plant cell wall. Other pathogens, including the powdery mildew fungus *Blumeria graminis* f. sp. *hordei (Bgh)* and rice blast fungus *Magnaporthe oryzae*, can directly penetrate the epidermis (Faulkner and Robatzek 2012). In addition, some bacteria pathogens employ the virulence factor, coronatine, to suppress the closure of guard cells. This leads to stomata reopening and facilitates pathogen invasion (Melotto *et al.* 2008).

1.1.2 PAMP-triggered immunity

Plants are resistant to the majority of potential pathogens (Senthil-Kumar and Mysore 2013). Two classes of receptors are involved in detecting pathogens that are capable of evading plants extracellular matrix protection layer in plant innate immunity (Faulkner and Robatzek 2012). One class is the plasma membrane (PM) - localized PRRs. The perception of PAMPs by PRRs triggers immediate physiological changes in plant cells, and therefore activates PTI. This is followed by subsequent defence events, which includes bursts of calcium (Ca^{2+}) and reactive oxygen species (ROS), activation of mitogen-activated protein kinases (MAPKs) – mediated signal transduction, transcriptional reprogramming of defence-related genes, callose deposition and HR-like cell death in some cases (Ingle *et al.* 2006, Monaghan and Zipfel 2012). Another class of receptor is plant R proteins, which are involved in ETI (see 1.1.3).

1.1.2.1 Pathogen Associated Molecular Patterns

PAMPs are necessary for microbial life and present as conserved molecular features of major microbial groups. These include flagellin (flg), elongation factor Tu (EF-Tu), cold shock protein, lipopolysaccharides (LPS), porins from gram-negative bacteria, peptidoglycan (PGN) in both gram-positive and negative bacteria cell wall, chitin and ergosterol present in fungi and elicitin with β-glucans in oomycetes (Wan *et al.* 2008, Zeng *et al.* 2010, Newman *et al.* 2013). The identified PAMPs are listed in (Table 1-1) (Newman *et al.* 2013). Based on their origins, these molecules are not only defined as PAMPs, but also named as MAMPs or DAMPs for microbe-associated or damage-associated molecular patterns, respectively (Segonzac and Zipfel 2011).

Table 1-1 MAMPs and DAMPs and their corresponding receptors (Newman *et al.* 2013).

Name	Corresponding plant receptor (PPR)	References
MAMPs		
Flagellin (Flg; flg22)	FLS2 (*Arabidopsis*)	(Felix *et al.* 1999, Gomez-Gomez *et al.* 2001)
Elongation factor TU (EF-TU; elf18/26)	ERF (*Arabidopsis*; *Brassicaceae*)	(Kunze *et al.* 2004)
Peptidoglycan (PGN)	Lym1 and Lym3 (*Arabidopsis*)	(Gust *et al.* 2007, Erbs *et al.* 2008, Willmann *et al.* 2011)
Lipopolysaccharide (LPS)	Not identified	(Newman *et al.* 1995, Felix and Boller 2003)
Bacterial cold shock proteins (RNP1 motif)	Not identified	(Felix and Boller 2003)
Bacterial superoxide dismutase (Sod)	Not identified	(Watt *et al.* 2006)
Activator of XA21 (Ax21)	XA21 and XA21D (rice)	(Song *et al.* 1995, Wang *et al.* 1998, Lee *et al.* 2009)
Beta-Glycan (GE)	GEBP (putative receptor soyabean)	(Darvill and Albersheim 1984, Umemoto *et al.* 1997)
Chitin	CeBip and CERK1 (rice); AtCERK1 (*Arabidopsis*)	(Felix *et al.* 1993, Kaku *et al.* 2006, Miya *et al.* 2007, Shimizu *et al.* 2010)
Avr9	Cf-9 (tomato)	(Rivas *et al.* 2004)
Xylanase (EIX)	Eix (tomato)	(Bailey *et al.* 1990, Ron and Avni 2004)
Pep-13 (An oligopeptide of 13 amino acids from *P. megasperma*)	Not identified	(Nürnberger *et al.* 1994)
Cellulose-binding elicitor lectin (CBEL) from *Phytophthora*	Not identified	(Mateos *et al.* 1997, Séjalon-Delmas *et al.* 1997, Gaulin *et al.* 2006)
DAMPs		
Pep1 (23 aa part of a cytosolic protein from *Arabidopsis*)	PEPR1 (*Arabidopsis*)	(Huffaker *et al.* 2006, Yamaguchi *et al.* 2006)
Cutin	Not identified	(Schweizer *et al.* 1996, Kauss *et al.* 1999)

1.1.2.2 Pattern Recognition Receptors

PRRs from the host are able to recognize PAMPs. This triggers the switch between growth and defence models in plants. Whereas many PAMPs are characterized from microbes, only a limited number of PRRs has been identified in plants (Table 1-1). PRRs are localized on the surface of cell at the PM. Their expression is often activated by the innate immune system (Newman *et al.* 2013).

In plants, based on their location or function, the known PRRs are classified into either membrane-bound receptor-like kinases (RLKs) or receptor-like proteins (RLPs) with functional domains. RLKs contain an extracellular domain (ECD) and a single-pass transmembrane domain (TM) linked to an intracellular kinase domain. Similarly, RLPs also have ECD and TM, but contain a short cytosolic domain instead of an intracellular kinase domain (Monaghan and Zipfel 2012). The key features of PRRs, including their PM localization and function, play an important role in their immune activities, because they determine the perception of extracellular PAMPs and transduction of intracellular signals (Faulkner and Robatzek 2012). For example, flg22 is the best studied PAMP. It contains 22 conserved amino acids from the N-terminus of flagellin (Felix *et al.* 1999). FLS2 is the receptor of flg22, which is encoded by *FLAGELLIN-SENSITIVE* 2 (*FLS2*) in *Arabidopsis* (Gomez-Gomez *et al.* 1999). As a member of RLKs, FLS2 contains a transmembrane domain, an intracellular serine/threonine kinase domain, together and an extracellular leucine rich repeat (LRR) domain for ligand binding function. Binding to the LRR domain leads to the changes in phosphorylation state of serine/threonine kinase domain, which subsequently activates the downstream signal cascade (Nicaise *et al.* 2009). Another example is the EFR (EF-Tu receptor), which detects the first 18 amino acids (elf18) in the N-terminus of EF-Tu. It is also an LRR-containing RLK (Kunze *et al.* 2004, Zipfel *et al.* 2006). In addition, the tomato LRR-RLPs, Eix1 (ethylene-inducing xylanase receptor 1) and Eix2, are the receptors of fungal xylanase (Ron and Avni 2004). The DAMP, AtPep1 (*Arabidopsis* peptide 1), can also be recognized by *Arabidopsis* LRR-RLKs PEPR1 (AtPep receptor 1) and PEPR2 (Huffaker *et al.* 2006, Yamaguchi *et al.* 2006, Krol *et al.* 2010). In total, these well-described LRR-containing proteins suggest that LRR domains of RLKs and RLPs constitute a major

clade of PRRs in plant innate immunity. RLPs with a lysine-motif (LysM) have also been identified. For instance, LysM proteins, LYM1 and LYM3 recognize bacterial PGN (Willmann *et al.* 2011), and CERK1 (chitin elicitor receptor kinase 1) and CEBiP (chitin elicitor binding protein) are the receptors of fungal chitin (Kaku *et al.* 2006, Shimizu *et al.* 2010). It has also been found that there are 615 RLKs encoding genes in *Arabidopsis* genome. However, based on the structure analysis, only 216 of them might show potential roles as PRRs in plant PTI (Boller and Felix 2009).

1.1.2.3 Mechanism model of PTI

PTI plays an important role in basal defence system and non-host resistance in plants, which respond to a broad-spectrum of non-specific pathogens. It involves PAMPs detection, PRRs-induced signal transduction and activation of downstream defence events (Monaghan and Zipfel 2012).

Flagellin perception by FLS2 is a well-studied model of PTI detection system (Figure 1-2) (Ingle *et al.* 2006). In this model, FLS2 requires association of brassinosteroid-insensitive 1 (BRI1)-associated kinase 1 (BAK1) and botrytis-induced kinase 1 (BIK1) for its function (Chinchilla *et al.* 2007, Lu *et al.* 2010). Bacterial flg22 first interacts with LRR domain, an extracellular ligand-binding domain of FLS2, which, in turn, triggers heterodimerization of FLS2-BAK1. The heterodimerization causes the activation of intercellular kinase domains and initiates immune signalling in a phosphorylation-dependent manner (Schwessinger *et al.* 2011). In cytoplasm, BIK1 is phosphorylated by BAK1, and then, it trans-phosphorylates both FLS2 and BAK1, and dissociates from the complex (Lu *et al.* 2010). Phosphorylated FLS2-BAK1 is then required in the flg22-responsive MAPK phosphorylation cascade. The phosphorylated AtMEKK1 (*Arabidopsis* MAPK kinase kinase 1) phosphorylates both AtMKK4 (*Arabidopsis* MAPK kinase 4) and AtMKK5, which subsequently activate AtMPK3 (MAPK3) and AtMPK6 through phosphorylation (Asai *et al.* 2002). Ultimately, this leads to expression of the transcription factors (TFs) WRKY22 and WRKY29. WRKY22 and WRKY29 regulate expression of flagellin-induced defence genes. WRKY29 is also involved in signal amplification through positive feedback on its own expression (Asai *et al.*

2002). In addition, dissociated BIK1 trans-phosphorylates membrane located nicotinamide adenine dinucleotide phosphate H (NADPH) oxidase complex to activate ROI production; however, only ROS burst has evidence showing that it requires flg22 heterodimerization with FLS2 (Robatzek *et al.* 2006, Lu *et al.* 2010).

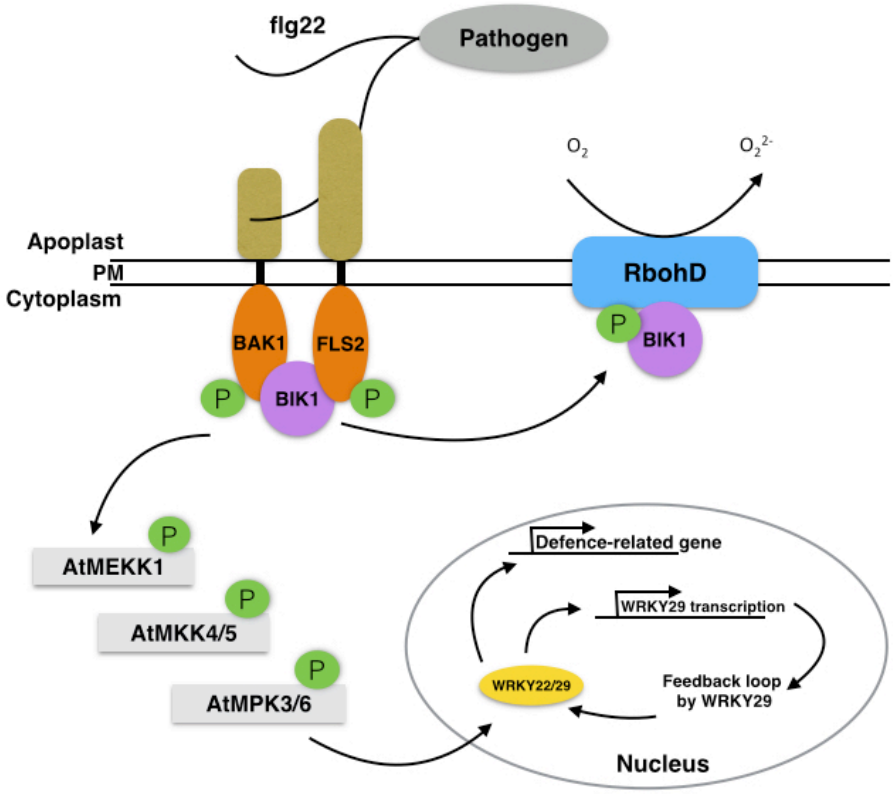

Figure 1-2 A working model of FLS2 in PTI (Ingle *et al.* 2006, Dodds and Rathjen 2010, Macho and Zipfel 2014).

After flg22 perception by ectodomain of FLS2, flg22-bound FLS2 rapidly forms a complex with BAK1, which leads phosphorylation of BIK1 by BAK1 in cytoplasm. BIK1 directly phosphorylates both FLS2 and BAK1, and is released from FLS2-BAK1 complex (Dodds and Rathjen 2010, Macho and Zipfel 2014). Phosphorylated FLS2-BAK1 then initiates downstream MAPK phosphorylation cascade that stimulates the expression of WRKY22 and WRKY29, which results in defence-related gene expression and a positive feedback loop of WRKY29 transcription (Ingle *et al.* 2006). Phosphorylated BIK1 associates the activation of NADPH oxidase (RbohD) to initiate ROI burst (Macho and Zipfel 2014).

1.1.3 Effector-Triggered Immunity

ETI is a key component of plant innate immunity. Based on its defence mechanism, it is also termed specific *R*-mediated innate immunity. In order to overcome PTI, adaptive pathogens have evolved to produce molecular effectors that target and supress the defence responses of PTI, which leads to the development of disease symptoms. In response to it, plants express R proteins that recognise the presence of effectors molecules. The interaction between the specific R proteins and their corresponding avirulent (Avr) effectors triggers downstream signal transduction in either directly or indirectly manner, and this results in activation of subsequent defence mechanisms and ultimate arrest of pathogen growth locally and/or systemically (Jones and Dangl 2006, Boller and He 2009).

1.1.3.1 Pathogen effectors

Although PTI protects plants from a broad-spectrum of diseases caused by pathogen invasion, the effector proteins are secreted by bacterial pathogens to suppress PTI, and delivered through the type III secretion system (T3SS) (Knepper and Day 2010). For example, degradation of FLS2 has been shown to terminate downstream signal transduction (Zhang *et al.* 2010). In addition, it was reported that phosphorylation of the kinase domain of BAK1, a RLS, which is required for most known PRRs, is inhibited when interacting with AvrPto/AvrAC; consequently, this supresses downstream signalling (Zhang and Zhou 2010). Finally, dephosphorylation also plays a role in blocking this signal transduction pathway. For example, two phosphothreonine lyases, HopF2 and HopAI1, dephosphorylate MKK4/5 and MPK3/6, respectively. As a result, PRR signalling is blocked (Asai *et al.* 2002, Guillaume *et al.* 2011, Maud *et al.* 2011).

Bacterial effectors not only supress activation of kinase cascades, but also directly interfere with the PAMPs-responsive downstream defence events. For example, HopM1 destabilizes AtMIN7 (*Arabidopsis* HopM interactor 7) and therefore inhibits the plant secretory pathway (Nomura *et al.* 2006, Nomura *et al.* 2011). XopD binds to transcriptional factor MYB30 and represses its transcriptional activity, which

consequently supresses the transcription of immune response genes (Canonne *et al.* 2011). HopI1 interacts with Hsp70 in the chloroplast, and this results in restriction of salicylic acid (SA) accumulation, a key hormone regulator of defence response in either local or systemic defence strategies (Dudler 2013).

Different from bacterial pathogens, fungi and oomycetes form specialized feeding structure, hausoria, to penetrate host cell wall and invaginate the PM of host cell (Petre and Kamoun 2014). The effectors, in order to supress PTI, are then secreted through this endomembrane system and delivered into host cell cytoplasm by unknown mechanism (Dodds and Rathjen 2010). However, evidence suggested that translocation domains of effectors are required for delivery into host cell cytoplasm. For example, AVR3a (avirulent protein 3a) of *Phytophthora. Infestans* (*P. infestans*) contains a motif Arg-X-Leu-Arg (RXLR), a consensus cell entry motif in oomycetes effectors, which is required for translocation into host cell cytoplasm (Whisson *et al.* 2007). The C-terminal Arg-Gly-Asp (RGD) motif of Ptr ToxA (*Pyrenophora tritici-repentis* toxin A) is required for the entry into plant cells (Manning *et al.* 2008). However, there is no consensus motif defined for fungi effectors.

1.1.3.2 Resistance (R) proteins

Genetic evidence suggests that pathogen effectors are highly diverse in both coding sequence and molecular functions (Glowacki *et al.* 2011). In contrast, R proteins are structurally conserved, and share some common features, such as LRR domain that mediates protein-protein interactions (Ellis and Jones 1998). There are 159 R protein-encoding genes (*R* genes) that have been identified in *Arabidopsis* (Meyers *et al.* 2003). NB-LRRs is the largest class of R proteins. As a sub group of signal transduction ATPases with numerous domains (STAND) family, NB-LRR proteins are involved in adenosine triphosphate (ATP)/ guanosine triphosphate (GTP) binding (Saraste *et al.* 1990), acts as a signal transduction switch. Based on the additional domain at the N-terminus NB-LRR proteins are divided into two major groups (Table 1-2) (Chisholm *et al.* 2006). One class contains a Toll interleukin 1 receptors (TIR) domain, named TIR-NB-LRRs (TNL) group; the other is the CC (coiled-coil)-NBS-LRR (CNL) group, which contains the CC domain. CNL is also considered as

the major member of the non-TIR-NB-LRRs family (Meyers *et al.* 2003, Tameling *et al.* 2006, Kohler *et al.* 2008, Porter *et al.* 2009). As TIR was originally identified as an intercellular region of *Drosophila* Toll and human interleukin 1 receptors, a group of intracellular immune receptors with similar structure, known as NLR proteins (nucleotide-binding oligomerization domain and LRR-containing proteins), exists in vertebrate immune system. However, instead of detecting pathogen effectors, NLRs play a role in PTI by responding to perception of PAMPs. For example, human Toll-like receptor 5 (TLR5), which is the homologue of *Arabidopsis* FLS2, responds to bacterial flagellin perception and triggers PTI rather than ETI (Danna *et al.* 2011). Furthermore, the *activated disease resistance* (*ADR*) *1* gene encodes a CC-NBS-LRR protein, ADR1. It is required for positive regulation of SA-dependent gene expression and conveys a broad-spectrum of disease resistance (Grant *et al.* 2003) and drought tolerance (Chini *et al.* 2004).

Table 1-2 Major classes of plants R proteins (Glowacki *et al.* 2011).

Domain structure		Example
TIR-NBS-LRR		
	TIR-NBS-LRR	RPS4
	TIR-NBS-LRR-WRKY	RRS1-R receptor
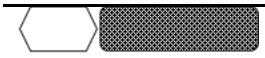	$NBS_{(TIR)}$-LRR	2 *Arabidopsis* *
Non-TIR-NBS-LRR		
	CC-NBC-LRR	ADR1; RPS5
	$NBS_{(CC)}$-LRR	4 *Arabidopsis**
	BED-NBS-LRR	Poptr_1:787192
Mixed		
	TIR-CC-NBS-LRR	2 *Populus**

 **NBS, LRR, TIR, CC, BED, WRKY. * Only the number of the NBS-LRR gene sequences is available.**

In terms of the structure of NBS-LRRs, different from typical TNL structure, subgroup member, RRS1-R protein from *Arabidopsis,* contains an additional C-terminal WRKY-like domain (Deslandes *et al.* 2003). Other proteins lack of TIR domain, but are classified as TNL due to the NBS domain determine that show sequence similarity to the NBS of classic TNL (Radwan *et al.* 2008).

In the non-TNL class, CNL is the largest group. Analysing the *Arabidopsis* genome, there are 4 gene sequences encode NBS-LRR proteins without C-terminal CC domains, and they are classified into non-TNL group due to the sequence similarity of NBS domain among the genes that encode classic typical CNL proteins (Kohler *et al.* 2008). In *Populus*, another member of non-TNL has been described as BED-NBS-LRR proteins that possess a zinc-finger DNA-binding domain at C-terminus. Furthermore, the members of a new NB-LRR class are determined that show both features of TIR and CC at C-terminus (Zhou *et al.* 2004).

1.1.3.3 Pathogen perception in ETI

The interaction between R protein and pathogen effector molecules is crucial to determine *R* gene-mediated resistance, the so-called gene-for-gene concept. The direct elicitor-receptor model was first demonstrated through the interaction between a tomato R protein and an effector from *P. syringae* pv. *tomato* (*Pst*) (Scofield *et al.* 1996, Tang *et al.* 1996). However, this theory has been controversial due to the widely different behaviours of pathogen spread and a finite number of *R* proteins with a limited number of functional motifs (Feys and Parker 2000). Thus, a "guard hypothesis" has been proposed (Dangl and Jones 2001). In this indirect recognition model, in the absence of pathogen attack, a given R protein, binds to a host guardee protein and forms a stable complex, this is inactivated through the inhibition of its kinase activity. This results in termination of downstream signalling. In the pathogen-challenged condition, the interaction between effector and guardee domain of the complex leads to the re-activation of the R protein through its conformational change. So, active R proteins can transduce signals and trigger downstream resistant responses (McDowell and Woffenden 2003).

This "guard hypothesis" model is supported by the studies on identifying resistance to *P. syringae* pv. *maculicola*, in which, (RPM1)-interacting protein 4 (RIN4) was recognized as a guardee protein (Figure 1-3) (Mackey *et al.* 2002). It has been reported that RIN4 might regulate the apertures of plant stomata in response to pathogen PAMPs (Liu *et al.* 2009).

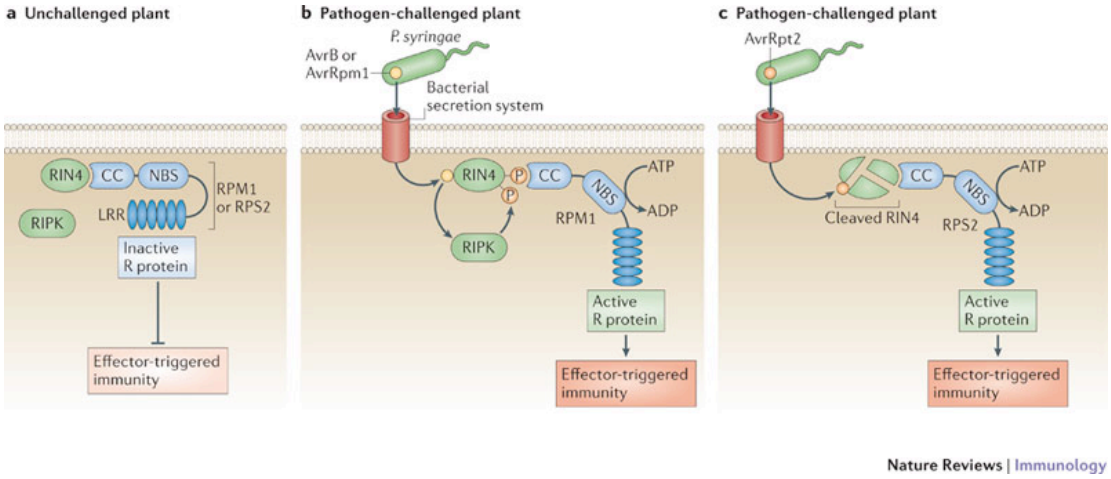

Figure 1-3 Guard model of RIN4 in response to different sets of R proteins from plants and corresponding Avr proteins from pathogens (Spoel and Dong 2012).

In unchallenged plants, RIN4 interacts with either RPM1 or RPS2 to form a RIN4 - RPM1 or RIN4-RPS2 complex, respectively. R proteins are therefore inactivated, and ETI is suppressed (a). In pathogen-challenged plants, three distinct *P. syringae* Avr factors, AvrRpm1, AvrB and AvrRpt2, are injected into the host through bacterial T3SS and target RIN4. Either AvrB or AvrRpm1 recruits phosphorylation of RIN4 threonine residues by RIPK (RPM1-induced protein kinase), a member of the receptor-like cytoplasmic kinase family, which leads to re-activation of RPM1. Therefore, ETI is activated (b). However, in the case of RIN4-RPS2, RIN4 is cleaved by bacteria cysteine protease of AvrRpt2, this cleavage results in the restoration of RPS2 activity, and therefore the activation of ETI (c).

1.1.4 Hypersensitive Response

After the activation of R proteins, signal transduction triggers the development of HR at the infection site. It is featured by a rapid death of cells surrounding the lesion, which prevents pathogens from spreading to neighbouring cells. This efficient defence response is associated with an accumulation of anti-microbial molecules and

programmed cell death (PCD) in the area of infection. As a result, pathogens are killed by secreted toxic compounds or nutrient deprivation (Hammond-Kosack *et al.* 1996).

H Marshall Ward first observed and described HR in wheat infected by the leaf rust, *Puccinia triticina* in the 19th century, but the name of HR was given by Stakman after 2 decades (Stakman 1915). The mechanism of the HR, including R-mediated recognition, signal transduction cascade and production of nature products, was only characterised relatively recently (Dangl and Jones 2001, Dixon 2001, Truman *et al.* 2006).

HR is described as a unique form of PCD (Chen and Dickman 2004). It plays a fundamental role during normal developmental and has a physiological function through regulated removal of certain cells from organisms. This genetically regulated process occurs across animals, plants, fungi and bacteria (Wang and Bayles 2013). However, there is little similarity between animal PCD (apoptosis) and plant HR.

HR is characterized by common physiological features: Ca^{2+} flux, ROS burst and changes in protein phosphorylation (Doke *et al.* 1996, Levine *et al.* 1996). The route from R protein activation to HR involves a cascade of signal transduction. An ion flux triggered by activation of R proteins leads to a quick alkalization of the apoplast. It involves an efflux of hydroxide (-OH) and potassium (K^+) outside the cells, accompanied by hydrogen (H^+) and Ca^{2+} influxes into the cells (Atkinson *et al.* 1996). Measurements of Ca^{2+} flux in *Arabidopsis* shows a continuous rise in cytoplasmic Ca^{2+} in response to avirulent bacteria and fungi (Xu and Heath 1998, Grant *et al.* 2000b). In both bacterial and fungal infections, progression to HR requires Ca^{2+} channels, as a Ca^{2+} cyclic nucleotide gated channel (CNGC) blocker abolished HR, implying a central function of Ca^{2+} flux in HR development (Clough *et al.* 2000, Ali *et al.* 2007).

Ca^{2+} influx is also thought to modulate the generation of ROS, including superoxide anions, hydrogen peroxide and hydroxyl radicals. In HR, early ROS production not only affects cellular membranes, causing lipid damage and contributing to cell death, but also plays a role in reinforcing the cell wall that surrounds lesions to inhibit the

spread of infection. Production of ROS is described as the "oxidative burst" present in the early stage of HR (Lamb and Dixon 1997, Grant *et al.* 2000b).

Enzymes have been proposed to contribute to ROS generation, such as amine oxide catalysing oxidative deamination of polyamines that releases hydrogen peroxide (H_2O_2) and ammonia, cell wall peroxidases and NADPH oxidase. Further, xanthine oxidase and oxalate oxidase are also thought to be sources of H_2O_2 (Bolwell and Wojtaszek 1997, Bolwell *et al.* 2002). However, genetic investigation focusing on homologues of mammalian NADPH oxidase, gp91phox, suggests that the respiratory burst oxidase homologues (Rboh) are the major source of extracellular ROS in plants. Rboh has been uncovered in rice, *Arabidopsis*, tomato, tobacco and potato (Groom *et al.* 1996, Keller *et al.* 1998, Torres *et al.* 1998, Amicucci *et al.* 1999, Yoshioka *et al.* 2001). In mammalian cells, the primary role of NADPH oxidase is to regulate ion fluxes, possibly through the involvement of the transmembrane spanning domains and EF hands at the N-terminus. By contrast, EF hands in Rboh are involved in Ca^{2+} regulation (Torres and Dangl 2005). Plant Rboh is considered the main source of extracellular ROS generation during plant-pathogen interaction (Bolwell *et al.* 2002).

Considering the defence signal is transduced through Ca^{2+} to produce ROS and activate cell death in the HR, the evidence from Rboh studies confirmed that NADPH oxidase regulates pathogen-induced ROS generation. However, recent physiological and molecular studies suggested that the ROS burst is important but not indispensable for HR. For example, a reduced HR was observed in the *rbohD* silenced *Arabidopsis* mutant with minor disruption on pathogenesis-related (PR) expression and SA accumulation (Delledonne *et al.* 1998, Durner *et al.* 1998, Dorey *et al.* 1999, Zhang *et al.* 2007). Meanwhile, pathogen-induced nitric oxide (NO) burst occurs during pathogen infection, the evidence report that HR is triggered after accumulation of NO and ROS (H_2O_2) (Delledonne *et al.* 1998, Yun *et al.* 2011). NO is a crucial signal molecule that regulates HR development.

In order to identify genes that are involved in HR, certain lesion mimic mutants (LMM) were identified by screening mutant lines in which cell death is misregulated. As a result, *Arabidopsis* mutant lines, *lsd* (*lesion simulating disease*) and *acd* (*accelerated cell death*) were identified and characterised (Lorrain *et al.* 2003). The

lsd1, *acd1* and *acd2* mutants cannot restrict PCD development; instead, they initiate a runway cell death (RCD) or follow the normal HR (Greenberg and Ausubel 1993, Greenberg *et al.* 1994). Additionally, *ACD1* and *ACD2* encode pheophorbide α oxygenase (PAO) and red chlorophyll catabolite reductase (RCCR), respectively, and account for chlorophyll breakdown in chloroplasts (Mach *et al.* 2001, Pattanayak *et al.* 2012). These mutants exhibit hallmarks of defence responses, such as callose deposition, *PR* expression, SA accumulation, ROS burst and normal HR (Lorrain *et al.* 2003).

Autophagy is a major system that contributes to PCD in mammalian and yeast. By characterising plant *BECLIN1*, an orthologue of mammalian autophagy gene (*ATG6/beclin1*), it demonstrated that autophagy contributes to plant disease resistance. Challenging *BECLIN1*-deficient plants with avirulent pathogen, HR is initiated at an infection site, but unrestricted PCD appears in distal health tissues. The results suggest that autophagy functions in restriction of HR PCD by unknown mechanisms (Liu *et al.* 2005).

As the distant relatives of animal caspases, metacaspases are also involved in HR regulation. *Arabidopsis* type1 metacaspases1 (AtMC1) has been demonstrated to be required for both superoxide (O_2^-) - dependent cell death and R protein – mediated HR by interacting with LSD1, a negative regulator of HR (Coll *et al.* 2010).

1.1.5 System acquired resistance

Using mobile immune cells that travel through the circulatory system, the adaptive immune system of vertebrates can detect potential pathogens throughout the body. However, in plants, each single cell is equipped with an integrated immune system to respond to pathogen attacks effectively. Avirulent pathogens not only elicit local HR, but also induce the production of anti-microbial PR proteins in uninfected, distal tissues to immunise the entire plant against secondary infections. This phenomenon is termed systemic acquired resistance (SAR), which provides a long-lasting, broad spectrum protection (Fu and Dong 2013). The expression of *PR* genes is the hallmark of SAR (Ryals *et al.* 1996).

The signalling hormone SA is a key molecule in the establishment of SAR and accumulation of SA appears at both the infection site and distal tissues, after *R* gene mediated pathogen perception. The introduction of the bacterial enzyme SA hydroxylase (*nahG*) into plants which converts SA into inactive catechol, blunts *PR* gene expression and the establishment of SAR against infection (Gaffney *et al.* 1993). As a result, *nahG* plants exhibit a strong susceptibility to a variety of pathogens (Delaney *et al.* 1994). Genetic studies indicate that SA accumulation is triggered in both local and systemic tissues, but the mechanisms of pathogen-induced biosynthesis of SA remain to be fully characterized. In addition, SA has long been known not to be a mobile signal of SAR. It is not the translocated signal responsible for the induction of SAR, but is required for local signal transduction. In infected cucumber plants with *P. syringae*, the primary leaves were removed at 6 hour after injection before SA accumulates in the phloem. However, accumulation of SA in distal tissue and *PR* genes expression remain normal (Rasmussen *et al.* 1991). This finding is further confirmed by grafting experiments between *nahG* and wild type tobacco plants. A *nahG* scion was grafted onto a wild type rootstock, following immunization to tobacco mosaic virus (TMV). There is no *PR* gene expression and no SAR development in the leaves of scion. In contrast, plants that have *nahG* rootstocks with wild type scion demonstrate the establishment of SAR and expression of *PR* genes occurs in the wild type scion (Vernooij *et al.* 1994)

The activation of SAR requires long-distance communication between the primary infected site and healthy distal tissues. In recent years, several metabolites have been identified that might be involved in long-distance, intra-plant signalling, these include methylsalicylic acid (MeSA), defective in induced resistance 1 (DIR1), glycerol-3-phosphate (G3P)-dependent factor, azelaic acid induced 1 (AZI1) and the non-protein amino acid pipecolic acid (Pip). In tobacco, MeSA is converted from SA by SA methyltransferase in the tissue with initial infection. In contrast, MeSA is converted into SA by the SA binding protein 2 (SABP2) with MeSA esterase activity in systemic tissue for signal perception. In addition, the accumulation of MeSA has been found in phloem following SAR activation, altogether, the results suggested that MeSA might be the phloem-mobile immune signal for SAR (Park *et al.* 2007). *DIR1* encodes an apoplastic lipid-transfer protein, and *dir1-1* in *Arabidopsis*

abolished SAR but retained local immune responses. This indicates that it is only required for SAR. Therefore, DIR1 may serve as a producer of immune signals or transporter of lipid-based immune signals to distal tissue (Maldonado *et al.* 2002). Another potential mobile signal is G3P. Blocking G3P synthesis failed to activate SAR, but SAR could be restored by application of exogenous G3P (Nandi *et al.* 2004, Chanda *et al.* 2011). Along with lipid-derived molecules, azelaic acid might also act as a mobile immune signal. AZI1 is a secreted lipid-transfer protein. Expression of *AZI1* primed SA accumulation, which suggests its involvement in translocated signalling (Jung *et al.* 2009). Pip is a common lysine-derived metabolite in plants that accumulates systemically and enriches in petiole exudates of inoculated leaves after infiltration of *P. syrinae* pv. *maculicola*. Exogenous application of Pip promotes *Arabidopsis* into a primed state through sufficient biosynthesis of SA and expression of *PR* genes. Thus, it may involve in SAR long-distance signalling (Navarova *et al.* 2012). The nature of the mobile signal for SAR remains debatable.

The *Arabidopsis nonexpressor of PR gene 1 (npr1)* mutant identified in a genetic screen failed to express *PR* genes after SAR induction (Cao *et al.* 1994). Wild type plants treated with SA induce the nuclear localization of NPR1 (Kinkema *et al.* 2000). NPR1 is a transcriptional coregulator and recruits transcription factors TGAs for the induction of *PR* genes (Zhang *et al.* 1999, Kim and Delaney 2002). To prevent untimely activation of SAR, the nuclear NPR1 concentration is mediated by two SA receptors NPR3 and NPR4 that bind SA with different affinities. In nucleus, NPR3 and NPR4 were found to adapt NPR1 degradation by directly interacting with Cullin3 ubiquitin E3 ligase (CUL3), which is targeted by proteasome (Figure 1-4) (Fu *et al.* 2012).

A primary infection can trigger accumulation of SA in distal tissue, which initiates transient oxidative and reductive changes (Spoel and Loake 2011). This in turn mediates a reversible switch between formations of the disulphide bond-mediated oligomeric complex and the monomeric state of NPR1 in the cytoplasm by cytoplasmic thioredoxins (TRXs) and S-nitrosoglutathione reductase (GSNOR) (Mou *et al.* 2003). Consequently, the translocation of monomeric NPR1 into the nucleus facilities its cooperation with TGAs that drives the expression of *PR* genes.

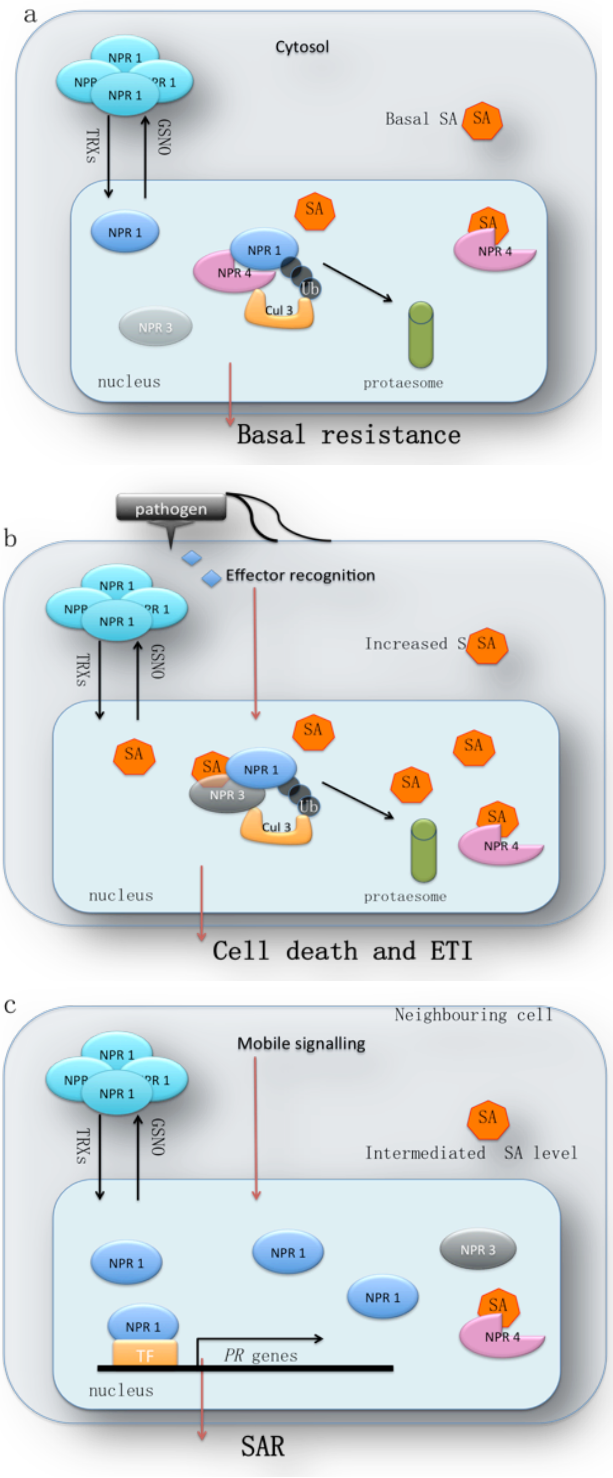

Figure 1-4 The mechanism of NPR1 involves SA-dependent SAR

In nucleus, the concentration of NPR1 is mediated by its paralogoues SA receptors NPR3 and NPR4. They are the adaptors of CUL3, which mediate the degradation of nuclear NPR1.

In the absence of SA, NPR1 interacts with CUL3-NPR4 for degradation. In wild type plants, basal SA binds to NPR4 and reduces NPR1-NPR4 interactions, which allows NPR1 assess to basal resistance (a). In response to pathogen attack, the increase in local SA leads to NPR1-NPR3 interactions followed by its degradation, which allows HR and development of resistance in lesion areas (b). Whereas in the neighbouring cells, the intermediate concentration of nuclear SA disrupts NPR1-NPR3 or NPR1-NPR4 interactions and results in the accumulation of NPR1 in distal cells. As a result, PCD is inhibited and SAR is established (c) (Fu *et al.* 2012).

1.2 Nitric oxide in plant disease resistance

Nitric oxide (NO) is a small and ubiquitous gaseous radical molecule. Its lipophilic nature allows it to easily cross through cell membranes and diffuse through organs. The *in vivo* chemical stability of NO indicates its potential biological functions and signalling roles (Arasimowicz and Floryszak-Wieczorek 2007). Compared with other known signalling molecules, NO has a distinctive half-life. In the gas phase, its stability depends on oxygen (O_2) concentration as it can be quickly oxidized by O_2 to form nitrogen dioxide (NO_2). This oxidation happens even faster with ozone (O_3) (Yamasaki and Sakihama 2000). The half-life of NO is less than 10 seconds in its aqueous phase (Wink *et al.* 1996). Oxidation of NO by O_2 and H_2O produces nitrite (NO_2^-) and H^+ or dinitrogen trioxide (N_2O_3), which is considered to be responsible for NO toxicity (vanderVliet *et al.* 1996). In cells, the half-life of NO is determined by interaction between ROS and NO, this cellular NO is converted to peroxynitrite ($ONOO^-$) by O_2^- (Rubbo and Freeman 1996). The nature of NO implies that NO and other reactive nitrogen species (RNS) are capable of targeting proteins, sugars, lipids, DNA and RNA in the process of switching the activities of protein, transducing signals and reprogramming transcription (Wink *et al.* 1996). In plants, RNS are produced to respond to pathogen infection. Evidence has shown that NO regulates plant defence responses, including the establishment of local PCD (Delledonne *et al.* 2001, Yun *et al.* 2011), cell wall reinforcement (Bradley *et al.* 1992) and SA-dependent defence responses (Feechan *et al.* 2005, Tada *et al.* 2008, Wang *et al.* 2009).

1.2.1 NO production

The activity of denitrifying bacteria (*Paracoccus denitrificans and Pseudomonas stutteri*) and autotrophic nitrifying bacteria (*Nitrosomonas eutropha & Nitrosopira briensis)* in soil was the only known biological source of NO for many years, until the discovery of NO synthesis in animal cells by nitric oxide synthase (NOS). NOS represents a family of enzymes catalysing L-arginine-dependent NO production.

There are two major pathways for NO production in cells: reductive and oxidative pathways, which are also referred to as nitrite-dependent and L-arginine-dependent, respectively (Moreau *et al.* 2008). In the absence of catalytic enzymes, the chemical reduction of nitrite requires an acidic environment, which limits the production to low pH condition (Yamasaki and Sakihama 2000, Bethke *et al.* 2004). Clear evidence shows that plants can produce NO from nitrite via a nitrite reductase (NR)-mediated pathway with NADPH as electron donor. In hypoxic conditions, the application of high nitrite concentrations increases NO production *in vitro* (Rockel *et al.* 2002). *In vivo* activity of NR-mediated NO production is also verified by characterisation of loss of NR function in plants. *Arabidopsis* genes *NIA1* and *NIA2* encode plant NRs. Inoculation of the pathogen *P. syringae* pv. *maculicola* into the knockout mutants, *nia1, nia2* and the double mutant *nia1 nia2* resulted in a significant suppression of NO synthesis and NO-mediated stomata closure (Desikan *et al.* 2002). In addition, a similar phenomenon was also revealed in wild type plants by the application of NR inhibitors like tungstate, sodium azide or potassium cyanide (Bright *et al.* 2006, Liu *et al.* 2007, Sang *et al.* 2008, Srivastava *et al.* 2009). Photosynthetic electron transport in chloroplasts and respiratory electron transport in mitochondria can also drive NO production in cells through the nitrite-dependent pathway (Yamasaki 2000, Gupta *et al.* 2005, Jasid *et al.* 2006). NR can also produce NO from nitrite; however, the efficiency is only 1% of NR activity (Moreau *et al.* 2010).

In the L-arginine-dependent pathway of NO production, NOS activity is the main source of NO in mammalian cells. All the NOS isoforms found in mammals catalyse a reaction of L-arginine by using NADPH in the presence of O_2 to produce L-

citrulline, NADP and free radical NO. The reaction requires cofactors, including flavin adenine dinucleotide (FAD), flavin mononucleotide (FMN), haeme and tetrahydrobiopterin (BH_4) (Figure 1-5) (Nathan and Xie 1994).

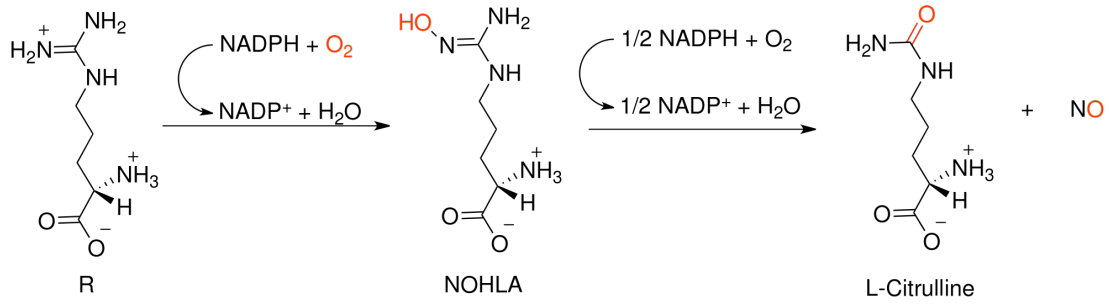

Figure 1-5 NO synthesis in mammals from L-arginine (Knowles and Moncada 1994).

Three known isoforms of NOS have been identified and well established in animals: neuronal NOS (nNOS/NOS 1), inducible NOS (iNOS or NOS 2) and endothelial NOS (eNOS/ NOS 3) (Nathan and Xie 1994)

nNOS, which was the first isoform described also known as constitutive NOS, is found in neuronal tissues and functions as a retrograde neurotransmitter. Apart from its role in cell communication, it is also important in response to memory and learning. Similar to nNOS, another constitutive NOS member, endothelial NOS (eNOS), is isolated from endothelium membrane and functions as a primary controller of smooth muscle. It is involved in regulation of vascular tone, secretion of insulin and growth of new blood vessels (Knowles and Moncada 1994, Liu *et al.* 1997). Described as a critical factor of host immunity, iNOS appears to form large amounts of NO and acts as a defence mechanism under an oxidative environment. This leads to peroxynitrite formation and cell toxicity, which exhibits antimicrobial and anti-tumour activity (Stuehr 1999, Mungrue *et al.* 2002). Bacterial NOS (bNOS) exists in gram-positive bacteria, such as plant-associated species, to protect bacteria against oxidative damage due to NO functioning as an antioxidant under some conditions (Crane *et al.* 2010).

Arginine-dependent NO formation is the primary source of endogenous NO formation from bacteria to mammals. However, no homologues of animal NOS proteins have been reported in higher plants. Evidence suggesting the existence of NOS in plants is indirect. Cryptogein is an elicitor of the tobacco defence response and can rapidly trigger an NO burst, which is sensitive to mammalian NO inhibitors (Delledonne *et al.* 1998, Foissner *et al.* 2000). The presence of a mammalian-like NOS in plants is evidenced by the fact that mammalian NOS inhibitors, which block the conversion of L-arginine to NO, can blunt the nitrosative burst in plants (Cueto *et al.* 1996, Delledonne *et al.* 1998).

Klessig (2003) first proposed a variant form of the P protein of glycine decarboxylase (GDC) as a pathogen-induced NO synthesis enzyme, which has been proved to be incorrect (Chandok *et al.* 2003). An *Arabidopsis* gene *At3g47450* was identified as a putative NOS encoding gene of plants by Crawford *et al.* (2006). AtNOS1 is a homologue of a hypothetical snail NOS and cross-reacts with mammalian NOS antibodies. However, it has been reported by several groups that this protein is not a NOS but might be associated with NO accumulation. Therefore, AtNOS 1 has been renamed NO-associated protein 1 (AtNOA1). This protein has now been shown to be a GTPase (Crawford *et al.* 2006)

The orthologs of NOA1 is YqeH in *Bacillus subtilis,* and this protein has no NOS activity but can hydrolyse GTP to GDP. Both YqeH and AtNOA1 contain the same C-terminal domain, the RNA-binding regulator (TRAP). TRAP is essential for RNA-binding and coupling GTP hydrolysis. This conserved structure suggests that AtNOA1 could be involved in NO generation by binding to RNA/ribosomes (Anand *et al.* 2010). NbNOA1, a homologue of AtNOA1 from *Nicotiana benthamiana*, regulates INF1 elicitor-induced NO production and *PR1* gene expression (Kato *et al.* 2008). The orthologs of AtNOA1 isolated from rice, OsNOA1, has been shown to control growth, development and NO production (Qiao *et al.* 2009). The early research on green algae *Scenedesmus* indicated that the formation of NO is due to the accumulation of nitrite. Further evidence supported this conclusion, as there is no effect on NO generation following application of NOS inhibitors L-N-nitroarginine methylester (L-NAME) and L-N-nitroarginine (L-NNA) (Mallick *et al.* 1999,

Mallick *et al.* 2000). Interesting, a NOS homolog has been reported in *Ostreococcus tauri* (Derelle *et al.* 2006). Thus, the *O. tauri* NOS provides direct evidence for the presence of a NOS-like enzyme in algae species. Recombinant *O. tauri* NOS expressed in *Escherichia coli* showed NOS enzyme activity similar to iNOS. Its function in NO production is influenced by light irradiance and growth phase (Foresi *et al.* 2010).

Polyamines, such as spermine and spermidine, support the oxidative formation of NO, as these activities can be repressed by NOS inhibitors but not an NR inhibitor (Gaupels *et al.* 2008). In addition, superoxide dismutase (SOD) is also capable of stimulating NO production from hydroxylamine even without cells. However, the role of this phenomenon is not clear (Rumer *et al.* 2009).

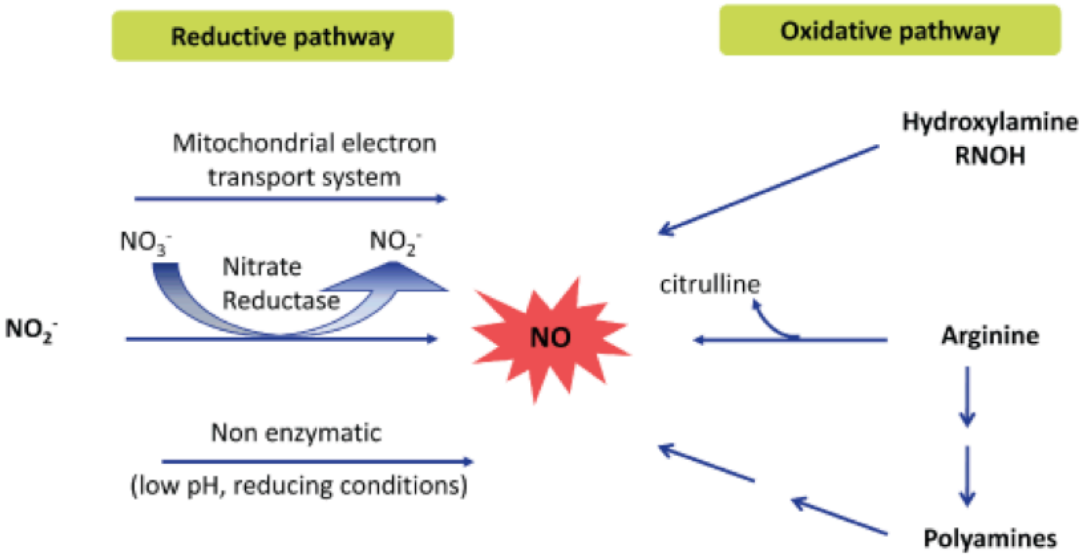

Figure 1-6 Two major pathways of NO production (Moreau *et al.* 2010).

As describe above, there are two major routes response for NO generation in plants, reductive and oxidative-dependent (Figure 1-6). The reductive pathway relies on the activity of NR, which produces NO from nitrite that requires electrons. The electrons can be provided through mitochondrial electron transport system from NADPH or under acidic reducing condition. In contrast to the reductive pathway, the existence of the oxidative pathway in plants is only revealed indirectly. Although the substrates

of the oxidative pathway are proposed, such as arginine, polyamines and hydroxylamines, the corresponding enzymes have not been identified from higher plants as yet.

1.2.2 NO chemistry and signalling

As described above, NO signalling functions are mostly attribute to its high diffusion, which allows this molecule to spread throughout the cytoplasm. The nature of NO, such as a small stock's radius and neutral charge, contributes to its mobility. These together establish the utility of NO in signalling (Arasimowicz and Floryszak-Wieczorek 2007).

The NO related signalling system is comprised of NOS activities and NO-dependent downstream factors. In mammals, NOS produces NO, which is the primary messenger. NO in turn activates a second enzyme, soluble guanylate cyclase (sGC). Consequently, the active sGC converts GTP to guanosine cyclic monophosphate (cGMP). cGMP is a second messenger for NO signalling that activates downstream signalling components, such as cGMP-dependent protein kinase (NO-G-kinase or PKG), CNGC and phosphodiesterases (PDE) (Figure 1-7) (Yamasaki *et.al,* 2011).

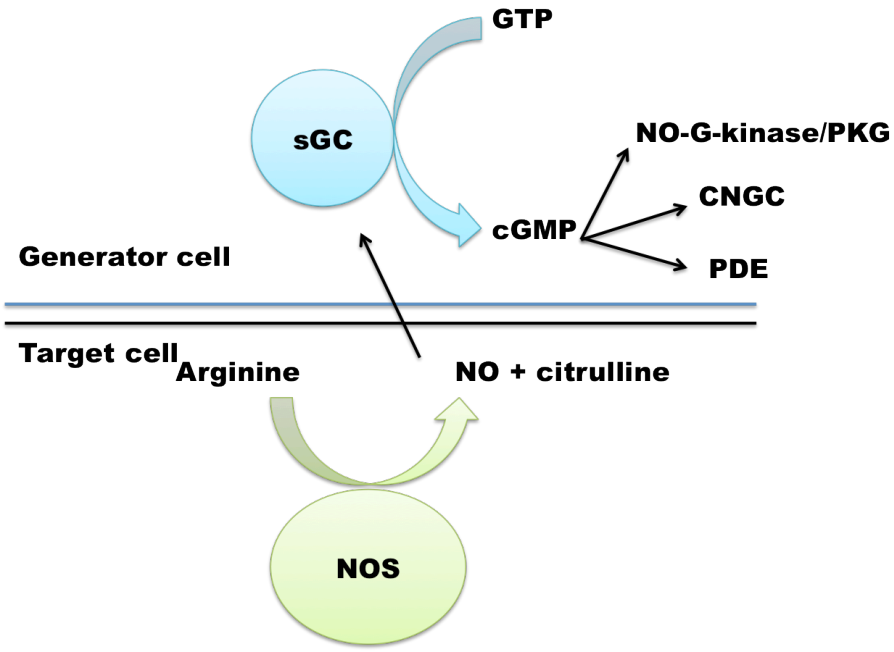

Figure 1-7 Mammalian model of NOS/sGC/cGMP signal system (Calabrese *et al.* 2007).

In this classic NO signalling model, activation of cGMP alters PKG that regulates the intracellular Ca^{2+} concentration, resulting in smooth muscle relaxation by phosphoric inositol 1,4,5 – triphosphate (IP_3) (Clementi 1998). Moreover, CNGC might be activated directly by cGMP to enhance the cytosolic free Ca^{2+} level (Ahern *et al.* 2002). Another substrate molecule, PDE is associated with NO downstream signal transduction (Beck *et al.* 1999).

As one of the principle factors of NO signalling, cGMP activity has also been demonstrated in plant species, including Norway spruce (Pfeiffer *et al.* 1994), barley (Penson *et al.* 1996) and tobacco (Durner *et al.* 1998) and *Arabidopsis* (Donaldson *et al.* 2004). The fact that the comparatively low level of endogenous cGMP is rapidly elevated after application of NO, NO donor, or abiotic stress suggested the existence of a classic NOS/sGC/cGMP signalling system in plants. Alongside the presence of cGMP in plants, the genes that encode mammalian-like sGC proteins have also been isolated from plant genomes recently. Firstly, *Arabidopsis* GC 1 (AtGC1) was identified, which lacks a typical GTP and Mg^{2+} binding moieties in comparison with mammalian sGC structure. Although the *in vitro* experiment demonstrated its Mg^{2+}-dependent GC activity, such activity is not connected with NO (Ludidi and Gehring 2003). The discovery of the *Arabidopsis* brassinosteroid receptor (AtBRI1) shows it may convert GTP to cGMP by a GC catalytic core in the cytosolic kinase domain (Kwezi *et al.* 2007). Furthermore, another 26 putative GC enzymes have been identified in the *Arabidopsis* genome through virtue of this cytosolic kinase domain. Within 27 potential plant GC enzymes, 13 showed LRR-PLKs structure, which predicts a direct interaction with plant hormones and extracellular ligands (Donaldson *et al.* 2004, Kwezi *et al.* 2007). These results suggest a potential large number of GCs in plants. Nevertheless, the rapid elevation of cGMP in plants seems to be caused by hormones rather than NO (Donaldson *et al.* 2004). Although the presence of mammalian type NO-signalling components, including sGC and cGMP, have been uncovered it may not be functionally relevant in plants (Yamasaki 2010).

1.2.3 NO-mediated Protein Post-Translational Modification

NO- and NO-derived species-dependent signalling pathways depend upon NO-regulated post-translational modifications (PTM) of proteins. Considered as a key mechanism underlying biological complexity, PTM modifies the properties of proteins and diversifies protein functions without changing gene transcription. For example, phosphorylation is a principle mechanism of PTM, others are glycosylation, methylation, acetylation and ubiquitination. NO-responsive PTM is celled nitrosylation. This chemical activity of NO allows it to bind to transition metals (metal nitrosylation) and interact with cysteine (Cys) (S-nitrosylation) and tyrosine (Tyr) (tyrosine nitration) residues of redox-sensitive proteins. In *Arabidopsis,* there are more than 100 proteins identified as NO targets (Besson-Bard *et al.* 2008).

Accumulating evidence suggest that NO-mediated signalling is regulated through NO turnover. An example is the reversible path between NO and S-nitrosoglutathione (GSNO), in which the intracellular level of GSNO is controlled by GSNO reductase (GSNOR). GSNOR can further reduce GSNO into GSSG and NH_3 (Leterrier *et al.* 2011). Rapid interplay between NO and ROS produces $ONOO^-$, which can be detoxified by peroxiredoxin II enzyme (PrxII E) in *Arabidopsis*. Indeed, S-nitrosylation of PrxII E increases the level of $ONOO^-$. Consequently, it promotes tyrosine nitration (Romero-Puertas *et al.* 2007). Therefore, NO turnover balances the bioavailability of NO signalling compounds, which are involved in NO signal transduction.

1.2.3.1 Metal nitrosylation

Metal nitrosylation occurs when NO donates electrons and reacts with metal atoms present in proteins, such as haem and zinc-finger proteins. This process turns on or off protein activities. Haem is a prosthetic group found in many proteins. In animals, haem-nitrosylation regulates many enzyme activities including inhibition of NOS and activation of sGC. Reactions between NO and haemoglobin (Hb), which regulates vasodilation to control the blood flow, have been well studied (Lima *et al.* 2010).

There are three major types of Hb in plants: symbiotic or so celled leghemoglobin (Lb), nonsymbiotic and truncated (Appleby 1984, Watts *et al.* 2001, Dordas *et al.* 2003) nonsymbiotic Hb, a ubiquitous molecule, is divided into two classes. Class-1 Hb is induced by hypoxia and has high affinity for O_2. In contrast, Class-2 Hb exhibits a low affinity for O_2. In plants, class-1 converts NO to NO_3^- by using NADPH acting as an electron donor, which could enhance tolerance to hypoxic stress during pathogen attack (Perazzolli *et al.* 2004).

In animals, NO initiates the cGMP signalling pathway by interacting with the haem ferrous iron to trigger its activity, which in turn induces cGMP production and finally initiates downstream cellular responses (Perazzolli *et al.* 2004). In plants, application of NO induces cGMP activity. Nevertheless, *in vitro* experiment shows that identified plant sGC activity could be altered in either the presence or absent of NO (Ludidi and Gehring 2003).

1.2.3.2 Tyrosine nitration

Tyrosine (Tyr)-nitration of proteins occurs through a chemical reaction of NO-derived species with the *ortho* position configuration of Tyr, which forms nitrotyrosine and results in altered protein function. Meanwhile, this prevents phosphorylation of Tyr (Schopfer *et al.* 2003). Tyr-nitration is mediated by $ONOO^-$, the product of the interaction between NO, ROS and nitroso-peroxocarboxylate ($ONOOCO^{2-}$), the latter being formed by $ONOO^-$ and CO_2. Unlike metal nitrosylation, Tyr-nitration mostly associates target proteins with loss of function, through nitration of relevant Tyr residues, which further prevents Tyr phosphorylation. For example, nitration of two Tyr residues of GSNOR by $ONOO^-$ can lead to inactivation of its function (Savvides *et al.* 2002). In addition, $ONOO^-$ could inhibit mitochondrial respiration and stimulate apoptosis through nitration of cytochrome c on tyrosine residues, which demonstrate that Tyr-nitration is involved in signalling events (Savvides *et al.* 2002). In *vitro* research shows that Tyr-nitration of NtMEK2 could turn off MAPK signalling transduction (Vandelle and Delledonne 2011). Further, *Arabidopsis* non-symbiotic haemoglobins (AtGLB) can also be Tyr-nitrosylated (Sakamoto *et al.* 2004). Pathogen perception, including concomitant NO

and ROS emission, suggests the importance of Tyr-nitration in plant defence signalling. The accumulated evidence suggests that Tyr-nitration may serve as a signal based on the possibility of its potential reversibility (Souza *et al.* 2008).

1.2.3.3 S-nitrosylation

S-nitrosylation is the covalent attachment of NO to the thiol side chain of Cys to form an S-nitrosothiols (SNO). The mechanism of reaction between NO and targeted proteins is ascribed to the electrophilic attack of NO^+ on thiolate, the direct interaction in the presence of NAD^+ as the electron acceptor or a non-enzymatic interaction with NO^- (Gow *et al.* 1997, Foster and Stamler 2004). The free thiol of Cys is modified in order to adapt nitrosative and oxidative stress to prevent toxicity. S-nitrosylation widely ranges in effect, such as regulation of protein function, including enzyme activity, ion channel, receptors and transcriptional factors (Stamler 1994, Hess *et al.* 2005). In *Arabidopsis,* 105 proteins have been identified as candidates for S-nitrosylation through the biotin-switch assay. These candidates are characterised as stress-related, redox related, signalling, cytoskeleton or metabolic (Lindermayr *et al.* 2005, Loake *et al.* 2007).

GSNO is formed through S-nitrosylation of glutathione (GSH), which is might function in NO storage and transport. To be considered a physiologically relevant transduction mechanism in plants, S-nitrosylation should be a reversible modification. GSNOR functions to breakdown GSNO to regulate the level of SNOs, and this process is celled de-nitrosylation. This enzyme has been found in bacteria, animals and plants (Liu *et al.* 2001). Analysis of the *Arabidopsis* GSNOR knockout mutant (*atgsnor1-3*), which contains high levels of SNO, shows that it affects development and compromises defence responses. In contrast, an enhanced GSNOR expression line that contains low levels of SNO exhibits enhanced resistance against pathogens (Feechan *et al.* 2005).

S-nitrosylation is an important redox-based regulation mechanism (redox regulation see 1.3.2). For example, in the regulation of gene expression, NPR1 is a key regulator in SA-mediated SAR and response to *PR1* expression. NPR1 exists as an

oligomer, which is formed from monomer subunits by intermolecular disulphide bonds in the cytosol. Monomer NPR1 is translocated into the nucleus to form a complex with TGA1. However, S-nitrosylation of NPR1 monomer results in the formation of NPR1 oligomer through promoting disulphide bond formation. Therefore, blocking the S-nitrosylation site prevents development of oligomers and SA-dependent gene expression is blunted (Tada *et al.* 2008). In addition, SA binding protein 3 (AtSABP3), which has been isolated from *Arabidopsis*, is also involved in the SA-dependent signalling system. Both activity and binding capacity of AtSABP3 are affected by S-nitrosylation (Wang *et al.* 2009). As mentioned in earlier, *Arabidopsis* metacaspases proteins are involved in pathogen-induced HR development (Uren *et al.* 2000). Evidence indicates that NO regulates the activity of *Arabidopsis* type II metacaspases AtMC9, not thought to function in plant immunity, via blocking its activation by S-nitrosylation through a catalytic Cys residue (Belenghi *et al.* 2007). In plants, S-nitrosylation is the key method of NO signal transduction due to the lack of a NO-modified sGC.

1.2.4 Nitric oxide-mediated transcriptional reprogramming in plants

In plants, NO-dependent signalling has been reported in various physiological processes, for instance, responses to abiotic and biotic stress (Delledonne *et al.* 1998, Tanou *et al.* 2012), stomata closure (Garcia-Mata and Lamattina 2002), seed germination (Sirova *et al.* 2011), root development (Pagnussat *et al.* 2002) and flowering (He *et al.* 2004). However, a clear picture of how NO achieves its action is still incomplete.

Analysis of NO-induced transcriptional changes in *Arabidopsis* through whole genome approaches has shown that there are a number of genes up- or down-regulated by NO (Huang *et al.* 2002, Polverari *et al.* 2003, Palmieri *et al.* 2008). For example, by cDNA-amplification fragment length polymorphism (AFLP) transcript profiling of plants infiltrated with sodium nitroprusside (SNP), 120 of 2500 transcripts were regulated by NO. Based on the analysis of sequence homologies, they were grouped into different functional categories: signal transduction, resistance and cell death, ROS generation and degradation, chloroplast, transport and basic metabolism (Polverari *et al.* 2003).

A whole-genome microarray has also been used to detect the expression of NO-responsive genes by Palmieri *et al.* (2008) in *Arabidopsis* treated with gaseous NO and SNP. There were 28 up-regulated genes and 26 down-regulated genes identified. Analysis of the transcriptional factor biding sites present in the promoter region of these genes revealed *GBOX* and *OCSE* elements were enriched. *GBOX* (CACGTG) contains an ACGT element, which is the core DNA-binding motif of bZIP (basic region/leucine zipper motif) transcription factors (TF) in plants. In addition, the analysis also revealed that *GBOX* elements were located around 250 bp upstream from the putative start of transcription in the promoters of these NO up-regulated genes. Another enriched binding element *OCSE*, the *Arabidopsis* octopine synthase (ocs) element-like sequences also belongs to the class of bZIP-binding elements. For example, the TGACG motif binding 1 TF (TGA1), which is a member of bZIP proteins, regulates *PR1* gene expression (Lebel *et al.* 1998). TGA interacts with NPR 1 to activate the expression of *PR1* (see 1.1.5), and both proteins are demonstrated to

be affected by NO through S-nitrosylation (Lindermayr *et al.* 2010). In *vitro* S-nitrosylation of TGA1 by GSNO promotes the TGA1-NPR1 interaction and enhances its DNA-binding efficiency (Lindermayr *et al.* 2010).

In animal cells, glyceraldehyde 3-phosphate dehydrogenase (GAPDH) is an important NO-mediated nuclear protein. The S-nitrosylation of GAPDH stabilised the E3 ubiquitin ligase Siah1 (seven in absentia homolog 1) by forming a complex. Then, the complex is translocated into the nucleus where nuclear proteins are degraded by Siah1. This ultimately leads to apoptosis (Hara *et al.* 2005). Recent research indicates that nitrosylated GAPDH can transnitrosylate nuclear proteins to affect transcription such as deacetylating enzyme sirtuin 1 (SIR1), histone deacetylase 2 (HDAC2) and DNA-binding protein kinase (DNA-PK) are proposed to be transnitrosylated (Kornberg *et al.* 2010). In contrast to animal cells, although *Arabidopsis* homologues of GAPDH, GapC1 and GapC2, are both able to be S-nitrosylated; the molecular function of S-nitrosylated GAPDH on transcriptional regulation in plants remains unclear (Holtgrefe *et al.* 2008).

Accumulating evidence suggests that NO-responsive signalling involves numerous physiological processes through reprogramming the genes transcription. However, in comparison with well-established model in animal cells, the mechanisms of NO-regulated transcriptional changes are still uncovered.

1.2.5 Nitric oxide modulates HR development

As an important signal in plant defence system, NO has been reported to play various roles in the HR (Delledonne *et al.* 2002, Yun *et al.* 2011, Wang *et al.* 2013). Pathogen recognition by a given R protein triggers an oxidative burst that precedes the development of HR at the site of infection. HR is the hallmark of pathogen-induced ETI in plants (see 1.1.4). A rapid elevation of NO synthesis is observed in parallel with the oxidative burst after pathogen recognition. The balance between NO-ROS interactions is considered as a key feature in the initiation of HR development (Delledonne *et al.* 2001, Wang *et al.* 2013). However, the role of NO in HR in plants is not as clearly understood as in animal PCD (Zhang *et al.* 2003, Lamotte *et al.* 2004, Tada *et al.* 2004).

Ca^{2+} influx is a key physiological feature of the HR (Doke 1996; Levine 1996). In animal cells, all existing L-arginine ─ dependent NO synthases require CaM (calmodulin) binding for activation (Ichimori *et al.* 1999). Although Ca^{2+} influx has also been demonstrated to be involved in signalling transduction, the classic mammalian-like NOS/sGC/cGMP signalling model is not applicable to the plant system (see 1.2.2). The evidence implies that Ca^{2+} influxes stimulate NO production, and in turn increase intercellular Ca^{2+} levels. An excess of Ca^{2+} leads to cytotoxicity and HR (Delledonne *et al.* 1998, Lamotte *et al.* 2004, Aboul-Soud *et al.* 2009). CNGC has been considered as a channel that directs Ca^{2+} influx (Cheval *et al.* 2013). The CNGC-dependent Ca^{2+} accumulation is an important component of HR. Inhibition of CNGC leads to an impaired HR, this phenotype can be restored by application of an NO donor (Clough *et al.* 2000, Jurkowski *et al.* 2004, Ali *et al.* 2007). So this implies NO might act as a downstream factor of Ca^{2+}signalling in HR development.

During the early ETI, the oxidative burst precedes HR and leads to accumulation of both ROS and NO in plants cells (Delledonne *et al.* 1998, Krause and Durner 2004). NO can rapidly interact with O_2^- and form $ONOO^-$, which drives programmed cell death in animals (Bonfoco *et al.* 1995). However, plants show more tolerance to $ONOO^-$ accumulation, and $ONOO^-$ facilitates Tyr-nitration, rather than functioning

as a cytotoxic factor (see 1.2.3.2). This implies a putative function of this PTM in NO-dependent signal transduction (Souza *et al.* 2008). Moreover, instead of NO interacting with O_2^-, HR has been proposed to be triggered by the interaction between NO and H_2O_2, derived from O_2^- by the action of superoxide dismutase (SOD). Although SOD is important to modulate NO/H_2O_2, the reaction of NO/O_2^+ is approximately three times faster than SOD (Delledonne *et al.* 2002). Therefore, the ratio of NO/ROSs might be a key feature to facilitate HR. *Arabidopsis nox1* (*NO overproducing 1*) and *atgsnor1-3* (see 1.2.3.3 & 1.2.6) plants challenged with avirulent bacterial strains showed an accelerated and enhanced cell death HR (CDHR) phenotype compared with wild-type *Arabidopsis*. This CDHR conveyed increased disease resistance against an obligate biotrophic pathogen. However, accelerated and enhanced CDHR did not offset the disablement of SA synthesis and signalling with respect to *Pst* DC3000 challenge, as in this case *nox1* and *atgsnor1-3* mutants exhibited increased disease susceptibility (Yun *et al.* 2011).

RbohD and *RbohF* respond to ROS generation during pathogen-induced HR (see 1.1.4), and *atrbohD* and *atrbohF* mutants showed impaired HR compared with the wild type (Torres *et al.* 2002) due to impeded ROS production. However, similar CDHR are observed in *atgsnor1-3 atrbohD*, *atgsnor1-3 atrbohF* and *atgsnor1-3 atrbohD atrbohF* plants, which intimates that S(NO) may induce cell death independently of *RbohD* and *RbohF*-mediated ROS (Yun *et al.* 2011).

The emerging evidence indicates that NO regulates HR in a positive manner; however, both *in vitro* and *in vivo* experiments showed that NO may also function in a negative loop by modifying NADPH oxidase activity (Yun *et al.* 2011). AtrbohD can be S-nitrosylated at Cys^{890} both *in vitro* and *in vivo*. Cys^{890} is localized behind Phe^{921} residue in AtrbohD, which is required for FAD binding (Ingelman *et al.* 1997). Impeded FAD binding by S-nitrosylated Cys^{890} of AtrbohD affects NADPH oxidase activity and inhibits ROS generation. The *in vivo* S-nitrosylation of AtrbohD occurs during plant immunity and suggests NO could restrict HR through this negative feedback loop by inactivating NADPH oxidase (Yun *et al.* 2011)

1.2.6 S-nitrosylation controls plant immune activities

PTM of proteins is the major strategy underpinning signalling processes. In this context, S-nitrosylation confers the ability to affect catalytic activity, change ligand-binding affinity and alter protein structure and protein-protein interactions, which results in alteration in protein activity, translocation and protein function. In NO-dependent signalling system, S-nitrosylation of target proteins is the key mechanism to convey bioactivity of NO (see 1.2.3).

In plants, the NO-dependent regulation of immunity is largely impacted by S-nitrosylation of defence-related proteins. For instance, PrxII E functions to detoxify $ONOO^-$ and results in tolerance of $ONOO^-$. S-nitrosylation of PrxII E could negatively regulate this immune response by causing increased ONOO accumulation (Romero-Puertas *et al.* 2007).

As described in 1.2.5, during HR development, S-nitrosylation also negatively regulates defence activities. The lack of GSNOR activity increases cellular SNO levels, leading to pathogen susceptibility due to repressed SA accumulation (Feechan *et al.* 2005, Yun *et al.* 2011).

AtSABP3 is an SA binding protein, which confers SA binding activity and chloroplastic CA activity. Infiltrated AtSABP3 loss of function *Arabidopsis* mutants (*atsabp3-1* and *atsabp3-2*) with *Pst* DC3000 (*avrB*) exhibited an enhanced pathogen growth compared with wild type. This phenotype can be rescued by expressing wild type AtSABP3. However, a C280S (Cys^{280}) mutant with reduced CA binding activity showed disease susceptibility. Thus, AtSABP3 is required for establishment of plant disease resistance and particularly the SA binding activity. In 1.2.3.3, S-nitrosylated AtSABP3 impairs both SA and CA binding activities, which may lead to disease development (Wang *et al.* 2009).

Another master factor of SA-dependent SAR is NPR1, which requires S-nitrosylation as a negative feedback to control *PR1* expression (see 1.1.5). The TFs that form a complex with NPR1 and then initiate *PR* gene expression have been demonstrated to be S-nitrosylated, which consequently enhances DNA binding affinity (see 1.2.3.3).

Thus, S-nitrosylation might control SAR through SA signalling and *PR* gene regulation.

1.3 NO-responsive transcriptional factor in Plant immunity

Plants have evolved transcriptional reprogramming in response to the environmental changes (1.2.4). Hence, the signal-induced transcription factors are the key class of regulators to protect plants from stress. Previous studies showed that a number of zinc finger proteins were up regulated by NO (Huang *et al.* 2002, Polverari *et al.* 2003, Palmieri *et al.* 2008). Most of these zinc finger proteins show transcription factor activity and are rich in Cys residues, which make these zinc finger proteins a target of NO-mediated redox regulation. Therefore, zinc finger transcription factors (ZnTFs) might play a role in NO-mediated defence response.

1.3.1 Zinc finger protein in plants

The zinc finger was first proposed as a repetitive zinc-binding motif in *Xenopus* transcriptional factor IIIA (TF IIIA) in 1983 (Miller *et al.* 1985). Zinc finger motifs are the representations of different number of Cys (C) and/or histidines (His, H) coordinating one or more zinc ions in the secondary structure of the finger, which zinc contributes to the stability of the domain. Zinc finger proteins are one of the most abundant proteins in eukaryotic genomes (Laity *et al.* 2001). Based on the different types of zinc finger motifs, proteins that contain zinc finger domains are classified into several different structural families (Table 1-3) (Berg and Shi 1996). Among the different zinc finger types, the classical C2H2 zinc finger is one of best-studied and largest families in eukaryotic genomes (Takatsuji 1998, Laity *et al.* 2001, Ciftci-Yilmaz and Mittler 2008). Most of eukaryotic zinc finger motifs have been documented in plants. Furthermore, some novel motifs have been identified in plants, such as the WRKY domain and the Dof domain. WRKY contains C2H2 type zinc finger domain, which is unique to plants and specifically binds to W boxes (TTGACC/T), the binding site for WRKY family of transcriptional factors. The Dof family shares a conserved domain, which is similar to the GATA 1 motif. However,

the difference in spacing between second and third fingers in Dof family and GATA 1 family makes them into a distinct class (Yanagisawa 1996). In addition, the Dof motif has not been found in yeast and animal genomes.

Table 1-3 Selected families of zinc-binding domains and their functions

Zinc finger type	Class		Function	Selected Reference
Cys2His2	TF IIIA	WRKY	Nucleic acid binding	(Miller *et al.* 1985, Ishiguro and Nakamura 1994)
Cys4	GATA	Dof	DNA binding	(Omichinski *et al.* 1993)
Cys2HisCys	FOG domain		Single-stranded nucleic acid binding	(Fox *et al.* 1999)
Cys8	Steroid-thyroid receptor		DNA-binding, oligomerisation	(Berg and Shi 1996)
Cys3HisCys4	RING finger		Protein-protein interaction	(Vonarnim and Deng 1993)
Cys2HisCys5	LIM domain		Protein-protein interaction	(Sanchez-Garcia and Rabbitts 1994)
Cys3His	FYVE domain		Lipid binding	(Kutateladze *et al.* 1999)
Cys4HisCys3	PHD domain		DNA binding	(Schindler *et al.* 1993)
HisCys3	TAZ domain		Protein-protein interaction	(De Guzman *et al.* 2000)

Some classes of motifs show direct nucleic acid binding in transcriptional or translational processes that include TF IIIA and GATA families. A conserved sequence QALGGH is located on the zinc fingers of TF IIIA proteins responding to DNA binding activity (Kubo *et al.* 1998). The study of the EPF family (renamed as ZPT) of petunia revealed that the spacing between fingers verifies the recognition of DNA-binding sites in a sequence-specific manner (Kobayashi *et al.* 1998). In comparison, other classes are mostly involved in protein-protein interactions, such as LIM and RING families. Many proteins that contain RING domains act as ubiquitin-protein ligases (E3 ligases) in ubiquitination reactions. For instance, ATL9, an *Arabidopsis* RING zinc finger protein shows E3 ligase activity in chitin- and NADPH oxidase-mediated defences (Stone *et al.* 2005, Berrocal-Lobo *et al.* 2010). In the order of ubiquitin-proteasome degradation, the ubiquitin is first activated by E1 activation enzyme, and then interacts with E2 conjugating enzyme that binds E3

ligase. The presence of E3 ligase responds to transfer ubiquitin to its target substrate (Vierstra 2003).

In plants, zinc finger proteins play a central role in the regulation of many physiological processes including flower development, light-regulated morphogenesis and environmental stimulation (abiotic and biotic stresses) (Takatsuji 1998). For example, members of TF IIIA family, SUPERMAN and EPF respond to flowering in *Arabidopsis* and petunia, respectively. The Dof1 is the transcriptional activator of C4-photosythetic phosphoenolpyruvate carboxylase (C4PEPC), which responds to light-stress (Yanagisawa 1996). Also, WRKY1, 2 and 3 regulate *PR1* expression in response to fungal infection.

1.3.2 Zinc finger proteins and redox regulation

Redox (reduction-oxidation) chemistry is a key feature of life, which results in the change of oxidation state. Through the regulation of oxidative burst, plants are able to adapt metabolism and gene expression under different stress. This involves ROS and/or RNS generation, cellular redox couples-mediate signalling and redox reactions in proteins through reversible PTM (Spoel and Loake 2011, Foyer and Noctor 2013). The generation of ROS relies on NADPH oxidases (Torres and Dangl 2005). In addition, NO production also requires NADPH (Modolo *et al.* 2005, Corpas *et al.* 2009). This NADPH/$NADP^+$ system involves redox signalling. To protect plants from oxidative damage and stress, low-molecular-weight antioxidants, such as GSH and ascorbate, can function together with ROS and/or RNS to mediate redox signal flow. During redox signalling, NADPH/$NADP^+$ initiates the electron flow, and subsequently regulates the GSH/GSSG regeneration system. The ratio of GSH/GSSG defines the cellular environmental redox potential that leads to redox sensor protein modifications. Additionally, the oxidised GSH is required in regeneration of reduced ascorbate (Figure 1-8) (Spoel and Loake 2011).

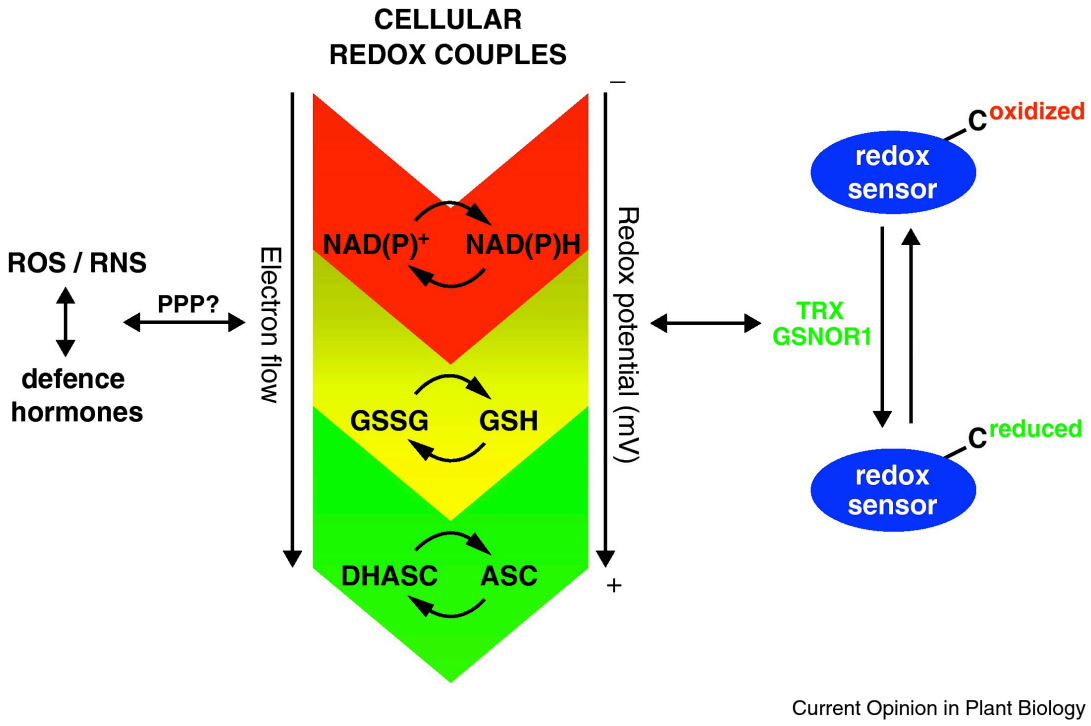

Figure 1-8 Redox signalling regulation by cellular redox couples (Spoel and Loake 2011). PPP, pentose phosphate pathway. ROS, reactive oxygen species. RNS, reactive nitrogen species.

In Figure 1-8, the production of ROS/RNS and defence hormones are sensed by listed cellular redox couples, which might involve pentose phosphate pathway (PPP). The increasing electron flow and enhancing cellular redox state alter protein structure and function. These redox sensor proteins are either transcriptional factors that affect gene expression or receptors that are involved in signal transduction network, including NPR1 and AtSABP3.

Through the regulation of redox homeostasis at the cellular level, plants confer capacity on growth, development and stress tolerance. As one of largest transcriptional regulator groups in plants, zinc finger proteins have been reported to be involved in redox regulation. For example, LSD1 contains three GATA-like zinc fingers. It negatively regulates programmed cell death in plants. In contrast, its highly conserved paralogue LOL1 is a positive regulator of cell death. They antagonistically regulate SOD and O_2^- accumulation (Epple *et al.* 2003). The elevation of zinc finger proteins ZAT12, ZAT7 and WRKY25 were observed in

cytosolic ascorbate peroxidase 1 (APX1)-deficient *Arabidopsis* plants. It implies that *ZAT12, ZAT7* and *WRKY25* respond to oxidative stress (Rizhsky *et al.* 2004). APX1 is a key H_2O_2 scavenging enzyme, which plays a key role in H_2O_2 mediated growth, development and might also respond to induction of heat shock protein under light stress (Pnueli *et al.* 2003). Results suggest that plants that express *ZAT12* and *ZAT7* could tolerate oxidative stress. However, APX1-deficient plants expressing *WRKY25* are unable to tolerate oxidative stress. In addition, lack of *ZAT12* leads to a reduction in expression of *APX1, ZAT7* and *WRKY25*, which suggests that *ZAT12* is required for the expression of these genes in response to oxidative stress. In addition, in *ZAT12* expressing plants, the transcripts that encode an NADPH oxidase are enhanced, which implies the role of ZAT12 in ROS generation (Rizhsky *et al.* 2004).

1.3.3 Zinc finger proteins regulate plant defence responses

Previous studies indicate that zinc finger proteins play a crucial role in various stress responses and defence, most of them belong to C2H2 family (Ciftci-Yilmaz and Mittler 2008).

The TF IIIA is one of the major groups of C2H2 family. An amino acid sequence is identified in finger domains that are responsive for specific DNA-recognition. TF IIIA zinc finger proteins function in transcription regulation. For example, it has been reported that Zat11 modulates paraquat-induced PCD in *Arabidopsis* (Qureshi *et al.* 2013). Necrotrophic pathogens trigger plants PCD by secreting host-selective *Alternaria alternate* f. sp. *Lycopersici*-toxin (AAL-toxin). AAL-toxin blocks the activity of ceramide synthesis, which is an sphinganine *N*-acyltransferase. This inhibition of ceramide leads to the accumulation of ceramide precursors and depletion of sphingolipids and ultimately cell death. *Alternaria stem canker* (*Asc*) from tomato confers tolerance to AAL-toxin, this gene is homologous to the yeast *longevity assurance gene 1* (*LAG1*) (Brandwagt *et al.* 2000). A knockout *Arabidopsis* mutant *loh2* (LAG one homologue 2) shows sensitivity to AAL-toxin treatment. However, when *ZAT11* was mutated in *loh2* background, plants exhibited an enhanced tolerance to paraquat-induced oxidative stress and PCD triggered by AAL-toxin. Interestingly, an enhanced PCD symptom occurred in a *zat11* T-DNA insertion

mutant, which implies that Zat11 might modulate ROS-induced PCD indirectly (Qureshi *et al.* 2013). However, the interaction between Zat11 and LOH2 is still unclear.

ZAT12, the paralog of *ZAT11*, has been demonstrated to be involved in different stress-and/or pathogen- induced defence activities, including light, oxidative, salinity and temperature (Davletova *et al.* 2005). In oxidative stress-related defence responses, ZAT12 is required for the expression of several defence-related genes (see 1.3.2) (Rizhsky *et al.* 2004). Recent studies suggest that the C2H2 zinc finger proteins may function as repressors during defence- and/or stress-mediated transcription changes. For example, although ZAT12 shows positive regulation of ROS-mediated defence activities, plants that lose ZAT12 function show enhanced tolerance to heat stress, which implies that the role of ZAT12 is to function as a repressor (Davletova *et al.* 2005). Similarly, ZAT10 is a stress-response protein that plays a dual role in plant defence responses. Overexpression of *ZAT10* in *Arabidopsis* increased tolerance to drought, heat, osmotic and slat stresses. Unexpectedly, both *ZAT10* knockout and RNAi knockdown transgenic plants are more tolerate to osmotic and salinity stresses (Mittler *et al.* 2006). It has been known that *ZAT10* overexpression increased expression of *APX1* and *APX2*, which are known to respond to ROS scavenging (Mittler *et al.* 2006). So, ZAT10 might either activate transcription of these genes or suppress the repressors of these genes.

The ethylene-responsive element-binding factor (ERF)-associated amphiphile repression (EAR) domain has been found in the C-terminus of zinc finger proteins that show repression activity (Ciftci-Yilmaz and Mittler 2008). The EAR domain has been demonstrated to be essential for protein repression activity. For example, NIMINI represses the expression of *PR1* (Kazan 2006). Accumulating evidence revealed that the EAR domain of ZAT10 might function in repression of ERFs (Ohta *et al.* 2001). Another oxidative-stress response protein ZAT7 may positively regulate tolerance to salinity, which requires the functional EAR motif (Ciftci-Yilmaz *et al.* 2007). Furthermore, the interaction of ZAT7 with defence-related transcription factor WRKY70 also requires an EAR motif (Ciftci-Yilmaz *et al.* 2007).

The WRKY family is another group of C2H2 zinc finger class. Unlike the TF IIIA group, WRKY family is a group of plant-specific C2H2 zinc finger proteins. The members of WRKY have been implicated in the regulation of plant immune responses (Eulgem and Somssich 2007). The WRKY family contains a large number of TFs that are widely involved in plant immunity. For example, WRKY22 and WRKY29 in *Arabidopsis* have been identified to be involved in the MAPK cascade pathway in PAMP-induced defence responses (Asai *et al.* 2002). WRKY70 is a regulator of the SA-dependent defence pathway. Furthermore, the expression of *NPR1*, the key regulator of SA-mediated SAR, is controlled by an unknown WRKY TF (Yu *et al.* 2001). In addition, the WRKY motif has been identified in several R proteins, which belong to the TIR-NBs-LRR class. For instance, *Arabidopsis* gene *RESISTANCE TO RALSTONIA SOLANACEARUM 1* (*RRS1*) encodes R protein RRS1 (also known as AtWRKY52) that responds to perception of pathogen effector PopP2 and consequently triggers ETI (Deslandes *et al.* 2003). Proteins that contain other types of zinc finger motifs have also been identified to be involved in the plant immune system, such as the CCCH-motif zinc finger protein. For example, HUA 1 has been reported to be involved in disease resistance in rice (Deng *et al.* 2012).

1.3.4 Zinc finger proteins regulate NO induced gene expression in yeast

NO-dependent signal transduction system is a key feature of innate immunity. Zinc finger proteins are prototypic targets for redox regulation. In plants, many zinc finger proteins have been identified to respond to the modulation of defence- and/or stress-induced responses. However, the pathways involved in NO-responses remain unclear. Zinc finger proteins-responsive redox changes are recently emerging as central to redox regulation in yeast. Recent data has implicated a C2H2 zinc finger transcription factor, Fzf1, as a regulator of nitrosative stress in *Saccharomyces cerevisiae* (Sarver and DeRisi 2005). Application of exogenous NO in *S. cerevisiae* results in an increase in both *YHB1* and *SSU1* transcription. *YHB1* is required for protection from nitrosative stress (Liu *et al.* 2000). It is an ortholog of *hmp* (*E. coli* flavohemoglobin protein) that is required for NO detoxification (Gardner *et al.* 1998). *SSU1* encodes a putative transmembrane sulphite efflux transporter that

confers resistance to sulfite stress, and its transcription is controlled by Fzf1 (Avram *et al.* 1999, Park and Bakalinsky 2000). Fzf1 is a key regulator in the nitrosative-dependent response. A strain lacking Fzf1 is compromised in nitrosative-specific transcriptional reprogramming. Oppositely, a gain of function strain exhibited this resistance in the absence of nitrosative stress (Sarver and DeRisi 2005).

Furthermore, a yeast specific zinc cluster protein, CTA4, has been shown to control the responses to NO in *Candida albicans* (Chiranand *et al.* 2008). Unlike Fzf1, CTA4 is a Zn(II)2-Cys6 transcription factor, which belongs to a zinc finger protein family that is unique to fungi. Under nitrosative stress *C. albicans* requires functional CTA4 to induce *Yhb1* expression in order to combat a nitrosative environment. A strain with a deletion of *CTA4* failed to activate *YHB1* transcription, leading to hypersensitivity towards nitrosative stress. This hypersensitive phenotype can be reversed through exogenous expression of *CTA4* or *YHB1*. In addition, *CTA4* also regulates transcription of the NO-inducible gene *SSU1*. However, deletion of *SSU1* does not have an effect on the sensitivity to nitrosative stress in *C. albicans*, which implies that *SSU1* might not function in NO detoxification. Significantly, lack of *CTA4* attenuates virulence of *C. albicans* (Chiranand *et al.* 2008).

1.4 Aims and Objectives

Despite the extensive studies of NO-mediated defence signalling, the mechanisms behind dynamics of NO signalling that lead to the establishment of defence response are still fragmental. The key regulators that respond to NO perception and signal transduction remain to be determined.

A NO-enriched *Arabidopsis* mutant, *nox1,* was isolated (He *et al.* 2004), which provides an effective platform for understanding how NO level regulates plant defence responses. We also aim to identify the proteins that regulate the initiation of NO signalling by establishing NO-reporter transgenic plants. We will explore the potential role of a group of transcriptional factors, which are NO-responsive zinc finger proteins, in the redox regulation of plant immunity.

Chapter 2 Material and methods

2.1 *Arabidopsis* seeds and growth condition

Arabidopsis ecotype Columbia (Col-0) was used. All used *Arabidopsis* mutant strains and transgenic lines were in Col-0 background and are outlined in Table 2-1. Seeds were placed on potting medium consisting of peat moss, vermiculite and sand (4:1:1), and then placed in a growth chamber and grown in long days (16 hours light and 8 hours dark) at 20°C.

For aseptic growth, seeds were sterilised with 10% (v/v) commercial bleach and a drop of Triton-X-100 for 20 minutes, washed 4 times in distilled water and maintained 4 days in the dark at 4ºC to improve germination uniformity. Plants were subsequently transferred to MS plates containing MS basal salts supplemented with 1% (w/v) sucrose and 1% (w/v) agar. Petri dishes were transferred to a growth chamber with 16 hours of light at 22ºC and 8 hours of dark at 18ºC.

Seeds of transgenic plants were sown in flats and selected by spraying a 150 mg/l BASTA solution twice: one was one week after germination; the other was four days later. Resistant plants were visually identified one week after treatment.

Table 2-1 *Arabidopsis* lines and mutant strains

Strains	Description	Source
Col-0	Wild-type	NASC
atgsnor1-1	T-DNA insertion resulting in the activation of the *Atgsnor*	SAIL
atgsnor1-3	T-DNA insertion resulting in the inactivation of the *Atgsnor*	Gabi-Kat
nox1	Point mutation resulting in loss of gene function	SALK
atgsnor1-1 nox1	Double mutant by crossing *atgsnor1-1* and *nox1*	Yun & Loake
atgsnor1-3 nox1	Double mutant by crossing *atgsnor1-3* and *nox1*	Yin & Loake

zat7	T-DNA insertion resulting in the inactivation of the *ZAT7*	SAIL
zat8	T-DNA insertion resulting in the inactivation of the *ZAT8*	JIC
zat16	T-DNA insertion resulting in the inactivation of the *ZAT16*	SAIL
zat12	T-DNA insertion resulting in the inactivation of the *ZAT12*	Gabi-Kat
zat7 zat8	RNAi transgenic	Yin & Loake
W-*zat7 zat8*	RNAi transgenic	Yun & Loake
GFP: ZAT8	*GFP: ZAT8* transgenic	Yin & Loake
P-3G: LUC	*P-3G: LUC* transgenic	Yin & Loake
P-1G: LUC	*P-1G: LUC* transgenic	Yin & Loake

2.1.1 Generation of transgenic lines

2.1.1.1 Generation of NO-reporter line

Transgenic *Arabidopsis* lines expressing *P-3G: LUC* or *P-1G: LUC* were generated by transferring the plant with pGreenII 0229 (John Innes Centre, JIC) (Hellens *et al.* 2000) plant expression vector that contains *P-3G: LUC* or *P-1G: LUC* gene expression cassette. In order to construct the reporter genes, the specific primers were designed with addition of selected restriction enzyme digestion sites on each end of the promoter sequences (Figure 5-3). The promoters regions of *At3g28740* (*P-3G*) and *At1g76600* (*P-1G*) were amplified from the Col-0 genome. *PR1*: *LUC* plasmid (pART27) containing the *LUC* sequence (Promega) and the *ocs* terminator was digested with *Nco* I and *Not* I to remove from vector backbone (Murray *et al.* 2002). The *LUC: TER* fragment were then fused with *P-3G* and *P-1G*, respectively. Subsequently, the products were cloned into pGreenII-0229 that employs a kanamycin (Kan) selection system in *E. coli*. The colonies that survived from Agar (Kan) selection plates contained transferred pGreenII-0229 vector. The selected plasmids were confirmed by digestion with *Eco* RI and *Nco* I and transferred into

Agrobacterium strain GV3101 (Loake lab). The floral dip method was employed for stable transformation. Transformation of female gametes was accomplished by dipping developing *Arabidopsis* inflorescences for 30 seconds into a 5% sucrose solution containing 0.01% (v/v) Silwet L-77 and resuspended *Agrobacterium* cells (Loake lab) carrying the genes to be transferred.

2.1.1.2 Generation of RNAi knockdown line

RNAi lines for the repression of *ZAT7* and *ZAT8* genes were generated by transferring the plant with modified pGreenII 0229 vector containing an inverted sequence repeat to produce a hairpin structure RNA. The sense and antisense fragments were amplified from cDNA library of Col-0 genome. The linear RNAi construct was cloned into modified pGreenII-0229 vector, and subsequently transformed into *E. coli* for antibody selection. The plasmids DNA were extracted from Kan-resistant colonies, and double digestion was applied to confirm the RNAi insertion. The floral dip method was employed for stable transformation as described above.

2.1.2 Nitrosative stress

Arabidopsis seeds were surfaced sterilised as described above for aseptic growth. The seeds were then placed on 1/2 MS agar plates with either 1.5 mM GSNO or 2 mM Cys-NO. The seeds were grown in dark at 22ºC for one week, as GSNO and Cys-NO are light sensitive. The seeds were placed on 1/2 MS plates and incubated at same condition as a control group.

2.2 Transient expression of GFP-fused protein

GFP: ZAT8 construct was generated by gateway cloning system, all procedures followed manufacturer's manual (Invitrogen). The PCR product of *ZAT8* was cloned into pENTR™/D-TOPO (Invitrogen) (Figure 2-1). The subsequent LR recombination reaction involved the attL sites of pENTR recombining with attR site of Destination vector (pK7FWGF2) (Karimi *et al.* 2002) (Figure 2-2) to generate

expression clone. The *GFP: ZAT8* recombinant plasmid was carried by *Agrobacterium* strain AGL1 (Oparka Lab). The *Agrobacteria* culture was then infiltrated directly into tobacco leaves to allow protein expression (Voinnet *et al.* 2003).

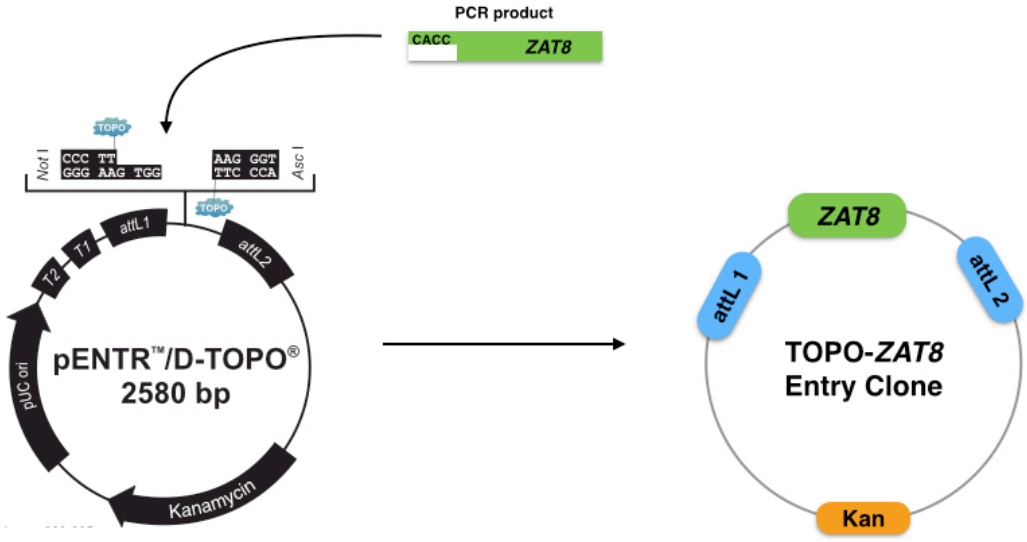

Figure 2-1 pENTR™/D-TOPO vector and TOPO cloning of pENTR™/TOPO-*ZAT8*.

The features of pENTR™/D-TOPO vector. The *rrn*B *T1* and *T2* transcription termination sequence reduces potential toxicity of insertion by preventing basal expression. pUC *ori* promotes replication of *Zat8* in *E. coli*. Kanamycin resistance gene provides selection system. TOPO: topoisomerase I recognition site. The *ZAT8* cDNA with additional "CACC" at 5' end of sequence were amplified by PCR with proofreading polymerase. The 5' *ZAT8* sequence was recognised by the overhang of 5' TOPO® recognition site in pENTR™/D-TOPO vector. The recognition allows insertion was cloned in the correct orientation and subsequently triggered the topoisomerase I.

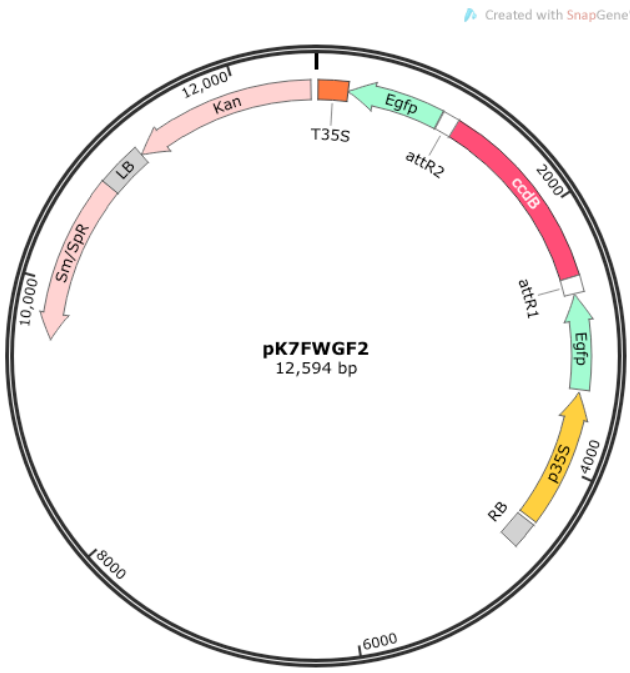

Figure 2-2 The features of GATEWAY™ pK7FWGF2 vector.

The destination vector, pK7FWGF2 consists of two *Egfp* sequences that located at 5' and 3' ends of GATEWAT™ cassette, which includes *att*R1, ccd*B* and *att*R2 orientation. The expression of insertion will be controlled by 35S promoter and terminator. Kan: plant selection marker kanamycin resistant gene. Sm/SpR: bacterial selection system. Spectinomycin resistance gene. LB: left T-DNA border. RB: right T-DNA border.

2.3 Growth of *Pst* DC3000 (*avrB* and *avrRps4*) and inoculation of plants

Pst DC3000 (*avrB* or *avrRps4*) was grown on Kings Broth (KB) supplemented with $MgCl_2$ (6 mM final concentration), 50 mg/l rifampicin and 50 mgl/l kanamycin. Liquid cultures were incubated on a shaker at 30°C at 250 rpm, and cells were harvested at cell density around OD_{600}=0.2 [the equivalent of 10^8 colony forming units per cm^{-2} (cfu/cm^2)] by centrifugation at 4000 g for 5 minutes. Cell pellet was washed and resuspended in 10 mM $MgCl_2$ and the cell density was further adjusted to OD_{600}=0.002 (10^6 cfu/cm^2). The abaxial side of leaves of 4 – 5 weeks old plants were inoculated with 1 ml needleless syringe. Successful inoculations were visualised by the appearance of a watery area under the epidermis (Yun *et al.* 2003).

2.3.1 Trypan blue staining

Leaves (half leaf) after 1 day of inoculation with *Pst* DC3000 (*avrB* or *avrRps4*) (OD_{600}=0.002) were cut out from the plant and boiled in trypan blue solution (containing 2.5 g/l trypan blue, 25% (w/v) lactic acid, 23% (w/v) water saturated phenol, 25% (w/v) glycerol and water) at 100°C for 2 minutes. After cooling, the trypan blue solution was replaced by saturated choral hydrate solution. After 24 hours, the leaves were taken out and mounted onto a microscopic slide (Yun *et al.* 2003).

2.3.2 Electrolyte leakage

Leaves were harvested 10 minutes after inoculation with *Pst* DC3000 (*avrB* or *avrRps4*) at OD_{600}=0.2. Leaf discs of uniform size (0.5 cm^2) were made from leaf samples using a cork border, and washed extensively with water for 10 minutes; and then 10 discs were placed in a clean petri dish with 6 ml distilled water. Each *Arabidopsis* line consisted of 3 replicates, and each replication contained 10 leaf discs. A DiST WP conductivity meter (HANNA instruments) was used to take meter reading every 2 hours (Dellagi *et al.* 1998).

2.3.3 Resistance assay

Three leaves per plant and three plants per line were infected with *Pst* DC3000 (*avrB* or *avrRps4*) (OD_{600}=0.002). Leaves were harvested at 4 days after inoculation. Three leaf discs (0.5 cm^2) from each plant were collected and ground in 500 µl 10 mM $MgCl_2$ solution in a 1.5 ml eppendorf tube. Serial dilutions of bacterial suspension were made and 100 µl of each dilution was spread onto KB plates containing 50 mg/l rifampicin, 50 mg/l kanamycin and $MgCl_2$ (6 mM final concentration). The plates were incubated for 2 days at 30ºC and the number of bacterial colonies for each sample were counted and recorded (Feechan *et al.* 2005).

2.4 Growth condition of *Pst* DC3000 and inoculation of plant

Pst DC3000 was grown in KB liquid media supplemented with 50 mg/l rifampicin and $MgCl_2$ (6 mM final concentration). The liquid culture was incubated and harvested as described above for *Pst* DC300 (*avrB*). Four weeks old plants were infected with a *Pst* DC3000 suspension (OD_{600}=0.0002) in 10 mM $MgCl_2$ by completely infiltrating the abaxial side of the leaf with a 1 ml syringe, as described above for *Pst* DC3000 (*avrB*). The measurements of bacterial growth were carried out as described for *Pst* DC3000 (*avrB*) (Feechan *et al.* 2005).

2.5 Growth of *Blumeria graminis* and inoculation of plants

Wheat power mildew *Blumeria graminis* f. sp. *tritici* (*Bgt*) was maintained on Col-0 plants in the greenhouse. Plants were inoculated via rubbing infection leaves against leaves of plants to be infected. Leaves were collected for SA measurements (0 and 48 hours post-inoculation) (Feechan *et al.* 2005).

2.6 Determination of SA levels

Free and conjugated endogenous SA levels were determined by HPLC analysis, as described previously (Aboul-Soud *et al.* 2004). 200 mg of leaf tissue per sample was collected and promptly frozen in liquid nitrogen. Each sample was then ground in 1.8 ml microtube using a tissue lyser machine, followed by addition of equal volume of 90% methanol and vortexed for 1 minute. The sample was then centrifuged at 1,5000 rpm for 5 minutes and the supernatant was transferred to a new tube. Pellet was resuspended in 1 ml 100% methanol and centrifuged. Two supernatant were pooled together and dried in a speed vacuum centrifuge at medium temperature. Each pellet was then resuspended in 1 ml 5% trichloroacetic acid, followed by the addition of 1 ml ethylacetate: cyclopentane: isopropanol (50:50:1) and vortexed for 1 minute. The organic phase was transferred to a new tube. The aqueous phase was re-extracted with another 1 ml of the 50:50:1 mix and the two supernatant pooled together and evaporated under heat in the vacuum centrifuge. The aqueous phase was then acidified to pH 1 (1 drop of 37% HCl), boiled for half hour to release conjugated SA and extracted with the organic mix twice. The two supernatant were pooled together and dried in the vacuum centrifuge. The residues were dissolved in 200 µl of 50% methanol and filtered through a 0.25 µM filter. The subsequent analysis was carried out by Dr. Yun. The extracts were diluted and introduced into an anion exchange column (Dionex IonPac® AS11) to elute SA. The eluents after column were passed through an anion self-regenerating suppressor (Dionex ASRS® -ULTRA suppressor) that converts NaOH in eluent into water to reduce background signals. The eluents were then sequentially through CD25 conductivity detector, PDA-100 UV-Vis diode array and RF2000 fluorescence detector to generate chromatograms (Aboul-Soud *et al.* 2004).

2.7 Measurement of SNO

Infected leaves of *Arabidopsis* (500 mg) were grinded in liquid nitrogen into fine powder and immediately transferred into a 1.5 ml eppendorf tube. 1 ml of ice-cold extraction buffer (50 mM K_2HPO_4, 50 mM KH_2PO_4 and 1 mM PMSF (Phenylmethanesulfonyl Fluoride)) was added to the leaf powder and dissolved by vortexing. Sample was then centrifuged at 4ºC at 8,000 rpm for 5 minutes. The supernatant was further centrifuged at 4ºC at 15,000 rpm for 20 minutes. The final supernatant containing crude protein extracts was filtered through a MicroBioSpin-6 column (Bio-Red). The protein extracts were then analysed by a chemiluminescence-based assay, and the procedure was carried out by Dr. Yun. During the procedure, protein extracts were injected into reaction chamber containing reducing agent to release NO form SNOs, and then NO released by reducing agent was brought into Sievers nitric oxide analyser. In the analyser, NO reacts with O_3 to produce excited NO_2, which emit light at 600-1800 nm. The light signals are detected by photomultiplier tube (Liu *et al.* 2004).

2.8 Extraction of genomic DNA from *Arabidopsis*

A leaf of *Arabidopsis* plant was grinded in 300 µl of CTAB (Cetyl trimethylammonium bromide) buffer in a 1.5 ml eppendorf tube and incubated at 65ºC for 20 minutes. The plant extract was mixed with 300 µl of chloroform by vortexing vigorously and centrifuged at 1,5000 rpm for 5 minutes. The supernatant was removed and the pellet was washed with 1 ml 70% ethanol. The ethanol was then removed and the pellet was air-dried and dissolved in 50 µl of water (Lukowitz *et al.* 2000).

2.9 Polymerase chain reaction (PCR) based methods

2.9.1 Reverse-transcription (RT)-PCR

Total RNA was extracted from 4 weeks old plants using TRI reagent (Invitrogen) according to the manufacturer's protocol. Omniscript RT Kit (Qiagen) was used for first-strand cDNA synthesis. Two-step RT-PCR was employed. To produce complementary DNA (cDNA): 1 µg RNA was taken into PCR tube and filled up to 14 µl with RNase free water. After denatured at 65ºC for 5 minuets and cooled on ice, 2 µl 10x buffer, 2 µl dNTP mix (5n nmol), 0.8 µl Oligo-dT primer (25 pmol), 0.25 µl Rnase inhibitor (40 units/µl) and 1 µl Ominiscript RT were added into tube and incubated at 37ºC for 1 hour and 70ºC for 5 minuets. To quantify RNA expression, PCR was carried out in following conditions: 1 µl of cDNA, dNTP mix (5 nmol), forward and reverse primer (5 pmol each), 1x buffer, *Taq* polymerase (1 unit) (Promega) at cycle 95ºC (30s), 55ºC (30s) and 72ºC (2 min), and optimized for 22 cycles. Reaction product (10 µl) was taken out to analyse in agarose gel electrophoresis. Primers were designed with Vector NTI.

Table 2-2 Primers used in RT-PCR

Gene	Forward (5' to 3')	Reverse (5' to 3')
PR1	AAGCTCAAGATAGCCCACAAG	CGTTCACATAATTCCCACGAG
NOX1	TCCAGATCTCAACGATGC	GAAGCAAAGGAGTACCTG
At3g28740	CGGCCGCGTAAACTAAACCTACC	CTGTCTCACGTGTTTAGCCTCGTTG
At1g76600	CGGTTGTGACGTTGAATCAG	GCCAATTTAGCTCGACCAGA
At5g42380	CCGGTGAAGAGCTACAAAGC	CAACGTCCTCCGTAAACTCG
Zat7	GGTTGCGAGAAGTGAGGAAA	AACTCCAAGAAATCGTTCTTCC
Zat8	GGTTGCGAGAAGTGAGGAAG	GTCGTCGTCTCCGGTAAAAA
Zat16	TGGTTGCTGAAAGTGATAATCG	ACATCGTTCTTCCCAACTCC
Zat12	ATCAAGTCGACGGTGGATGT	AAACTGTTCTTCCAAGCTCCA

2.9.2 Genotyping PCR

Genotyping PCR was carried out in the following condition: 1 µl genomic DNA, dNTP (5 nmol), forward and reverse primer (5 pmol each), T-DNA insertion Left Border (LB) primer (5 pmol), 1x buffer, *Taq* polymerase (1 unit) (Promega) at cycle 95ºC (30s), 52ºC (30s) and 72ºC (2 min) for 35 cycles. Reaction product (10 µl) was taken out to analyse in agarose gel electrophoresis. The primers were designed by SALK institute genomic analysis laboratory.

Table 2-3 Primers used in genotyping

	Line	Forward (5' to 3')	Reverse (5' to 3')
SAIL line	*atgsnor1-1*	TATATAATGGTTCGACGCATATTT	GTCGGGTCGGGTCGTTAATA
	zat7	TTCAATCGGTGATCATATGGAG	TGGACAAGGATCCAAGAAGTG
	zat16	GTAAAAGGCGGCTTAAGAAGG	GTTCTTCCCAACTCCAATTCC
Gabi-Kat line	*atgsnor1-3*	TATATAATGGTTCGACGCATATTT	CCACCAACACTCTCAACAATC
	zat12	TCTCTTAAGCTACGCGGTGTC	TTGTTTTTATTCGTGATGGGG
JIC SM line	*zat8*	TGACTATCCAACCTAGGAAAAGTTC	TTCATAGATCAAACTTCAAGGGC

Table 2-4 Left border primers of different T-DNA lines

T-DNA lines	Left Border primer	Sequence (5' to 3')
SAIL	SL-LB	TTCATAACCAATCTGGATACA
Gabi-Kat	GK-LB	ATAATAACGCTGCGGACATCTACATTTT
JIC SM	Spm32	TACGAATAAGAGCGTCCATTTTAGAGTGA

2.9.3 PCR for transgenic material

PCR was carried out in the following: 1 µl DNA, dNTP mix (5 nmol), forward and reverse primer (5 pmol each), 1x buffer, *Pfu* proofreading polymerase (1 unit) (Promega) at cycle 95ºC (30s), 55ºC (30s) and 72ºC (2 min) for 35 cycles. *Taq* polymerase (0.5 unit) was added after the PCR reaction and incubated at 72ºC for 10 minutes to add a 3' an overhang for TA cloning purpose. The PCR product was separated in agarose gel electrophoresis and purified in distilled water by a gel extraction kit (Qiagen). Primers below were designed with Vector NTI.

1). *P-3G: LUC*

PCR was used to amplify a 2000 bp promoter fragment (*P-3G*) from Col-0 genomic DNA with *Eco* RI and *Nco* I sites at respective 5' and 3' ends using the following primers:

5' primer 5'-CCACAACGTTGGGAGCTACATCGACTTTCTT-3'
3' primer 5'-CCACAACGTTGGGTATGTTAACGTTAGGATA-3'

The purified PCR product was cloned into pGEM-T Easy (Promega) for amplification and sequencing. Confirmed DNA fragment was then sub-cloned into an expression vector pGreenII-0229 (JIC) through the designed restriction sites and transferred into *Agrobacterium* GV3101 for floral dip purpose. The *P-1G*: *LUC* cassette was generated with same method and the following primers:

5' primer 5'-CCACAACGTTGGAATCATTTATGTTAAATAGA-3'
3' primer 5'-CCACAACGTTGGATATACAGAGTTGGTTCCAGGT-3'

2). RNAi

PCR was used to amplify two desired products from Col-0 cDNA: sense fragment with *Eco* RI and *Xba* I sites, and antisense (plus linking sequence) with *Pst* I and *Xba* I sites at respective 5' and 3' ends using following primers:

Table 2-5 Primers used in RNAi cassette

Sense	**5'**	**3'**
5' primer	GCGGCCGCAACGAGTTTTCCGATGCAAGACTTGTC	
3' primer	TCTAGAAGTTTCTTGTGGCTTGCACGATGACCTC	
Antisense	**5'**	**3'**
5' primer	ACTAGTAACGAGTTTTCCGATGCAAGACTTGTC	
3' primer	TCTAGATTCAAAGTCGTCACCGTCGTCGTCTCCG	

The purified PCR product was cloned into pGEM-T Easy (Promega) for amplification and sequencing. The confirmed DNA fragments were then sub-cloned into a modified pGreenII 0229 (which containing a 35S promoter – terminator cassette) through the designed restriction sites and transferred into *Agrobacterium* GV3101 for floral dip purpose.

3). *GFP: ZAT8*

PCR was used to amplify *ZAT8* cDNA fragment with addition 4 bp (ATAA) immediately adjacent to the start (ATG) using following primers:

5' primer 5'-CACCATGGTTGCGAGAAGTGAGGAAGTT-3'
3' primer 5'-TCAAGAAATCGTTCTTCCCA-3'

This fragment was subsequently cloned into pENTR™/D-TOPO vector (TOPO cloning kit, Life Technology) for sequencing and Gateway Cloning. The confirmed DNA fragments were then cloned into a destination vector (pK7FWGF2) using LR reaction kit (Invitrogen), and this vector was then used to transform *Agrobacterium.*

All the constructs were generated in accordance with manufacturers' instructions.

2.10 Bacterial transformation

2.10.1 Transformation of *E. coli* XL1-blue

A 10 µl aliquot of competent cells (STRATAGENE) was placed on ice and allowed to thaw, and subsequently 1 µl of plasmid DNA was added to the cells. The sample was mixed and incubated on the ice for 30 minutes. The cells were then heat shocked at 42ºC for 60 seconds. The cells were chilled on ice for 2 minutes before 100 µl of pre-warmed LB liquid media added. The sample was incubated at 37ºC, 250 rpm for 1 hour. The total volume of the transformation was added to selective LB medium agar plates and incubated at 37ºC (on inverted plates) until colonies were visible.

2.10.2 Plasmid extraction

Plasmid DNA was extracted using either the QIAprep® Miniprep (Qiagen) or GeneJET™ Plasmid Miniprep Kit (Fermentas) in accordance with the manufacturer's instructions.

2.10.3 Transformation of *Agrobacterium*

A 100 µl of competent cells (Loake lab) was thawed on ice for approximate 1 hour, and 10 µl of plasmid DNA were added to the cells and chilled on ice for a further 5 minutes. The sample was then snap frozen in liquid nitrogen, and immediately incubated at 37ºC for 5 minutes and allowed to thaw. The sample was mixed with 1 ml LB medium and incubated at 28ºC, 250 rpm for 2~4 hours. The cell pellet was then harvested by centrifugation at 8000 rpm for 30 seconds, and resuspended in 100 µl of LB medium. The total volume of the transformation was added to selective LB medium agar plates and incubated at 30ºC (on inverted plates) until colonies were visible.

2.11 Real time imaging of luciferase (LUC) activity

5mM luciferin in 0.01% solution of Triton X-100 was sprayed on the seedlings. And then plants were placed in dark for 20 minutes in order to allow the luciferin to dry and to minimise background bioluminescence. All LUC imaging was detected by using an ultra low light imaging camera system (Berthold, Redbourn, UK). Images were collected over a 30 second time period (Grant *et al.* 2000a).

2.12 GFP fluorescence imaging

5 days after transient expression (2.2), 0.5 cm^2 tobacco leaf disk were cut from infiltration site and imaged using a laser scanning confocal microscope set to 40x optical zoom. The confocal microscope using a Melles Griot Argon Ion and Argon-Krypton lasers mounted on an Olympus IX70 Fluorescence Microscope. The GFP signal was excited with the 488 nm line of an Argon Laser and detected via a 495-540 nm emission filter (Geilfus *et al.* 2014).

Chapter 3 Characterization of the disease phenotype of the NO overproducing mutant (*nox1*)

3.1 Introduction

NO has been emerging as a key signalling molecule in both plant development and immunity (He *et al.* 2004, Yu *et al.* 2012, Wang *et al.* 2013). Formation of SNO is an important route for NO bioactivity and the extent of S-nitrosylation controls the cellular level of SNO formation (Feechan *et al.* 2005). This reversible redox modification is indirectly governed by GSNOR (Liu *et al.* 2001). Through studies of the homologue of animal GSNOR, in *Arabidopsis* mutants, *atgsnor1-1* and *atgsnor1-3,* it has indicated that SNO formation highly influences plant defence responses (Feechan *et al.* 2005). Loss of *Atgsnor* function in *atgsnor1-3* leads to an increased SNO accumulation and enhanced pathogen susceptibility. In contrast, gain of *Atgsnor* function in *atgsnor1-1* reduces SNOs level and results in increased disease resistance in comparison to Col-0 *Arabidopsis* wild type plants. In addition, removal of *Atgsnor*, which disrupts the balance of S-nitrosylation/de-nitrosylation, raises the SNO accumulation and ultimately results in multiple impaired defence modes. These include *R*-gene resistance, basal resistance and SA-dependent signalling (Feechan *et al.* 2005).

In plants, S-nitrosylation has been considered as a major pathway in NO signalling due to the lack of a NO-sensitive sGC. However, the increased SNOs appeared without increased NO burst after attempted pathogen infection in *atgsnor1-3* (Feechan *et al.* 2005), and NO burst has been intensively described during plant defence response (Delledonne *et al.* 1998, Durner *et al.* 1998). Thus, NO and SNO might undertake distinct roles in plant defence responses

An *NO overproducing 1 (nox1)* mutant in *Arabidopsis* has been isolated through an NO-hypersensitive screen. The fast-neutron-mutagenized *Arabidopsis* (Col-0) seeds were screened for seedlings with inhibited root growth under 10 μM SNP, an NO donor. Map-based cloning indicated that *NOX1* is identical to *CUE1* (*chlorophyII a/b*

binding protein (*CAB*) *under-expression 1*), which encodes a chloroplast phosphoenolpyruvate (PEP)/phosphate translator (PPT) (He *et al.* 2004). Identical morphological phenotypes have been revealed in both *nox1* and *cue1*, including small size and pale green leaf with reticulate pattern. Furthermore, *cue1* mutant showed hypersensitivity to SNP and an NO elevation (Streatfield *et al.* 1999, He *et al.* 2004). Therefore, the *nox1* mutant is an NO elevated endogenous platform that provides an effective tool to investigate NO-related plant development and immunity.

Several developmental phenotypes of *nox1* have been reported, but there is no report of the effects of *nox1* on plant immunity (He *et al.* 2004). A possible disease phenotype of *nox1* mutant may extend the understanding of how NO regulates plant immunity. The works herein reported, the enhanced SNO levels and reduced SA accumulations in *nox1* mutant- were examined in response to various pathogens. Together, increased pathogen-induced hypersensitive response (HR) and pathogen susceptibilities were determined in *nox1* plants. In addition, the *atgsnor1-3* plants are included in the experiments as a positive control.

3.2 Results

3.2.1 Pathogen-induced defence signals accumulation

The *atgsnor1-3* line was known to show a significant increase in cellular SNO level upon *Pst* DC3000 challenge, which weakens multiple defence responses (Feechan *et al.* 2005). Moreover, SA has been long recognised as a defence signal molecule in both local and systemic resistances (Uknes *et al.* 1992, Shirasu *et al.* 1997). Reduced SA concentrations in response to pathogens have been demonstrated in the *atgsnor1-3* mutant (Feechan *et al.* 2005). Therefore, SNO concentrations and SA accumulations were determined in the *nox1* mutant in response to several pathogens.

3.2.1.1 Increased SNO concentration in *nox1* mutant

The Col-0 plants are susceptible to bacteria pathogen *Pst* DC3000 (Whalen *et al.* 1991). However, the Col-0 ecotypes are resistant to *Pst* DC3000 expressing the AvrB effector protein, which is recognized by the R protein, RPM1. Ultimately ETI is triggered (Grant *et al.* 2000b). Thus, the given plant lines, Col-0, *atgsnor1-3* and *nox1*, were challenged with *Pst* DC3000 (*avrB*) at 1×10^6 colony forming units (cfu)/ml. In the absence of AvrB, an enhanced initial SNO level was determined in *nox1* plants, which was twice as high as that found in Col-0 plants. After inoculation with *Pst* DC3000 (*avrB*), the SNO concentration increased over time in all lines, but *nox1* plants exhibited enhanced SNO accumulation when compared to Col-0 (Figure 3-1). Statistical analysis of variance (ANOVA, GraphPad Prism 6) suggests that *nox1* plants show significantly enhanced SNO concentrations in comparison with Col-0 (P, Figure 3-1), but is at similar level to that of *atgsnor1-3* mutant (P, Figure 3-1).

In Col-0 plants, the product of *Pst* DC3000 avirulent gene *avrRps4* is recognized by the *R* gene product RPS4, which belongs to a R protein subclass that is distinct from RPM1 (Gassmann *et al.* 1999). The given lines were challenged with *Pst* DC3000 (*avrRps4*) at 1×10^6 cfu per ml, a similar pattern of SNO accumulations was observed in all tested *Arabidopsis* lines (Figure 3-2). The SNO contents in *nox1* mutant were

approximately twice higher than these found in Col-0 plants over 48 hours post inoculation (hpi). The difference between SNO content in *nox1* and Col-0 plants is significant, P, in 0.0001 (Two-Way ANOVA with Tukey's multiple comparisons tests). In contrast, *nox1* mutant exhibited a similar SNO level relative to *atgsnor1-3* plants (P, 0.4839). In addition, the statistical analysis suggested that there was no significant difference between *nox1* and *atgsnor1-3* plants (P, Figure 3-2).

Collectively, *nox1* plants exhibited enhanced SNO levels in comparison with Col-0 plants (Figure 3-1 & Figure 3-2), which might be due to the increased NO production. However, statistical analysis indicated that there is no significant difference in SNO concentration between *nox1* and *atgsnor1-3* mutants. Therefore, it would be worth examining if increased SNO in *nox1* mutant is GSNOR-dependent.

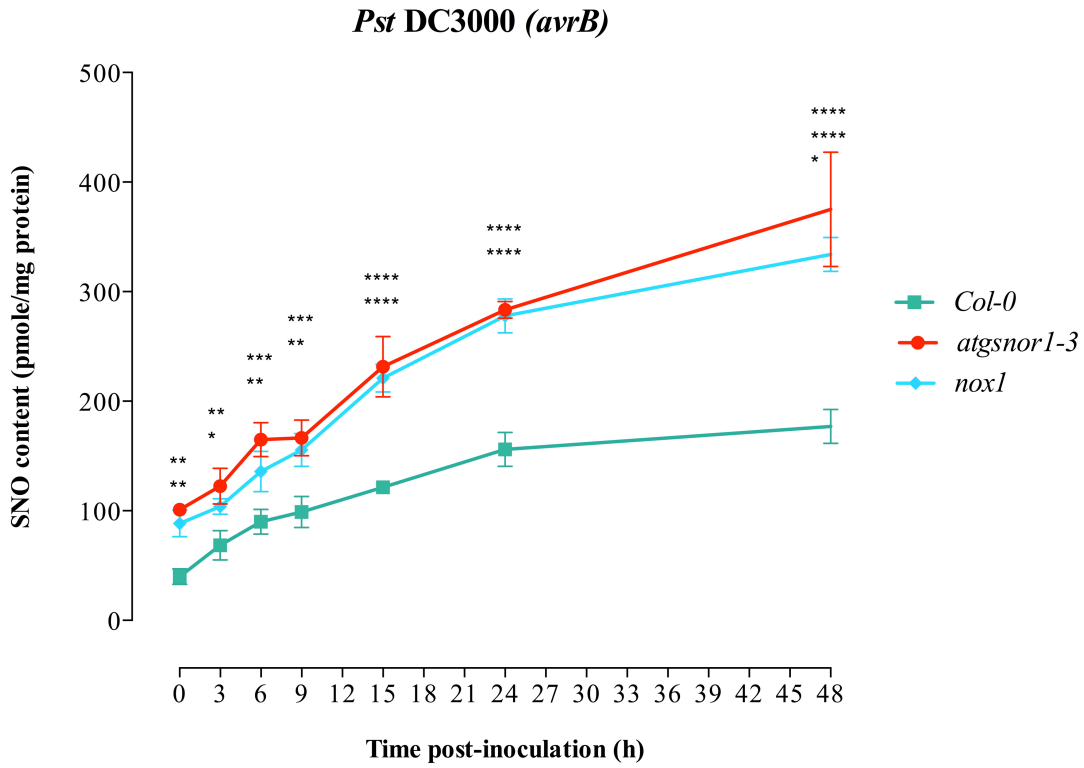

Two-Way ANOVA **Tukey's multiple comparisons test**

	0h		3h		6h		9h		15h		24h		48h	
	Significant	P-value	Significant	P-value	Significant	P-value	Significant	P-value	Significant	P-value	Significant	P-value	Significant	P-value
Col-0 & *atgsnor1-3*	**	0.0013	**	0.0033	***	0.0002	***	0.0006	****	< 0.0001	****	< 0.0001	****	< 0.0001
Col-0 & *nox1*	**	0.007	*	0.0427	**	0.0099	**	0.0023	****	< 0.0001	****	< 0.0001	****	< 0.0001
atgsnor1-3 & *nox1*	ns	0.608	ns	0.3539	ns	0.1021	ns	0.6777	ns	0.7008	ns	0.905	*	0.0199

P-values above are multiplicity adjusted P values. The threshold of family-wise significant is set at 0.05.

Figure 3-1 SNO contents in Col-0 and mutant plants following *Pst* DC3000 (*avrB*) challenge.

Profile of SNO accumulation over time in stated *Arabidopsis* lines following attempted *Pst* DC3000 (*avrB*) inoculation. The total SNO levels were determined in leaf extracts derived from the stated *Arabidopsis* lines. Data points were the mean of 3 replicates ± standard error (S.E). following ANOVA. *Pst* DC3000 (*avrB*) suspension was infiltrated at 1×10^6 colony forming units (cfu)/ml.

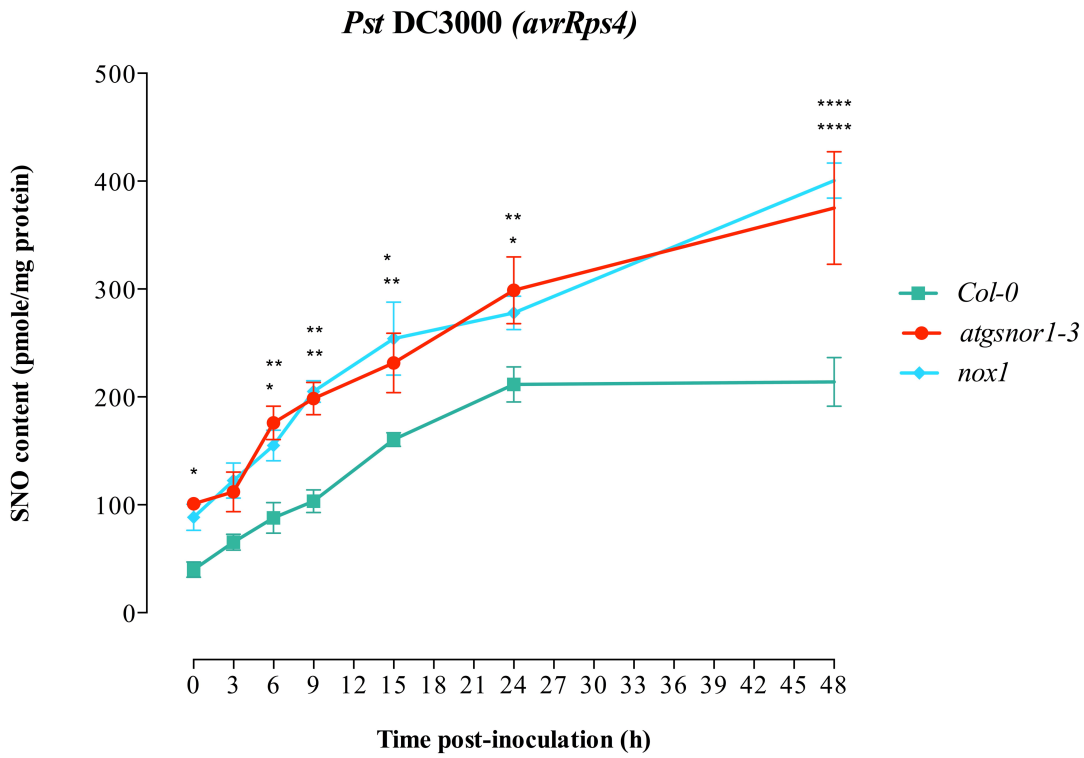

Two-Way ANOVA **Tukey's multiple comparisons test**

	0h		3h		6h		9h		15h		24h		48h	
	Significant	P-value	Significant	P-value	Significant	P-value	Significant	P-value	Significant	P-value	Significant	P-value	Significant	P-value
Col-0 & *atgsnor1-3*	*	0.0373	ns	0.1173	**	0.004	**	0.0022	*	0.0162	**	0.0041	****	< 0.0001
Col-0 & *nox1*	ns	0.1021	ns	0.9405	*	0.0226	**	0.0013	**	0.0025	*	0.0236	****	< 0.0001
atgsnor1-3 & *nox1*	ns	0.8328	ns	0.2001	ns	0.6053	ns	0.9512	ns	0.5639	ns	0.6053	ns	0.4839

P-values above are multiplicity adjusted P values. The threshold of family-wise significant is set at 0.05.

Figure 3-2 SNO profile of *nox1* plants following *Pst* DC3000 (*avrRPS4*) challenge.

Profile of SNO content in the four *Arabidopsis* genotypes stated following challenge with *Pst* DC3000 (*avrRps4*). Data points were the mean of 3 replicates ± standard error (S.E). following ANOVA. *Pst* DC3000 (*avrB*) suspension was infiltrated at 1×10^6 colony forming units (cfu)/ml.

3.2.1.2 Reduced SA accumulation in *nox1* plants

Leaf samples from Col-0, *atgsnor1-3* and *nox1* were collected at 0 and 48 hours after *Pst* DC3000 (*avrB*) inoculation at 1×10^6 cfu/ml. The concentration of total SA from leaf extracts, which consists of free SA and SA-β-glucoside (SAG), was then determined by high-performance liquid chromatography (HPLC) (Feechan *et al.* 2005). A reduced total SA accumulation was detected in *nox1* mutant compared to Col-0 at 0 hpi and 48 hpi (Figure 3-3 A). The total SA determined in *nox1* mutant is less than half that of Col-0. The difference between *nox1* and Col-0 plants at 48 hour post inoculation (hpi) is statistically significant (P, 0.001).

To further explore the role of *NOX1* in defence-related SA signalling, the total SA level was measured in *nox1, atgsnor1-3* and Col-0 plants upon infection with other pathogens, including *Pst* DC3000 (*avrRps4*), *Pst* DC3000 and *Blumeria graminis* f. sp. *tritici* (*Bgt*) (Figure 3-3). As described above, *nox1* plants were infiltrated with *Pst* DC3000 (*avrRps4*) at 1×10^6 cfu/ml. Similar results were obtained relative to AvrB-induced SA accumulation, the total SA in *nox1* mutant was only half of that determined in Col-0 at 48 hpi. The statistics demonstrated that the difference is significant at P, 0.0001.

Reduced level of SA was also detected in *nox1* plants when compared to Col-0 after *Pst* DC3000 inoculation at 1×10^5 cfu/ml (Figure 3-3 C). The statistical analysis showed the difference is significant at P, in 0.025. The SA accumulation was also repressed in *nox1* plants in response to *Bgt* inoculation. The difference between *nox1* and Col-0 plants is statistically significant (P, 0.0008).

Interestingly, *nox1* mutant showed similar SA accumulation as that of *atgsnor1-3* plants in response to both avirulent strains and virulent strain of *Pst* DC3000. The statistics also indicated that there were no significant differences between *nox1* and *atgsnor1-3* plants at both 0 hpi and 48 hpi (P, 0.8381 and 0.1019). However, the difference of SA level between *nox1* and *atgsnor1-3* plants is significant at P in 0.0285 after *Bgt* infection.

Furthermore, the statistical analysis demonstrated that no significant difference between the different bacterial lines in *nox1* mutant background was found (P, 0.99).

The result suggests that enhanced NO production might compromise capability of SA accumulation in *nox1* mutant both during basal resistant and ETI. It is also possible that *nox1* mutant regulates SA accumulation through S-nitrosylation.

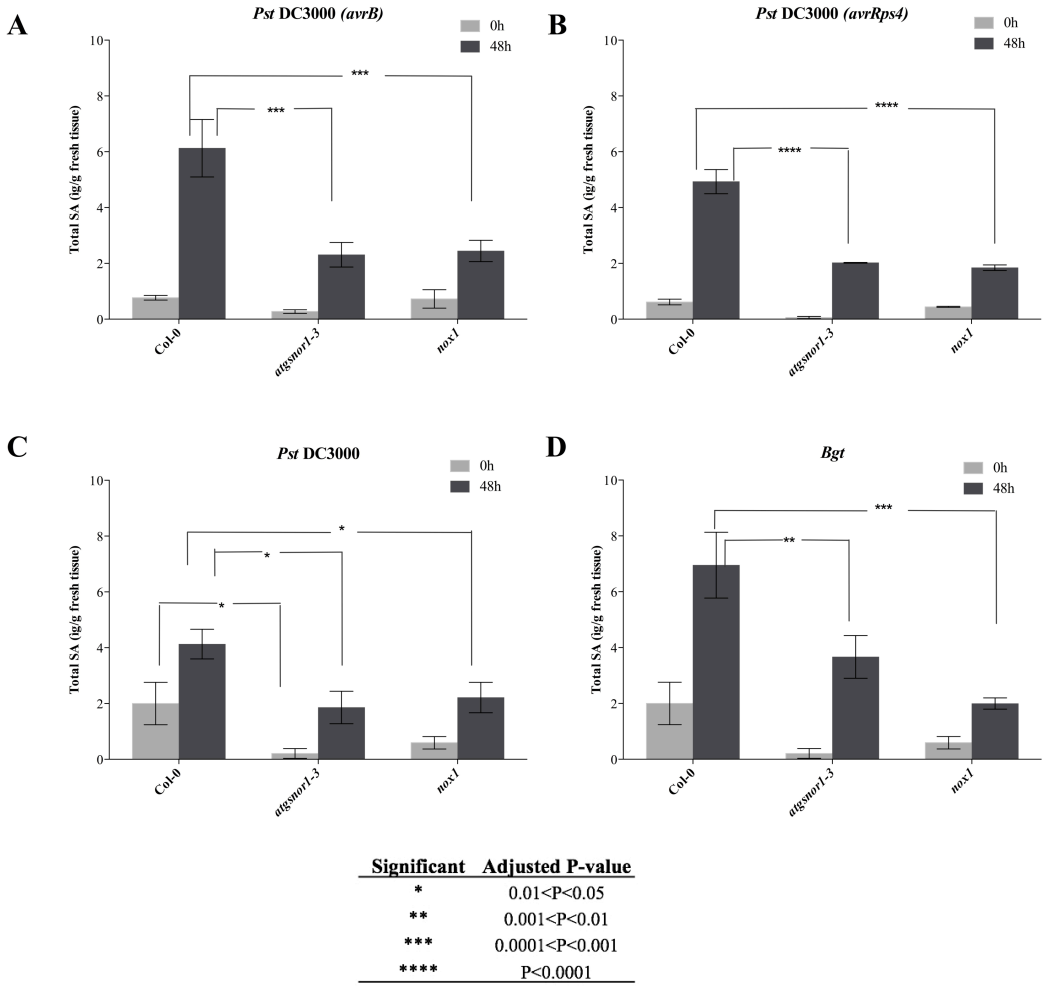

Significant	Adjusted P-value
*	0.01<P<0.05
**	0.001<P<0.01
***	0.0001<P<0.001
****	P<0.0001

P-values above are multiplicity adjusted P values. The threshold of family-wise significant is set at 0.05.

Figure 3-3 Reduced total SA levels were determined in *nox1* mutants in response to various of pathogens.

A. Total SA accumulation in response to attempted *Pst* Dc3000 (*avrB*) at 1 × 10^6 cfu/ml. **B**. Detection of SA accumulations following challenge with *Pst* DC3000 (*avrRps4*) at 1 × 10^6 cfu/ml. **C**. Accumulation of SA upon treatment of *Pst* DC3000 at 1 × 10^5 cfu/ml. **D**. Total SA levels was detected following *Bgt* challenge. Data points are mean of 3 replicates ± S.E. following ANOVA.

3.2.2 Impaired *R* gene-mediated resistance in *nox1* plant

Arabidopsis WT ecotypes express *R* gene-specific resistance against host-specific pathogens, which results in ETI. GSNOR is required for regulating SNO concentration to establish *R* gene-mediated resistance (Feechan *et al.* 2005). In addition, the concentration of SA is remarkably increased during HR (Shirasu *et al.* 1997). The *nox1* mutant revealed an accelerated SNO accumulation and suppressed SA accumulation towards to treatments of various pathogens. In order to explore the possible role of *NOX1* in *R* gene-mediated defence responses, *nox1* plants were infiltrated with *Pst* DC3000 (*avrB*) and *Pst* DC3000 (*avrRps4*), respectively. As a result, *nox1* plants exhibited stronger HR development and enhanced disease susceptibility compared to Col-0 plants in response to both treatments.

3.2.2.1 HR development in response to avirulent *Pst* DC3000 in *nox1* mutant

HR development is the hallmark of *R* gene-mediated resistance. In Col-0, the perception of AvrB by RPM1 leads to HR development at infection sites, which might limit the further spread of pathogens (Grant *et al.* 2000b). HR-induced cell death can be visualised using trypan blue, which specifically stains dead or dying cells blue (Figure 3-4). The Col-0, *atgsnor1-3* and *nox1* plants were challenged with *Pst* DC3000 (*avrB*) at 1×10^7 cfu/ml. As a result, *nox1* and *atgsnor1-3* plants revealed an enhanced HR-induced cell death in comparison with Col-0 (Figure 3-4 A). Furthermore, similar symptoms were observed when infiltrated with *Pst* DC3000 (*avrRps4*) at 1×10^7 cfu/ml, leaves of *nox1* and *atgsnoe1-3* mutants exhibited stronger HR development when compared to Col-0 (Figure 3-4 B). In contrast, there is no difference among Col-0, *atgsnor1-1* and *nox1* plants in response to *Pst* DC3000 infection at 1×10^7 cfu/ml (Figure 3-4 C).

In order to corroborate these findings, HR-responsive cell death in Col-0, *atgsnor1-3* and *nox1* were quantified using cell death-induced electrolyte leakage (Figure 3-5). The initiation of HR starts from a change in ion flux, which involves an efflux of $^-$OH and K^+ out of and an influx of H^+ and Ca^{2+} into cells (Atkinson *et al.* 1996). Therefore, the measurement of electrolyte leakage of leaves following challenge with

pathogens provides an important tool to quantify HR development during the disease resistance. Challenged with *Pst* DC3000 (*avrB*) at 1×10^8 cfu/ml, the electrolyte leakage increased over time in all stated *Arabidopsis* plants. When compared to Col-0, both *nox1* and *atgsnor1-3* mutants showed an accelerated electrolyte leakage (Figure 3-5). In all given lines, there is no significant increase before 4 hpi; however, a substantial raise occurred between 4 hpi and 6 hpi. In addition, the acceleration of electrolyte leakage in Col-0 was slow down after 6 hpi. In contrast, *nox1* exhibited an enhanced acceleration in electrolyte leakage, which is approximately twice higher than that in Col-0 at 24 hpi. The differences between different *Arabidopsis* genotypes are clarified by two-way ANOVA, which is statistically significant at P, in 0.0006 (Figure 3-5). Furthermore, both *nox1* and *atgsnor1-3* mutants show enhanced HR relative to Col-0 and the difference between *nox1* and *atgsnor1-3* is statistically significant.

Similar results were revealed in response to *Pst* DC3000 (*avrRps4*) treatment at 1×10^8 cfu/ml (Figure 3-6). Triggered by AvrRps4, the results of electrolyte leakage showed a significant rise in all stated genotypes after 4 hpi, and the measurements in *nox1* plants were significantly greater than those in Col-0. The difference between different lines is statistically significant at P, 0.0005. In addition, HR development between *nox1* and *atgsnor1-3* plants showed significant difference after 4 hpi. Collectively, increased NO production promotes cell death during ETI, which might regulate HR development through S-nitrosylation.

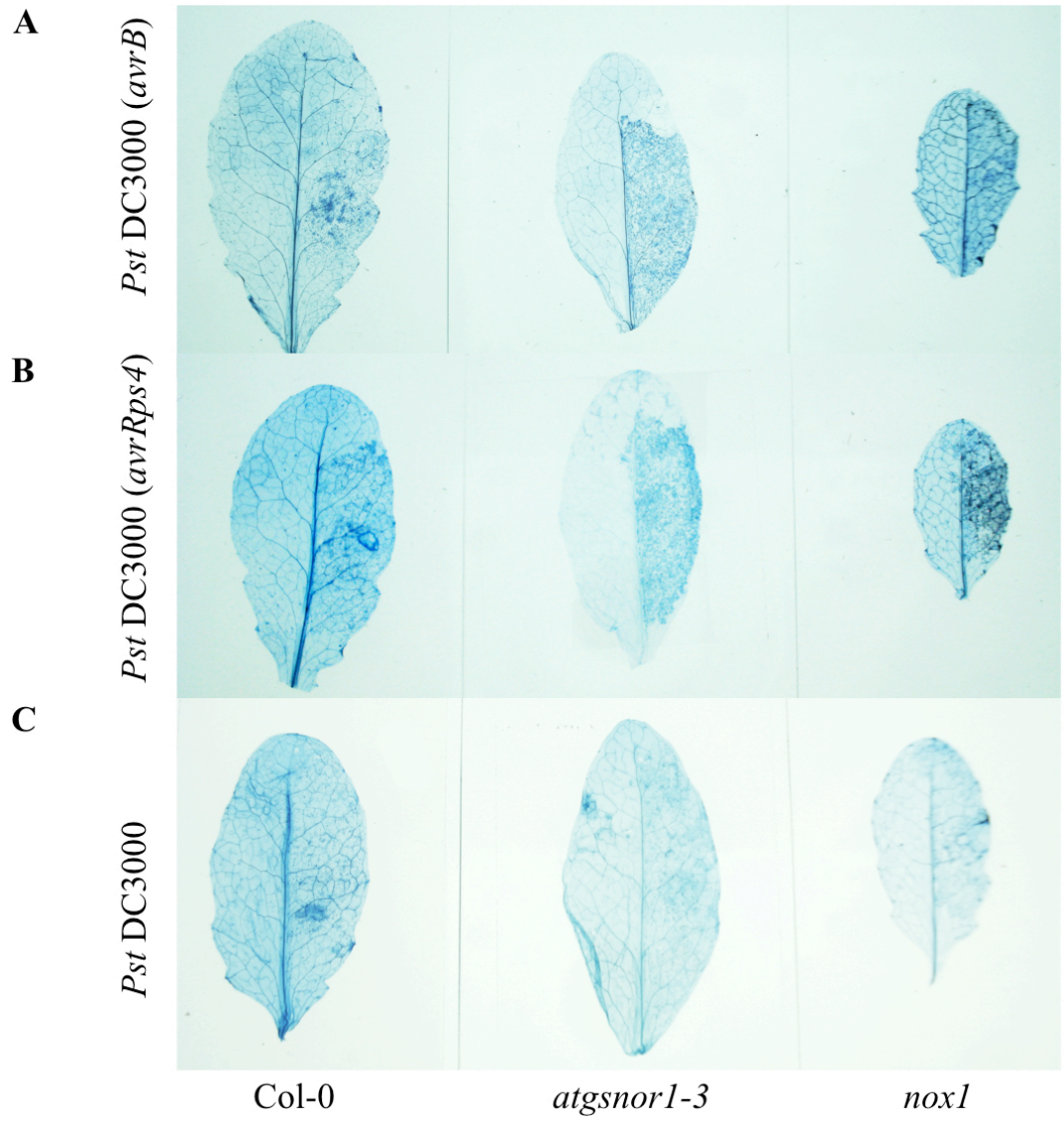

Figure 3-4 HR-induced cell death in Col-0 and mutants upon treatments of various strains of *Pst* DC3000

A. Cell death development in stated *Arabidopsis* genotypes was determined by trypan blue staining upon infection of *Pst* DC3000 (*avrB*) at 1 × 10^7 cfu/ml for 15 hour post inoculation (hpi). **B.** Cell death developments in *Arabidopsis* genotypes was triggered by *Pst* DC3000 (*avrRps4*) at 1 × 10^7 cfu/ml for 15 hpi and scored by trypan blue staining. **C.** Cell death development in the given *Arabidopsis* genotypes, triggered by 1 × 10^7 cfu/ml *Pst* DC3000 at 15 hpi. Only half leaf has been inoculated in all three experiments.

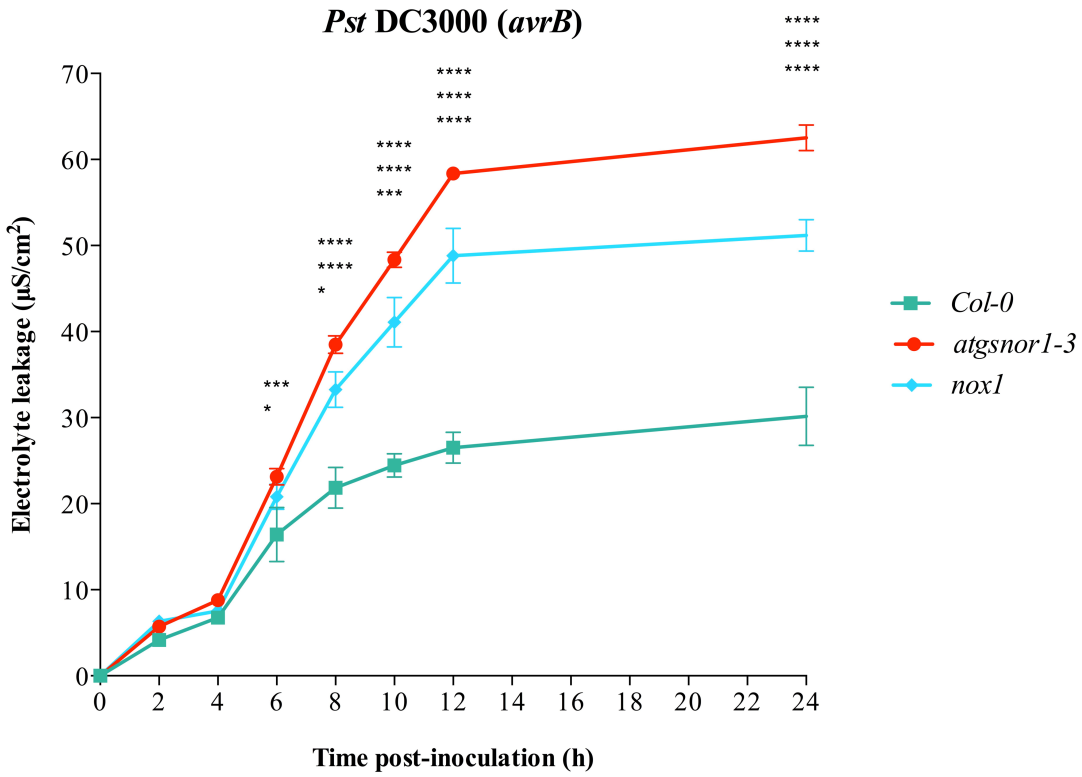

Two-Way ANOVA	Tukey's multiple comparisons test															
	0h		2h		4h		6h		8h		10h		12h		24h	
	Significant	P-value	Significant	P-value	Significant	P-value	Significant	P-value	Significant	P-value	Significant	P-value	Significant	P-value	Significant	P-value
Col-0 & *atgsnor1-3*	ns	> 0.9999	ns	0.5765	ns	0.3954	***	0.0005	****	< 0.0001	****	< 0.0001	****	< 0.0001	****	< 0.0001
Col-0 & *nox1*	ns	> 0.9999	ns	0.355	ns	0.8694	*	0.022	****	< 0.0001	****	< 0.0001	****	< 0.0001	****	< 0.0001
atgsnor1-3 & *nox1*	ns	> 0.9999	ns	0.9203	ns	0.6963	ns	0.299	**	0.006	***	0.0002	****	< 0.0001	****	< 0.0001

P-values above are multiplicity adjusted P values. The threshold of family-wise significant is set at 0.05.

Figure 3-5 Quantification of HR development in *nox1* plants against *Pst* DC3000 (*avrB*).

Quantification of cell death development in given *Arabidopsis* lines following challenge with *Pst* DC3000 (*avrB*). The data points represented the mean of 3 replicates ± S.E. The strains of avirulent *Pst* DC3000 were infiltrated at 1×10^8 cfu/ml. µS/cm^2 (microSiemens per cm^2).

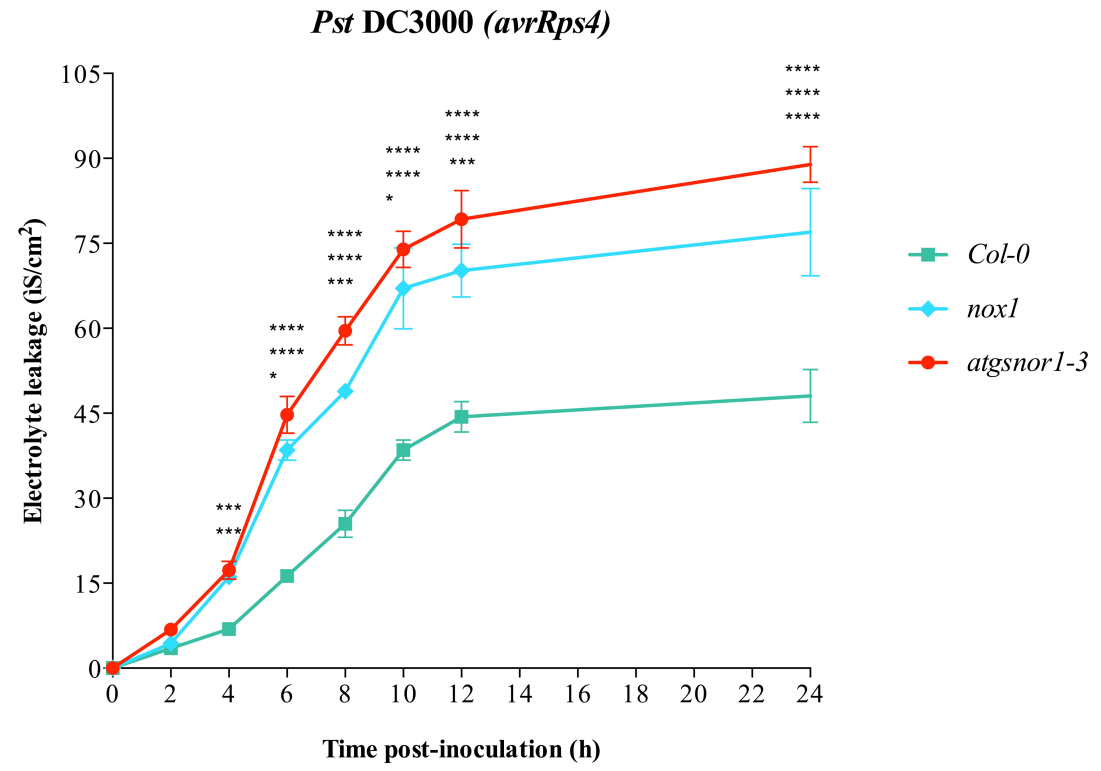

Two-Way ANOVA **Tukey's multiple comparisons test**

	0h		2h		4h		6h		8h		10h		12h		24h	
	Significant	P-value	Significant	P-value	Significant	P-value	Significant	P-value	Significant	P-value	Significant	P-value	Significant	P-value	Significant	P-value
Col-0 & *atgsnor1-3*	ns	> 0.9999	ns	0.3186	***	0.0002	****	< 0.0001	****	< 0.0001	****	< 0.0001	****	< 0.0001	****	< 0.0001
Col-0 & *nox1*	ns	> 0.9999	ns	0.9254	***	0.0008	****	< 0.0001	****	< 0.0001	****	< 0.0001	****	< 0.0001	****	< 0.0001
atgsnor1-3 & *nox1*	ns	> 0.9999	ns	0.5232	ns	0.855	*	0.0234	***	0.0001	*	0.0123	***	0.0009	****	< 0.0001

P-values above are multiplicity adjusted P values. The threshold of family-wise significant is set at 0.05.

Figure 3-6 Avirulent *Pst* DC3000 (*avrRps4*) induced HR in the stated lines.

HR-induced cell death determined by electrolyte leakage in stated lines in response to *Pst* DC3000 (*avrRps4*). The data points represented the mean of 3 replicates ± S.E. The strains of avirulent *Pst* DC3000 were infiltrated at 1×10^8 cfu/ml. μS/cm^2 (microSiemens per cm^2).

3.2.2.2 Enhanced *Pst* DC3000 (*avrB*) susceptibility of *nox1* plants

To determine the possible impact of *nox1* in *R* gene-mediated immune responses, the growth of avirulent pathogens were measured within infiltrated leaves. *nox1*, *atgsnor1-3* and Col-0 plants were challenged with *Pst* DC3000 (*avrB*) at 1×10^6 cfu/ml, and leaf extracts were collected at 4 days post inoculation (dpi). The leaf extracts were diluted and spread on agar plates. The growth of bacteria was quantified by counting the number of colonies on the agar plates. The *atgsnor1-3* mutant is known to be susceptible to *Pst* DC3000 expressing either *avrB* or *avrRps4* (Feechan *et al.* 2005).

In response to *Pst* DC3000 (*avrB*) infection, both *nox1* and *atgsnor1-3* lines showed enhanced bacterial susceptibilities relative to Col-0 (Figure 3-7 A). ANOVA was applied to verify the reliability of the result. The difference between *nox1* and Col-0 plants is statistically significant (P, 0.0029), In contrast, statistical analysis demonstrated there is no significant difference (P, 0.5098) between *nox1* and *atgsnor1-3* mutants.

Furthermore, increased bacterial susceptibilities were determined in *nox1* and *atgsnor1-3* mutants upon treatment of *Pst* DC3000 (*avrRps4*) when compared to Col-0 (Figure 3-7 B). The statistical results showed that difference between *nox1* and Col-0 plants is significant at P, in 0.0007. Conversely, the bacterial susceptibility in the *nox1* mutant was indistinguishable from that of *atgsnor1-3* line, because the difference is not statically significant (P, 0.5038).

The results suggest that *R*-gene mediated resistance is compromised in *nox1* plants relative to Col-0, which might be due to enhanced NO production.

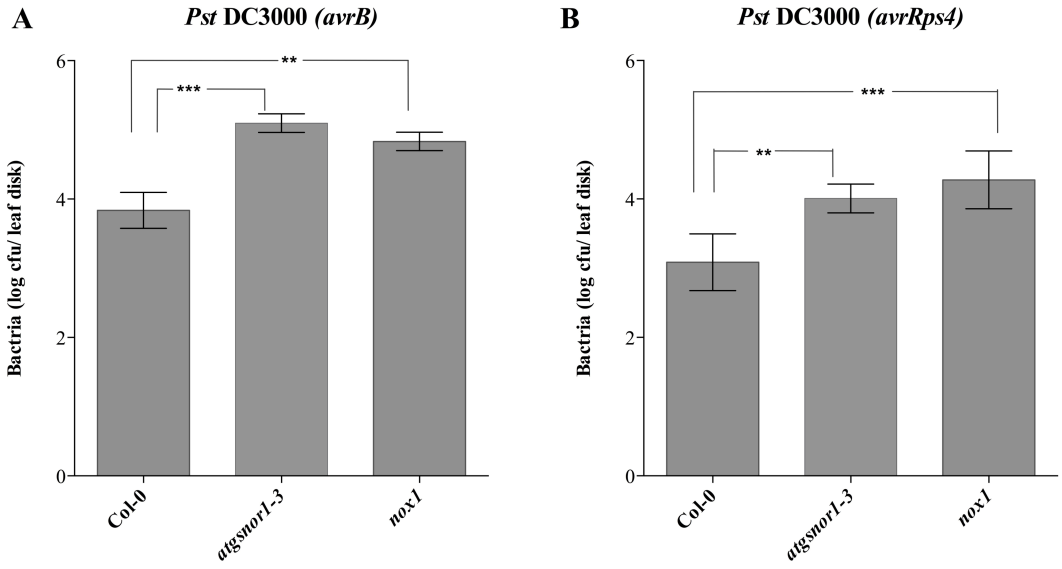

Two-Way ANOVA	Tukey's multiple comparisons test			
	Pst DC3000 (*avrB*)		*Pst* DC3000 (*avrRps4*)	
	Significant	P-value	Significant	P-value
Col-0 & *atgsn*	***	0.0004	**	0.005
Col-0 & *nox1*	**	0.0029	***	0.0007
atgsnor1-3 &	ns	0.5098	ns	0.5038

P-values above are multiplicity adjusted P values. The threshold of family-wise significant is set at 0.05.

Figure 3-7 Pathogenicity test in *nox1* plants upon infiltration of avirulent strains of *Pst* DC3000.

A. Growth of *Pst* DC3000 (*avrB*) at 4 dpi in the leaves of stated genotypes. **B.** Number of *Pst* DC3000 (*avrRps4*) colonies recorded by inoculated leaf extracts in all given lines upon 4 dpi. The data proposed the mean of 3 replicates ± S.E. The strains of *Pst* DC3000 were infiltrated at 1×10^6 cfu/ml.

3.2.3 Impact of *NOX1* in basal resistance

Pst DC3000 is virulent on Col-0 ecotype and results in the development of disease symptoms (Whalen *et al.* 1991). *Arabidopsis* expressing basal resistance confers ability to limit the growth of virulent pathogens (Glazebrook *et al.* 1996). However, the basal resistance is substantially compromised in *atgsnor1-3* line (Feechan *et al.* 2005). Herein, we explored that NO overproduction influences the development of basal resistance by challenging *nox1* with *Pst* DC3000.

Upon infiltration of *Pst* DC3000, the difference in susceptibility between different plant lines was reflected by the leaf appearance 4 days after infection (dpi) (Figure 3-8 A). However, *nox1* and Col-0 plants showed similar level of leaf chlorosis, alongside *atgsnor1-3* mutant showed relatively stronger leaf chlorosis. This result implies that basal resistance might not be compromised in *nox1* background relative to Col-0. To investigate basal resistance in *nox1* mutant, the 4 dpi leaf extracts were collected from stated lines to quantify the bacterial growth on agar plates (Figure 3-8 B). As a result, an increased susceptibility was determined in *nox1* plants when compared to Col-0 line; however, the difference is not statistically significant (P, 0.0563). In contrast, statistical analysis indicated that *atgsnor1-3* mutant showed significant increased susceptibility relative to Col-0 (P, 0.0099).

Interestingly, the pathogen susceptibility in *nox1* mutant is at similar level as that found in *atgsnor1-3* line, and difference is not statistically significant (P, 0.3498). Therefore, basal resistance might be defected in *nox1* plants against *Pst* DC3000 when compared to Col-0, but *nox1* mutant also showed more resistance to *Pst* DC3000 relative to *atgsnor1-3* line. The findings also suggest that over producing NO might weaken plant basal resistance by regulating S-nitrosylation, but not as strong as that of *atgsnor1-3*.

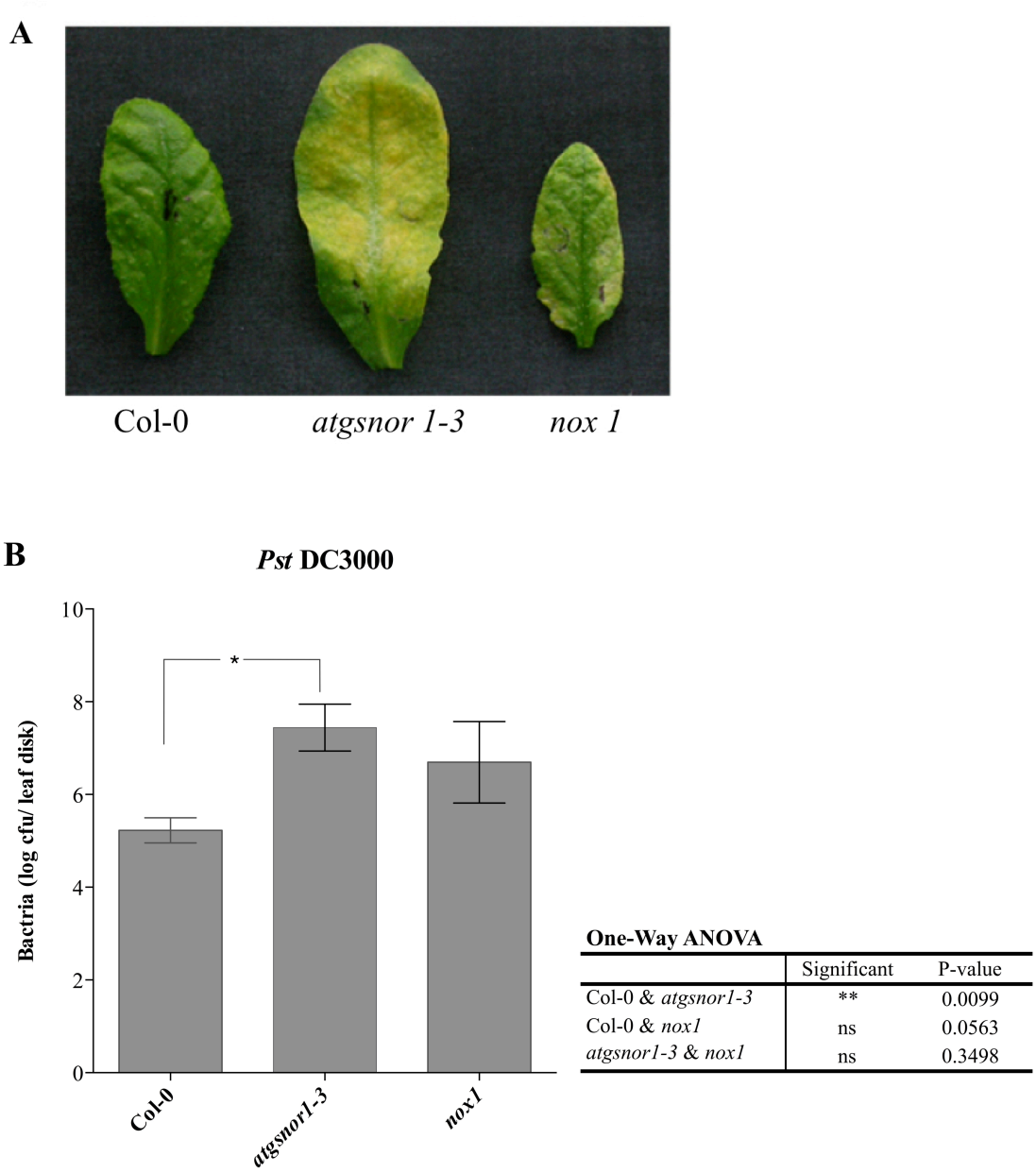

Figure 3-8 Pathogenicity test in *nox1* and *atgsnor1-3* mutants upon infiltration of *Pst* DC3000.

A. Appearance of leaves after 4 days of infiltration with *Pst* DC3000 at 1 × 10^5 cfu/ml. **B.** Number of colonies recorded upon 4 dpi towards *Pst* DC3000 at 1 × 10^5 cfu/ml. The data represented the average of 3 replicates ± S.E. *Psp* (NPS1125) infiltrated at 1 × 10^6 cfu/ml.

3.3 Discussion

It has been found that *nox1* contains a substantially high concentration of L-Arginine and L-Citrulline, which suggests that an enhanced endogenous NO in the *nox1* mutant might be due to an iNOS-like NO synthesis activity. Although the phenomenon of a pathogen-triggered NO burst has been extensively described in plants (Delledonne *et al.* 1998), NOS enzymes, which are structurally related to these found in animals, have not been identified in higher plants (Qiao *et al.* 2009). Herein, we report defence-related phenotypes of *nox1* mutant, which include key aspects of NO signalling not previously demonstrated.

A pool of GSH exists in plants and it is rapidly oxidized by NO to form GSNO. GSNO is a low molecular weight tripeptide considered as a stabilised reservoir of NO, which can be reduced by GSNOR into GSSG and NH_3 (Leterrier *et al.* 2011). GSSG can be recycled back to the GSH pool through further reduction. Thus, a GSNOR-regulated reversible mechanism of NO bioactivity underlies NO signalling. GSNOR has been demonstrated to control the global SNO content, which is a key regulator of multiple plant defences (Feechan *et al.* 2005).

It has been reported that SNO formation can be altered by challenging with *Pst* DC3000 (*avrB*) (Feechan *et al.* 2005). Total SNO concentrations were determined in *nox1* plants following infiltration of *Pst* DC3000 (*avrB*) and *Pst* DC3000 (*avrRps4*), respectively. As expected, the *nox1* mutant exhibited higher initial SNO concentration and accelerated SNO accumulation in comparison with Col-0. However, the level of SNO concentration and accumulation in *nox1* plants were similar to these found in *atgsnor1-3* mutant. Thus, it is reasonable to presume that overproducing NO increased SNO level that might influence the defence response in *nox1* mutant.

Therefore, the activity of *R* gene-mediated resistance was examined in the *nox1* line by HR development and pathogenicity testing. HR is a hallmark of ETI and acts to prevent the pathogen from spreading into distal healthy tissue (Greenberg *et al.* 1994). Inoculation of avirulent strains of *Pst* DC3000 result in cell death by HR (CDHR) in *nox1* plants (Figure 3-5 & Figure 3-6). The AtrbohD produces ROI to

activate HR in *R*-gene mediated resistance. However, its activity is repressed in *nox1* mutant. In addition, S-nitrosylation of AtrbohD at Cys890 might impede its capability to bind with FAD (Yun *et al.* 2011). Hence, ROI production might be blocked in *nox1* and *atgsnor1-3* mutants due to the S-nitrosylation of AtrbohD, which implies that the cell death formation is ROI-independent, but might be promoted by increased SNO concentration in *nox1* and *atgsnor1-3* plants. Moreover, the accumulation of SA, another activator for cell death, is repressed in *nox1* plants, alongside the CDHR is increased in *nox1* and *atgsnor1-3* relative to Col-0 line. It is known that S-nitrosylation of SA-binding protein, such as AtSABP3, results in repression of SA signalling (Wang *et al.* 2009) Therefore, it is reasonable to presume that ROI and SA mediated HR development pathway might be blocked in *nox1* and *atgsnor1-3* backgrounds, and instead, a SNO-mediated pathway might be responsible for HR development during ETI, but the mechanism behind SNO-promoted HR development is unknown.

Furthermore, the growths of *Pst* DC3000 (*avrB*) and (*avrRps4*) were enhanced in *nox1* when compared to Col-0. However, the bacterial titres were statistically similar between *nox1* and *atgsnor1-3* mutants. The results suggest that overproducing NO compromise *R*-gene mediated resistance, which might be GSNO-dependent.

In order to examine the impact of basal resistance in *nox1*, the *nox1* line was infiltrated with *Pst* DC3000 (Figure 3-8). Similar to the *atgsnor1-3* plants, basal resistance was defected in *nox1* mutant during pathogenicity test, suggesting the mechanism might be GSNO-related.

SA has long been known as a signal molecule that is involved in both local and systemic defence response (Vernooij *et al.* 1994). The accumulation of SA is reduced in *nox1* plants in response to various pathogens, such as *Pst* DC3000 (*avrB*), *Pst* DC3000 (*avrRps4*), *Pst* DC3000 and *Bgt*. GSNOR-regulated SNO content impacts the SA-signalling pathway. In the absence of *Atgsnor*, SA accumulation is repressed upon *Pst* DC3000 (*avrB*) infection. In addition, accumulation of *PR1* transcripts is substantially reduced and delayed in *atgsnor1-3* in response to both non-specific and specific pathogens, which cannot be restored by infiltration of exogenous SA. The change in SA concentration leads to *PR* gene expression, which, in turn, results in

immune activities (Tada *et al.* 2008). Thus, the evidence indicated that GSNOR positively regulates the SA signalling network both upstream and downstream of SA (Feechan *et al.* 2005).

Furthermore, the *Arabidopsis* SA-binding protein, AtSABP3 represses SA signalling through S-nitrosylation. However, the loss of function mutant, *atsabp3*, exhibited enhanced pathogen growth when compared with Col-0, which suggested that AtSABP3 is required for a negative feedback loop of SA-signalling in the defence response (Wang *et al.* 2009). Collectively, it is reasonable to assume that SA accumulation and SA-mediated signalling transduction might be blunted in *nox1* plants through S-nitrosylation, consequently, resulting in defect of *R*-gene and basal resistance.

In conclusion, the compromised defence immunity of *nox1* plants might be due to increased protein S-nitrosylation. There are similar results that SNO concentration, SA accumulation and pathogen susceptibility were observed in *nox1* relative to *atgsnor1-3* plants, and hence, GSNOR might be related. However, in order to verify this hypothesis, further experiments are required. For instance, the *nox1 atgsnor1-3* double mutants are generated and being characterised. In addition, as one of the key defence signals, it is reasonable to further investigate the SA-signalling in *nox1* plants, and several key regulators of SA-pathway will be examined. These include the change of transcripts of *PR1*, activity of NPR1 and TGA1, together with accumulation and activity of AtSAP3 in *nox1* plants against pathogen attack. The resulting findings will further clarify possible mechanisms underpin NO-regulated defence response.

Chapter 4 Construction of *atgsnor1-3 nox1* plants

4.1 Introduction

Previous findings suggest that *nox1* plants exhibit increased SNO content and accelerated HR symptoms after infection with *Pst* DC3000 (*avrB*). Furthermore, decreased SA accumulation and defected ETI against avirulent *Pst* DC3000 were observed. As a result, *nox1* plants displayed promoted disease development relative to Col-0, which may be due to the elevation of GSNO caused by excessive NO production.

GSNOR has been shown to control the global level of S-nitrosylation *in vivo*, which plays a key role in the establishment of plant defence activities (Feechan *et al.* 2005). It has been demonstrated that GSNOR is highly specific for the metabolism of GSNO (Liu *et al.* 2001). In comparison with the *nox1* line, *atgsnor1-3* showed stronger HR symptoms and enhanced pathogen susceptibility. However, the statistical analysis indicated that there was no significant difference between these two lines. In order to dissect NO signalling in the establishment of defence responses and investigate whether the disease phenotype of *nox1* plants is GSNO-dependent or -independent, *atgsnor1-3* and *nox1* single mutants were crossed to generate the *atgsnor1-3 nox1* double mutant.

Interestingly, the results implicated that NO and GSNO function additively to alter developmental phenotypes and enhance pathogen susceptibility.

4.2 Results

4.2.1 Identification of the *atgsnor1-3 nox1* double mutant

The single mutants *nox1* and *atgsnor1-3* were crossed to generate the double mutant. *atgsnor1-3* was used as the pollen donor to *nox1*. Therefore, the next generation will acquire the *Atgsnor* insertion as well as sulfadiazine resistance from the T-DNA insertion located in *atgsnor1-3*. The *atgsnor1-3* and *nox1* heterozygous plants (F1 progeny) were screened on an agar plate supplemented with sulfadiazine. The resulting sulfadiazine resistance plants were transplanted into soil and allowed to set seed. The seeds were collected from each F1 individual candidate and grown into F2 progeny plants, which were then further verified by genotyping PCR. In order to confirm the presence of T-DNA insertion in F2 plants, PCR was performed using two gene specific primers and one T-DNA left border primer. A size of 1.2 Kb PCR product was amplified with Col-0 genomic DNA, whereas a 650 bp fragment was produced with DNA from homozygous *atgsnor1-3* plants and both bands were found in PCR products from heterozygous plants (Figure 4-1). Progeny from homozygous plants were then verified by PCR to confirm that this double mutant (*atgsnor1-3 nox1*) was homozygous for the *Atgsnor* insertion (Figure 4-2). The genotyping PCR of *nox1* mutation in *atgsnor1-3 nox1* candidates was not performed because *nox1* is a recessive mutant. However, *nox1* is a point mutation at TRP 54, which changes TRP codon (TGG) into a stop codon (TGA). Therefore, the identification of *nox1* in F2 and F3 candidates were confirmed by DNA sequencing (Figure 4-3).

The phenotypic characterization of F3 progeny plants showed phenotypes of both *nox1* and *atgsnor1-3* single mutants (Figure 4-4 A). For instance, reduced size of rosettes and pale green leaves and the reticular pattern of the *nox1* single mutant were all found in *atgsnor1-3 nox1* double mutants. Furthermore, *atgsnor1-3 nox1* double mutants possessed curly leaves, loss of apical dominance and reduced fertility as seen in *atgsnor1-3* plants. Collectively, the *atgsnor1-3 nox1* double mutant phenotypes suggest that GSNO and/or SNO content is important during vegetative and reproductive development. Mutations in *Atgsnor* lead to a further reduction of

fertility in comparison with the *nox1* single mutant. In addition, *nox1*-related phenotypes might be, at least partially, due to the limitation of shikimate pathway because of a defect in a chloroplast phosphoenolpyruvate (PEP)/phosphate translator (PPT) (Voll *et al.* 2003).

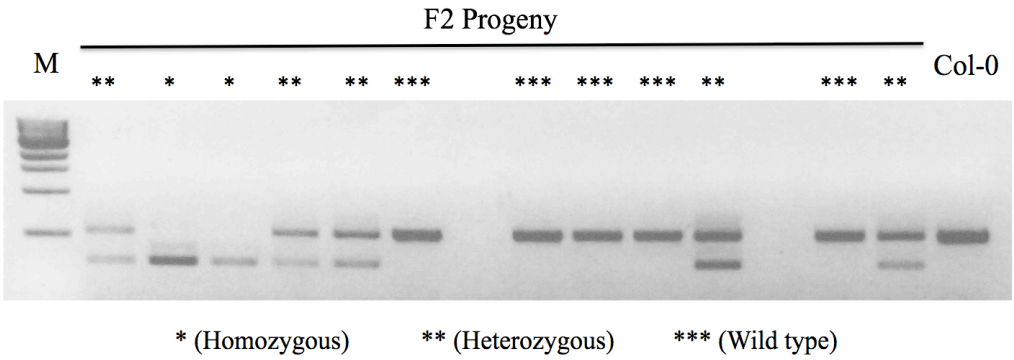

Figure 4-1 Identification of the T-DNA insertion in F2 progeny plants by PCR.

PCR with two gene specific primers and one T-DNA left border primer were used to identify the T-DNA insertion in an F2 segregating population. Homozygous knock-out (*) mutants were identified and allowed to set seed.

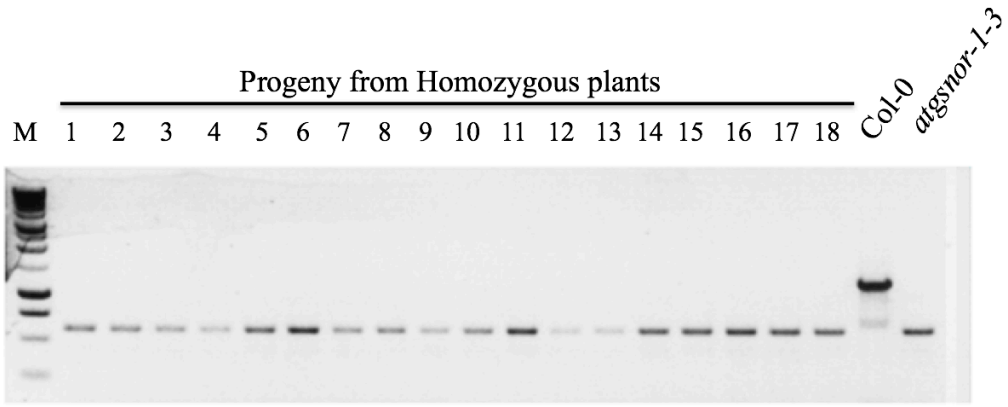

Figure 4-2 Confirmation of *atgsnor* homozygosity in *atgsnor1-3 nox1* by PCR.

Progeny of the *atgsnor1-3 nox1* F2 progeny (*) were confirmed as homozygous for the T-DNA insertion in *Atgsnor*.

Figure 4-3 Confirmation of *nox1* mutation in *atgsnor1-3 nox1* mutant

The DNA fragments were amplified from genomic DNA of *atgsnor1-3 nox1*, *nox1* and Col-0. The resulting fragments were sequenced to confirm the point of mutation.

Figure 4-4 The phenotype of *atgsnor1-3 nox1* mutants (4 weeks old plants).

A. Additive phenotypes in *atgsnor1-3 nox1* plants. The *Arabidopsis* rosettes are about 45 millimetres (mm) in diameter. The largest leaves are approximately 7 mm across and 13 mm long. **B.** In the *atgsnor1-3* mutant, rosettes are about 85-90 mm in diameter. Scale indicted larger leaves are approximately 18-19 mm across and 35 mm long. **C.** The phenotypes of *nox1*. The largest leaves are about 10 mm across and 19.5 mm long; the rosettes are 50-51 mm in diameter.

4.2.2 Defence-related phenotypes of *atgsnor1-3 nox1* double mutants

The *atgsnor1-3 nox1* double mutant is expected to have constitutive NO accumulation and abolished GSNOR activity. To investigate if NO and GSNO play mutual or distinctive roles in manipulation of plant immune systems, their defence-related phenotypes were determined.

4.2.2.1 HR is accelerated in *atgsnor1-3 nox1* double mutant plants

Previously we determined that *nox1* plants have enhanced HR symptoms, which is similar to that of *atgsnor1-3*. Therefore, the HR was investigated in the *atgsnor1-3 nox1* double mutant. Following infiltration of *Pst* DC3000 (*avrB*) the development of HR was performed in Col-0, *atgsnor1-3, nox1* and *atgsnor1-3 nox1* plants. Cell death was visible in *nox1, atgsnor1-3* and double mutant lines after 24 hpi relative to Col-0, with more cell death in double mutant plants (Figure 4-5). To clarify the impact of HR in these double mutants, cell death was quantified by using electrolyte leakage measurements following inoculation with *Pst* DC3000 (*avrB*) (Figure 4-6).

Application of *Pst* DC3000 (*avrB*) triggers HR-induced cell death, this was examined in all given lines from 2 hpi. In Fig 4-6, the *atgsnor1-3 nox1* double mutant showed strong enhanced HR development in comparison with other tested lines. The difference between double mutant and Col-0 is statistically significant (P, 0.0001). Statistical analysis indicated that *atgsnor1-3 nox1* only showed significant difference relative to *atgsnor1-3* at 2 hpi (P, 0.018) and 4 hpi (P, 0.0085) within 10 hours after inoculation. In addition, the difference between *nox1* and *atgsnor1-3 nox1* is statistically significant after 4 hpi (P, 0.0058).

These results suggest that removal of both GSNOR and NOX1 function leads to an acceleration of HR relative to both parental plants. Thus, the phenotypes of *nox1* and *gsnor1-3* are additive in the context of the kinetics of HR development caused by *Pst* DC3000 (*avrB*).

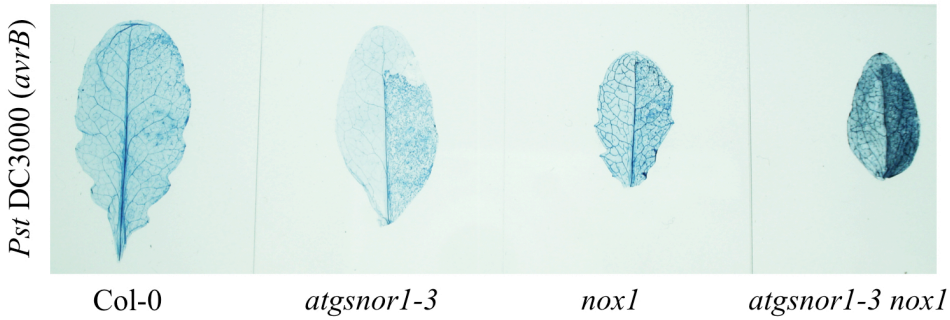

Figure 4-5 *Pst* DC3000 (*avrB*) induced cell death in all given lines.

Cell death development in stead *Arabidopsis* genotypes was determined by trypan blue staining upon infection of *Pst* DC3000 (*avrB*) at 1 × 10^7 cfu/ml for 24 hpi**.**

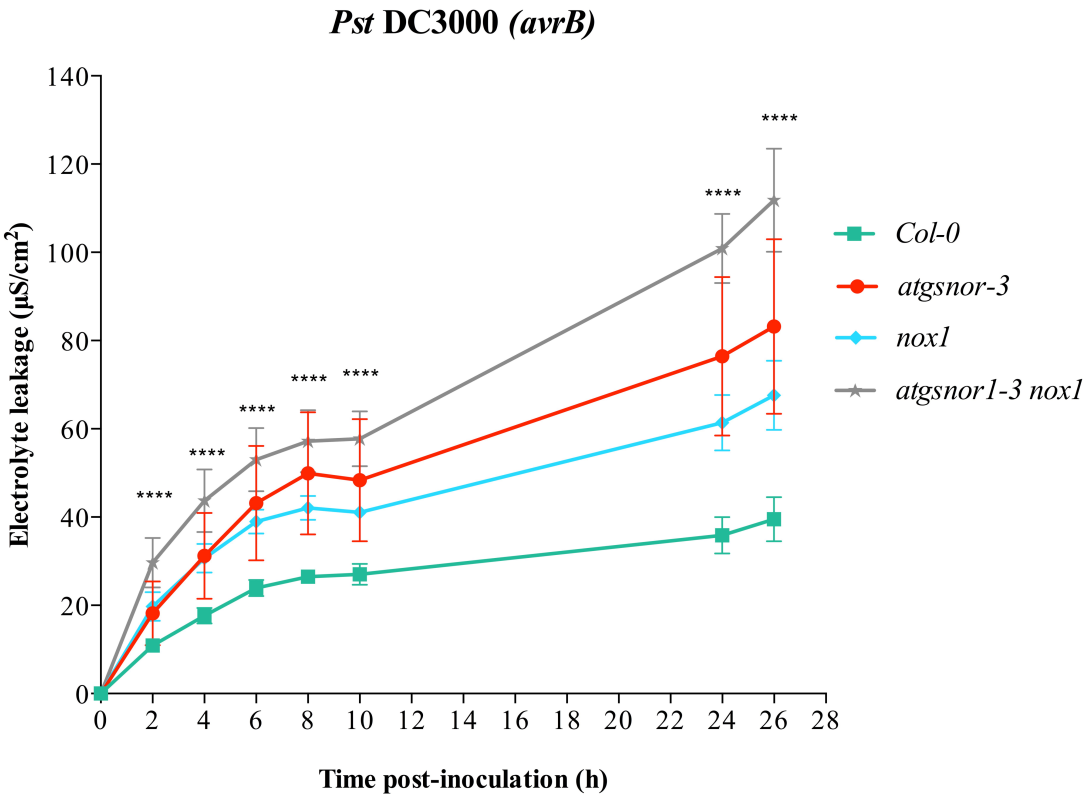

Two-Way ANOVA	Tukey's multiple comparisons test							
	0h		2h		4h		6h	
	Significant	P-value	Significant	P-value	Significant	P-value	Significant	P-value
Col-0 & *atgsnor1-3*	ns	> 0.9999	ns	0.2176	**	0.0039	****	< 0.0001
Col-0 & *nox1*	ns	> 0.9999	ns	0.0955	**	0.0058	**	0.0011
Col-0 & double	ns	> 0.9999	****	< 0.0001	****	< 0.0001	****	< 0.0001
atgsnor1-3 & *nox1*	ns	> 0.9999	ns	0.9746	ns	0.999	ns	0.6777
atgsnor1-3 & double	ns	> 0.9999	*	0.018	**	0.0085	ns	0.051
nox1 & double	ns	> 0.9999	ns	0.051	**	0.0058	**	0.0026
	8h		10h		24h		26h	
	Significant	P-value	Significant	P-value	Significant	P-value	Significant	P-value
Col-0 & *atgsnor1-3*	****	< 0.0001	****	< 0.0001	****	< 0.0001	****	< 0.0001
Col-0 & *nox1*	***	0.0007	**	0.0026	****	< 0.0001	****	< 0.0001
Col-0 & double	****	< 0.0001	****	< 0.0001	****	< 0.0001	****	< 0.0001
atgsnor1-3 & *nox1*	ns	0.1682	ns	0.2176	**	0.0011	***	0.0007
atgsnor1-3 & double	ns	0.2176	ns	0.0703	****	< 0.0001	****	< 0.0001
nox1 & double	**	0.0011	***	0.0003	****	< 0.0001	****	< 0.0001

P-values above are multiplicity adjusted P values. The threshold of family-wise significant is set at 0.05.

Figure 4-6 The *atgsnor1-3 nox1* double mutant shows an accelerated HR phenotype.

HR-induced cell death was determined by electrolyte leakage in stated lines in response to *Pst* DC3000 (*avrB*). The data points represented the mean of 3 replicates ± S.E. The strains of avirulent *Pst* DC3000 were infiltrated at 1×10^8 cfu/ml.

4.2.2.2 Additive pathogen susceptibility in *atgsnor1-3 nox1* double mutants

Four-week old Col-0, *atgsnor1-3, nox1* and *atgsnor1-3 nox1* plants were infiltrated with *Pst* DC3000 (*avrB*). Disease symptoms development, such as leaf collapsing, was monitored. It has been determined previously that disease symptoms were maximal at four dpi in Col-0 and, approximately, three days in *atgsnor1-3* and *nox1* plants. However, double mutant plants showed accelerated disease symptoms at 48 dpi (Figure 4-7). To investigate pathogen susceptibility of double mutant, the bacterial titres were recorded after 3 days post *Pst* DC3000 (*avrB*) challenge at 1×10^6 cfu/ml (Figure 4-8 A). Among the tested lines, *atgsnor1-3 nox1* plants were the most susceptible to *Pst* DC3000 (*avrB*), with bacteria titre 3 logs higher than that found in Col-0, and approximately 0.5 to 1 log higher in comparison with both *atgsnor1-3* and *nox1* plants, respectively. The difference between double mutant and Col-0 is statistically significant (P, 0.0001). In addition, the difference between *atgsnor1-3 nox1* and *nox1* plants is significant at P, 0.001. In contrast, statistical analysis indicated that no significant difference between *atgsnor1-3* and double mutant was found. The finding suggests that enhanced disease symptoms development in *atgsnor1-3 nox1* after inoculation with *Pst* DC3000 (*avrB*) might be due to the suppression of GSNOR activity.

Pst DC3000 suspensions were inoculated in 4-weeks old Col-0, *atgsnor1-3, nox1* and *atgsnor1-3 nox1* plants, and plants were scored for the presence of bacteria titre as described above (Figure 4-8B). Bacteria colonies in double mutant were 2 logs higher than that found in Col-0, which is statistically significant (P, 0.0001). The increased bacterial growth was identified in *atgsnor1-3 nox1* mutant relative to either *atgsnor1-3* or *nox1* single mutant. The statistical analysis demonstrated that the difference between double mutant and *atgsnor1-3* is significant (P, 0.0024), and there is also a significant difference between *atgsnor1-3 nox1* and *nox1* (P, 0.005). The results suggest that the additively compromised basal resistance in double mutant might be due to the removal of GSNOR activity and increased protein-nitrosylation.

In conclusion, both *R*-gene mediated resistance and basal resistance are defected in *atgsnor1-3 nox1* mutant relative to parental plants and Col-0. Therefore, GSNO and NO might additively function in regulation of immune responses.

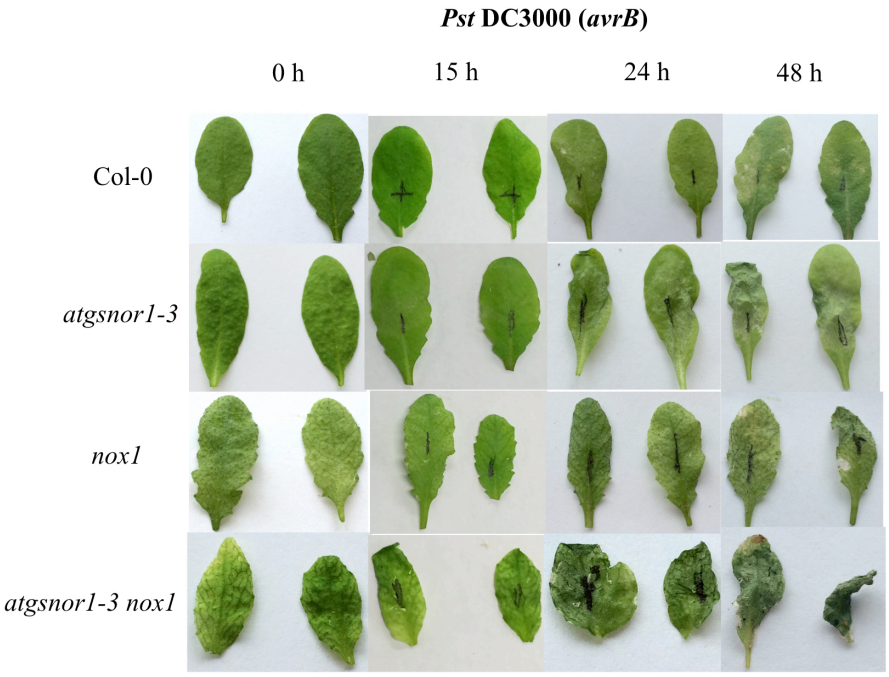

Figure 4-7 Disease symptoms development

Kinetics of disease symptom development in the leaves of stated *Arabidopsis* genotypes over time post *Pst* DC3000 (*avrB*) challenge at 5×10^7 cfu/ml.

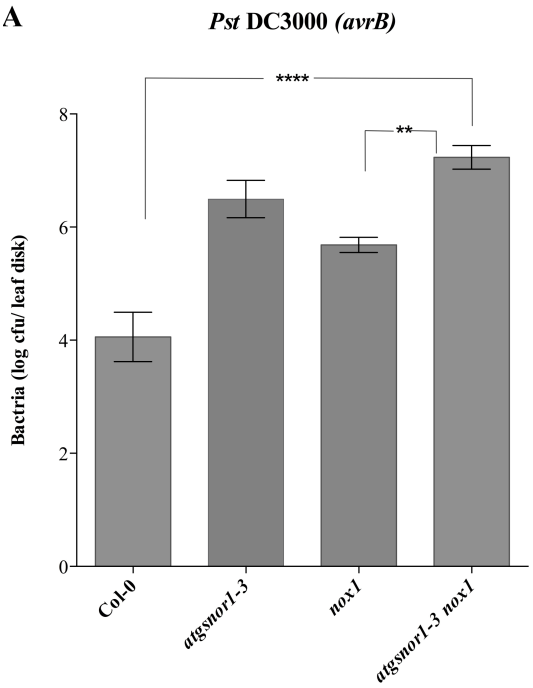

One-Way ANOVA

	Significant	P-value
Col-0 & *atgsnor1-3*	****	< 0.0001
Col-0 & *nox1*	***	0.0007
Col-0 & double	****	< 0.0001
atgsnor1-3 & *nox1*	*	0.0431
atgsnor1-3 & double	ns	0.0657
nox1 & double	**	0.001

P-values above are multiplicity adjusted P values. The threshold of family-wise significant is set at 0.05.

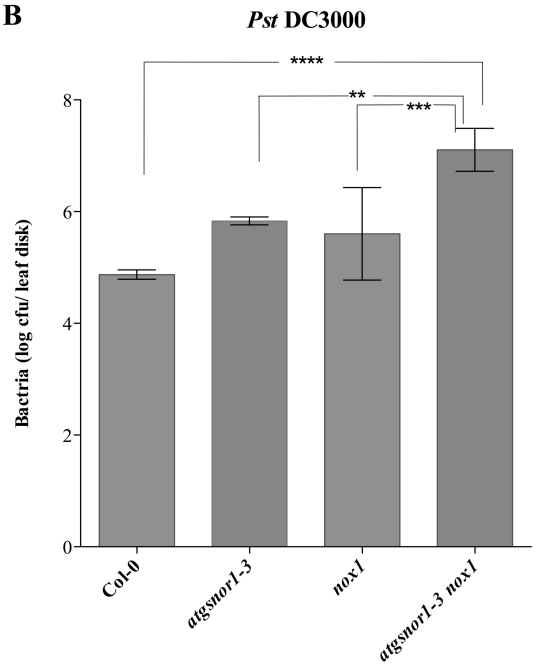

One-Way ANOVA

	Significant	P-value
Col-0 & *atgsnor1-3*	*	0.0209
Col-0 & *nox1*	ns	0.0963
Col-0 & double	****	< 0.0001
atgsnor1-3 & *nox1*	ns	0.8552
atgsnor1-3 & double	**	0.0024
nox1 & double	***	0.0005

P-values above are multiplicity adjusted P values. The threshold of family-wise significant is set at 0.05.

Figure 4-8 Enhanced pathogen susceptibility in *atgsnor1-3 nox1* plants compared with WT and single mutants.

A. Columns showed growth of bacteria after 3 days of infiltration with *Pst* DC3000 (*avrB*) at 1 × 10^6 cfu/ml. **B.** The columns indicated number of colonies recorded upon 3 dpi towards *Pst* DC3000 at 1 × 10^6 cfu/ml. The data points represented the average of 3 replicates ± S.E.

4.3 Discussion

atgsnor1-3 nox1 double mutants maintain some *nox1*-related phenotypes. These included reduced rosettes and leaf size, together with reticulate leaf pattern (Figure 4-4). It has been known that re-establishment of the ability to transport PEP, or alternatively form PEP from pyruvate inside the chloroplasts could rescue *nox1* phenotype, such as recovery of reticulate leaf phenotype, improvement of silique numbers and biomass production (Voll *et al.* 2003). Accordingly, alongside GSNO-dependent pathway, the restriction of the shikimate pathway by a defect in a PPT production might contribute to the development phenotypes of *nox1*.

Studies indicated that *nox1* and *atgsnor1-3* lines displayed different expression patterns of floral-related genes, such as *FLOWERING LOCUS C* (*FLC*), *LEAFY* (*LFY*) and *CONSTANS* (*CO*) (He *et al.* 2004, Kwon *et al.* 2012). Although, there is no direct evidence implicating that a delay of flowering time effects seed development, the reduced fertile capability in the double mutant might be contributed by both *nox1* and *atgsnor1-3* mutations. Therefore, it would be interesting to compare expression patterns of floral-related genes in *atgsnor1-3 nox1* double mutant with its parental plants. In summery, the phenotypes of double mutant line might be conveyed by both NO- and GSNO-derived protein regulations.

During the characterization of resistance–related phenotypes, the accelerated HR symptoms were found in *atgsnor1-3 nox1* plants in comparison with both *atgsnor1-3* and *nox1* mutants following the infiltration of *Pst* DC3000 (*avrB*) (Figure 4-6). Furthermore, enhanced pathogen susceptibilities were determined in *atgsnor1-3 nox1* plants following challenge with *Pst* DC3000 (*avrB*) and *Pst* DC3000, respectively (Figure 4-8). These results suggest that NO and GSNO may function additively in disease resistance, with a more dominant role for GSNO. Although it has been known that the activity of NADPH oxidase was repressed in both *atgsnor1-3* and *nox1* plants (Yun *et al.* 2011), the additive HR-induced cell death from electrolyte leakage indicated that a potential protein nitrosylation pathway, which is not regulated by GSNOR, might be implicated in the establishment of HR during attempted *Pst* DC3000 (*avrB*) infection. However, the details of both GSNO-

dependent and independent pathway that underpin elevated HR development remain unknown.

It is known that SA is a key regulator for establishment of systemic resistance. In addition, previous results exhibited reduced SA accumulation in both *atgsnor1-3* and *nox1* plants. Hence, it is conceivable that SA accumulation might be suppressed in *atgsnor1-3 nox1* plants, and consequently results in defects of SA-related defence response. However, to confirm this hypothesis, it will be necessary to further characterise *atgsnor1-3 nox1* plants by monitoring the disease symptoms in distal leaves, kinetics of SA accumulation and *PR1* transcription levels during pathogen infection. If this is found to be the case, the finding may contribute to the understanding of NO-derived protein modification in SAR.

In conclusion, these results indicated that both GSNO-dependent and GSNO-independent pathways contribute to the additive disease-related phenotypes in *atgsnor1-3 nox1* double mutants, while a more dominant role was taken by GSNO relative to NO during HR development and disease symptoms development. Because the lack of identification of NOS and NO-sensitive sGC in plant genomes, the mechanisms underlying plant model of NO signal transduction remains fractional. The current module of NO signal transduction in plants suggests that GSNO and/or SNOs are the formation of endogenous NO sources, and response to the equilibrium of protein S-nitrosylation and de-S-nitrosylation. However, this study suggests that NO and GSNO/SNOs might mediated their effects on plant defence responses through different type of protein modifications. Unlike GSNO/SNOs, which strictly influence the level of protein S-nitrosylation, NO might be involved in differential protein nitrosylation, these include S-nitrosylation and metal-nitrosylation. It has been known that the formation of protein XNOs is predominantly NO dependent but GSNO concentration-independent in the yeast *Saccharomyces cerevisiae* (Foster *et al.* 2009). It is conceivable that compromised defence responses in *nox1* and *atgsnor1-3 nox1* plants might be partially due to the increasing of NO-dependent XNOs. However, to confirm this hypothesis, it will be necessary to further characterise *atgsnor1-3 nox1* plants by monitoring the kinetics of XNO accumulation and compare with SNO levels during pathogen infection. The resulting findings

might further contribute to the understanding of SNO and NO function in plant immunity.

Chapter 5 Generation of NO-Reporter Systems

5.1 Introduction

NO is a key player in plant signalling involved in a range of protein functions associated with development and defence regulation (Delledonne *et al.* 2001, Feechan *et al.* 2005, Tada *et al.* 2008, Wang *et al.* 2009, Yun *et al.* 2011). NO is known to affect protein activities through post-translational modifications (PTMs), including S-nitrosylation, metal-nitrosylation and tyrosine nitration (Astier 2010). In particular S-nitrosylation, which affects the thiol group of cysteines, has been demonstrated to be a major PTM in plant pathophysiological processes (Feechan *et al.* 2005, Wang *et al.* 2009, Yun *et al.* 2011).

Being a reversible and specific mechanism, S-nitrosylation requires enzymatic processes to govern its cellular status. Although GSNOR, one important player in this context, has already been identified, this enzyme only regulates S-nitrosylation indirectly through GSNO turnover (Feechan *et al.* 2005, Yu *et al.* 2012). In addition, in the last chapter, results indicated its activity lacks specificity to fine-turn NO-signalling; this implies that other genes and/or proteins might contribute to NO-signalling in addition to GSNOR.

To facilitate genetic dissection of the dynamic events in the NO signalling network, transgenic *Arabidopsis* lines were engineered that would report accumulation of a gene transcript closely correlated with NO signalling during defence responses. The principle advantages of this approach are: (1) spatial and temporal accumulation of marker transcripts can be imaged in real-time; (2) the results are able to reflect mechanisms that are actually occurring in the plant; (3) high-throughout saturating mutant screens can be carried out with transgenic lines.

In the research described in this chapter, NO-inducible marker genes were identified and NO-reporter cassettes were generated. To engineer the reporter cassette for subsequent plant transformation, the promoter region of the marker genes were fused

to the firefly luciferase gene (Murray *et al.* 2002). Such transgenic plants may also be utilised for high-throughout mutant screens (Grant *et al.* 2003, Chini *et al.* 2004).

5.2 Results

5.2.1 Identification of NO-inducible marker genes

Marker genes are useful for monitoring dynamic events in the NO-derived signalling pathway. There is a large number of genes that are regulated by NO in *Arabidopsis*, some of which might be involved in plant disease resistance and could fulfil an important role in NO-regulated signalling (Huang *et al.* 2002, Polverari *et al.* 2003, Palmieri *et al.* 2008). In order to identify NO-inducible marker genes, microarray data from both in-house and public databases were mined for potential candidates that are listed in Table 5-1.

Table 5-1 Transcriptional changes of selected genes in WT plants following challenge with 0.5mM SNP.

ID	Description	NO-induced ratio of expression (SNP: NO donor)
At3g28740	Encodes a member of cytochrome P450 family	9.9
At1g76600	Unknown nuclear protein	15.7
At5g42380	Calmodulin like 37 (CML 37)	10.22345675

The selection of three candidates is based on analysis of microarray data (Ahlfors *et al.* 2009) and cross-reference with published data (Palmieri *et al.* 2008). The *Arabidopsis* leaves were harvested at 3 hours after treatment. The data were generated using three biological replicates.

Among these three candidates, cytochrome P450 family (CYP) is a large and diverse group of enzymes that have been identified across all the life kingdoms. They are primarily involved in redox processes (Nelson 2011). In total, there are 272 genes belonging to the CYP450 family in *Arabidopsis* (Werck-Reichhart D 2002).

At3g28740 encodes CYP81D11 (Cytochrome P450, Family 81, Subfamily D and Polypeptide 11) (Heazlewood *et al.* 2005). In contrast, *At1g76600* encodes an unknown nuclear protein (Klok *et al.* 2002). The CML37 encoded by *At5g42380* has a Ca^{2+} binding activity (McCormack *et al.* 2005). However, the functions of these genes remain unknown.

In order to experimentally confirm the expression of these genes that are specifically regulated by NO, Col-0 was treated with GSNO, whereas $MgCl_2$ and GSH (reduced form of glutathione) were used as controls. The leaf samples were collected at 3-hour intervals, and the transcript levels of these three genes was determined by reverse transcriptase (RT) PCR (Figure 5-1). For *At5g42380*, there was no visible difference in the transcription level between GSNO-treated and untreated (control) leaves. In contrast, no basal expression was observed in *At3g28740* control treatments, a significant GSNO-induced transcription was observed at 3hpi. Accordingly, *At3g28740* was deemed to be a suitable NO-inducible marker gene. In addition, *At1g76600* was included as enhanced accumulation at 1 and 3 hpi of GSNO treatment was shown in comparison with $MgCl_2$ and GSH treatments. Furthermore, a strong accumulation of *At1g76600* transcript was detected at 10 min in all treatments, which might be triggered by wound of infiltration. Hence, *At1g76600* might be NO inducible.

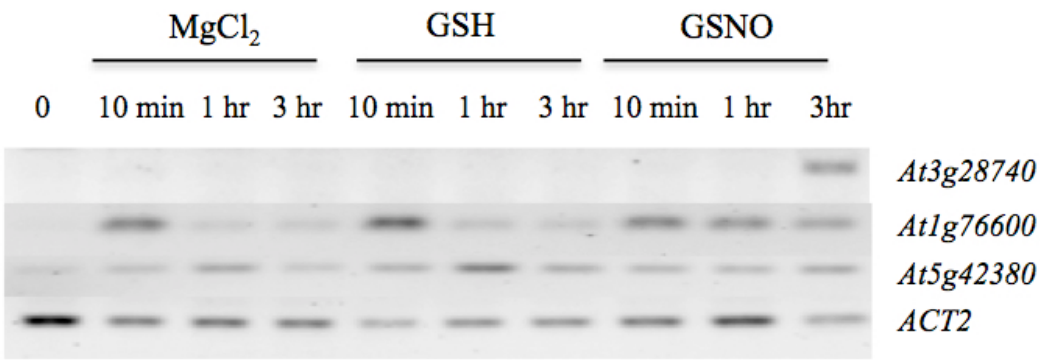

Figure 5-1 RT-PCR of selected genes following 10 mM GSNO inoculation.

Arabidopsis leaves were harvested at stated time points. *ACT2* was used as a loading control. 10 mM $MgCl_2$ and 10 mM GSH were used as controls. The experiment was repeated 3 times with similar results. RT-PCR was optimized for 22 cycles.

To further characterise the expression patterns of selected genes, the marker transcripts were monitored in Col-0, *atgsnor1-1* and *atgsnor1-3* plants. *atgsnor1-1* is a gain of *Atgsnor* function *Arabidopsis* transgenic plant (Feechan *et al.* 2005). A SA-biosynthesis impaired mutant *SALICYLIC ACID INDUCTION DEFICIENT 2* (*sid2*) was included, which exhibits an increased susceptibility to *P. syringae* and a reduced SAR (Nawrath and Metraux 1999). Col-0, *atgsnor1-1, atgsnor1-3* and *sid2* lines were each challenged with *Pst* DC3000 (*avrB*), and the fluorescence signals of relative expression of marker transcripts were recorded in both non-induced and pathogen-induced conditions in microarray assay (Loake unpublished data) (Figure 5-2).

There was no significant difference in accumulation of *At3g28740* transcript in Col-0, *atgsnor1-1 or sid2* plants. However, the transcription level of *At3g28740* was significantly increased in *atgsnor1-3* plants compared to it in Col-0 in both non-induced and pathogen-induced conditions (Figure 5-2A). This suggested that the expression of *At3g28740* might be SNO-dependent but pathogen-independent. Alongside, the transcription level of *At1g76600* showed an increase in all tested lines under infection compared to the non-induced condition (Figure 5-2 B). Hence, the expression of *At1g76600* might be activated in response to *Pst* DC3000 (*avrB*), especially in the *atgsnor1-3* line, which shows that the difference between non-induced and induced condition is statistically significant at P, 0.0002. However, whether this elevation is caused by high cellular SNOs content requires further investigation.

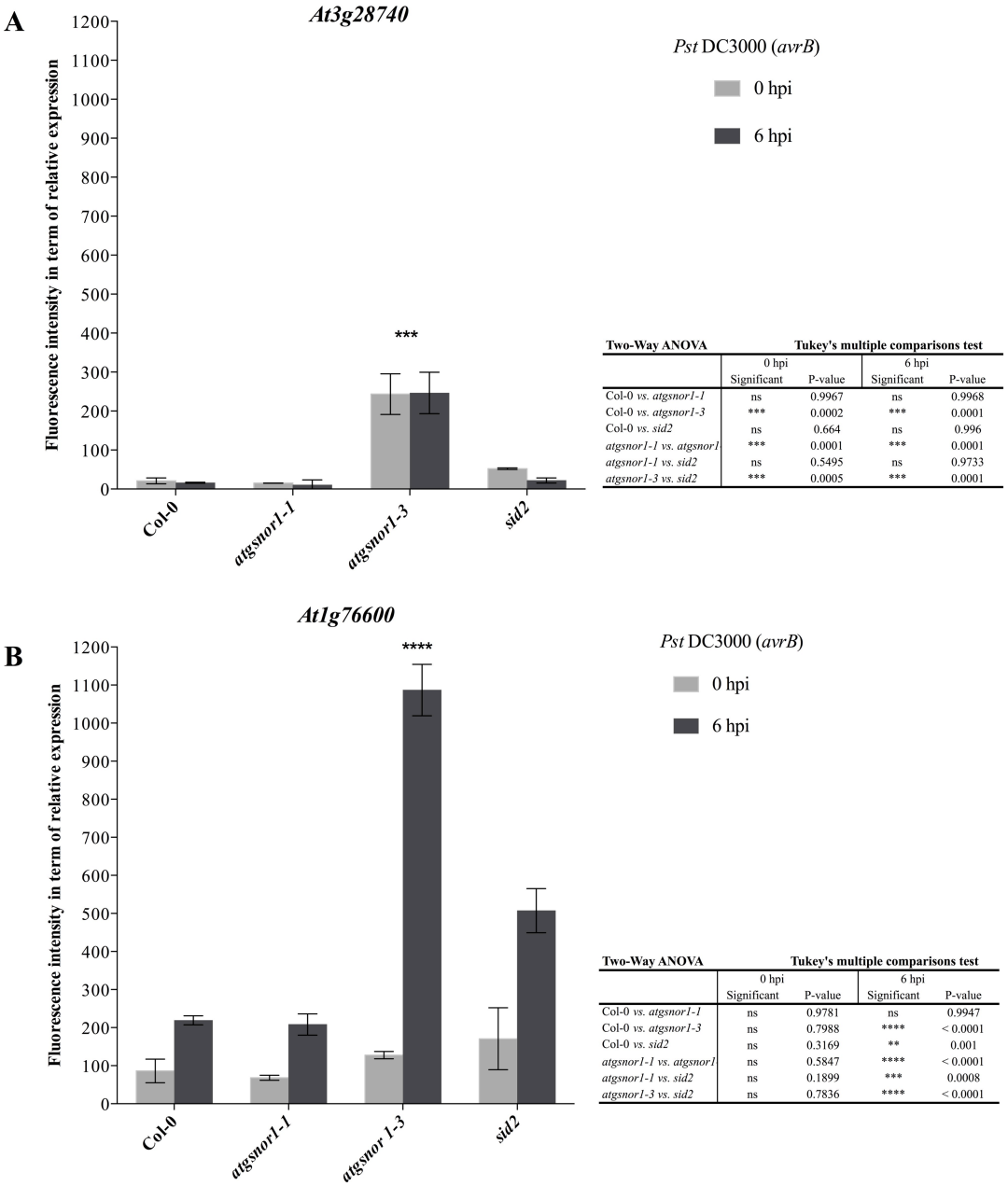

Two-Way ANOVA	Tukey's multiple comparisons test			
	0 hpi		6 hpi	
	Significant	P-value	Significant	P-value
Col-0 *vs. atgsnor1-1*	ns	0.9967	ns	0.9968
Col-0 *vs. atgsnor1-3*	***	0.0002	***	0.0001
Col-0 *vs. sid2*	ns	0.664	ns	0.996
atgsnor1-1 vs. atgsnor1	***	0.0001	***	0.0001
atgsnor1-1 vs. sid2	ns	0.5495	ns	0.9733
atgsnor1-3 vs. sid2	***	0.0005	***	0.0001

Two-Way ANOVA	Tukey's multiple comparisons test			
	0 hpi		6 hpi	
	Significant	P-value	Significant	P-value
Col-0 *vs. atgsnor1-1*	ns	0.9781	ns	0.9947
Col-0 *vs. atgsnor1-3*	ns	0.7988	****	< 0.0001
Col-0 *vs. sid2*	ns	0.3169	**	0.001
atgsnor1-1 vs. atgsnor1	ns	0.5847	****	< 0.0001
atgsnor1-1 vs. sid2	ns	0.1899	***	0.0008
atgsnor1-3 vs. sid2	ns	0.7836	****	< 0.0001

P-values above are multiplicity adjusted P values. The threshold of family-wise significant is set at 0.05.

Figure 5-2 Transcription profiles of selected genes in stated lines upon *Pst* DC3000 (*avrB*) challenge.

A. The transcription profile of *At3g28740* in stated lines. **B.** The transcription profile of *At1g76600* in all given lines. *Arabidopsis* leaves were infiltrated with avirulent strain of *Pst* DC3000 at 1 × 10^6 cfu/ml. The data from 6 hpi measurements with two repeats. Plot the data from microarray source (Loake unpublished data).

5.2.2 Construction of NO-Reporter Cassettes

At3g28740 and *At1g76600* were deemed to be NO marker genes that positively respond to NO. Hence, the promoters of these NO marker genes were used to generate NO-reporter cassettes. In order to engineer such cassettes, the predicted promoter regions from 2000 bp upstream from the transcriptional start site (TSS), were selected as NO-responsive promoters and fused to the reporter gene *luciferase* (*LUC*) (Murray *et al.* 2002). The linearized *Promoter* (*P*): *LUC* reporter constructs were then subsequently cloned into a binary vector (pGreenII-0229) (Hellens *et al.* 2000). The integrated plasmids were transferred into *E. coli* genome to generate *E. coli* strain that carries *P*: *LUC* reporter construct (Figure 5-3).

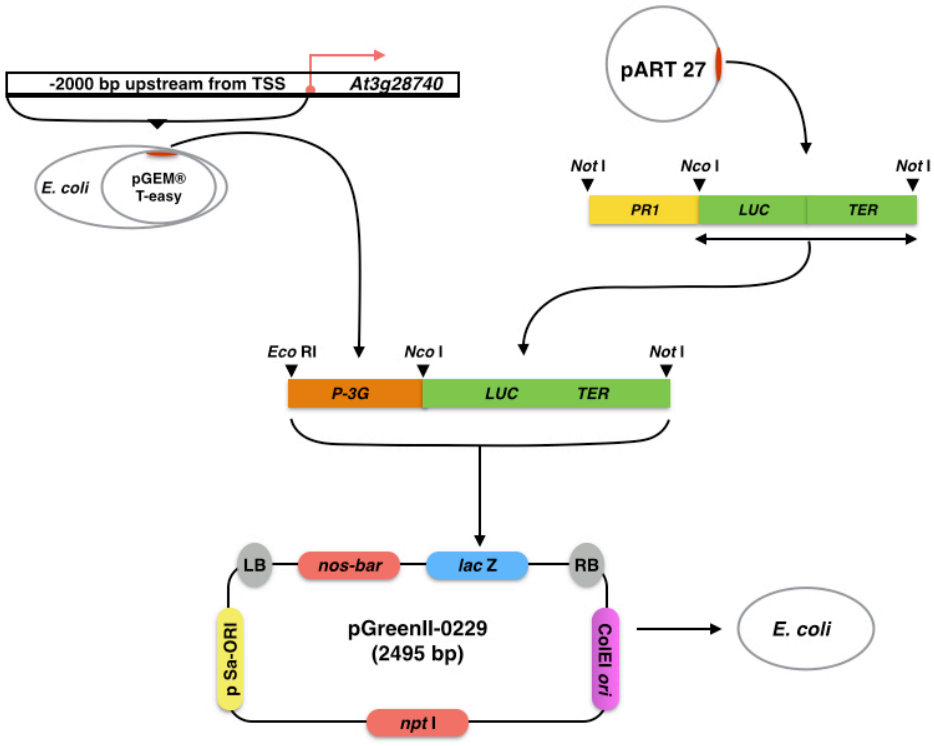

Figure 5-3 Establishment of bioluminescence cassettes for bacteria transformation.

TSS: transcriptional start site. *PR-1*: promoter of *PR1*. *TER*: terminator. *P-3G*: promoter of *At3g28740*. LB: left border. RB: right border. *nos-bar*: nopaline synthase promoter drive *bar* (*bialaphos* resistance) gene. The pSa-ORI: is the broad host range replication origin that used in most of *Agrobacterium* vector. ColEI *ori*: a common replication origin in *E. coli* vectors. These replication origins promote number of plasmids in *Agrobacterium* and *E. coli* cells, respectively. *nptI*: kanamycin resistance gene, the selection marker of pGreenII vector.

5.2.3 Identification of putative regulatory motifs in promoters

A number of putative regulatory motifs were found in the promoter regions of *At3g28740* and *At1g76600*, which were concordant with NO-regulated gene expression (Table 5-2) (Palmieri *et al.* 2008, Mengel *et al.* 2013). Previous study showed that G-box, OCSE, MYCL, MYB and W-box motifs all frequently occur in the promoters of NO-regulated genes (Palmieri *et al.* 2008).

In the promoter region of *At3g28740*, single motif of G-box, MYB and OCSE were found in the first 500 bp (all positions of motifs are given in relation to TSS) upstream of *At3g28740,* but four MYCL motifs were located at this region. In addition, one MYCL and one MYB motif were found between -1000 and -1500 bp upstream.

Similar to that found in promoter of *At3g28740,* one motif of OCSE and MYB, together with two MYCL motifs, were identified within -500 upstream of *At1g76600*. However, there are two W-box found within first 500 bp of promoter that bind to WRKY family. Furthermore, the G-box motif was located at -1075 bp upstream and two additional MYCL motifs were identified at -744 and -1740 bp upstream of transcription start, respectively.

Therefore, 2000 bp upstream from TSS of two marker genes were selected to be promoter regions.

Table 5-2 *Cis*-elements identified in the promoter regions of *At3g28740* and *At1g76600*.

Gene	Base pairs upstream from TSS			
	1-500	500-1000	1000-1500	1500-2000
	Cis-element name			
At3g28740	G-box MYCL×4 MYB OCSE		MYCL MYB	
At1g76600	MYCL×2 WRKY×2 MYB OCSE	MYCL	G-box	MYCL

5.2.4 Generation of NO-reporter transgenic plants

The NO-reporter bioluminescence plasmids were generated as described as in 2.1.1.1. The plasmids were integrated into Col-0 genome by using *Agrobacterium*-mediated transformation method, which is an efficient tool to generate stable transgenic plants without the need of tissue culture (Clough and Bent 1998). Transgenic plants were screened with BASTA resistance. The luciferase activity was further detected in selected candidates (Figure 5-4). The activity of LUC in plants is triggered by treating leaves with its substrate, luciferin, and can be monitored by an ultra low-light imaging camera (Murray *et al.* 2002). As results, the plants with 10 mM GSNO pre treatment showed luciferase activities. In contrast, there is no luciferase activity detected in plants without GSNO pre-treatment. Seedlings with successfully induced luciferase expression were transplanted for seeds.

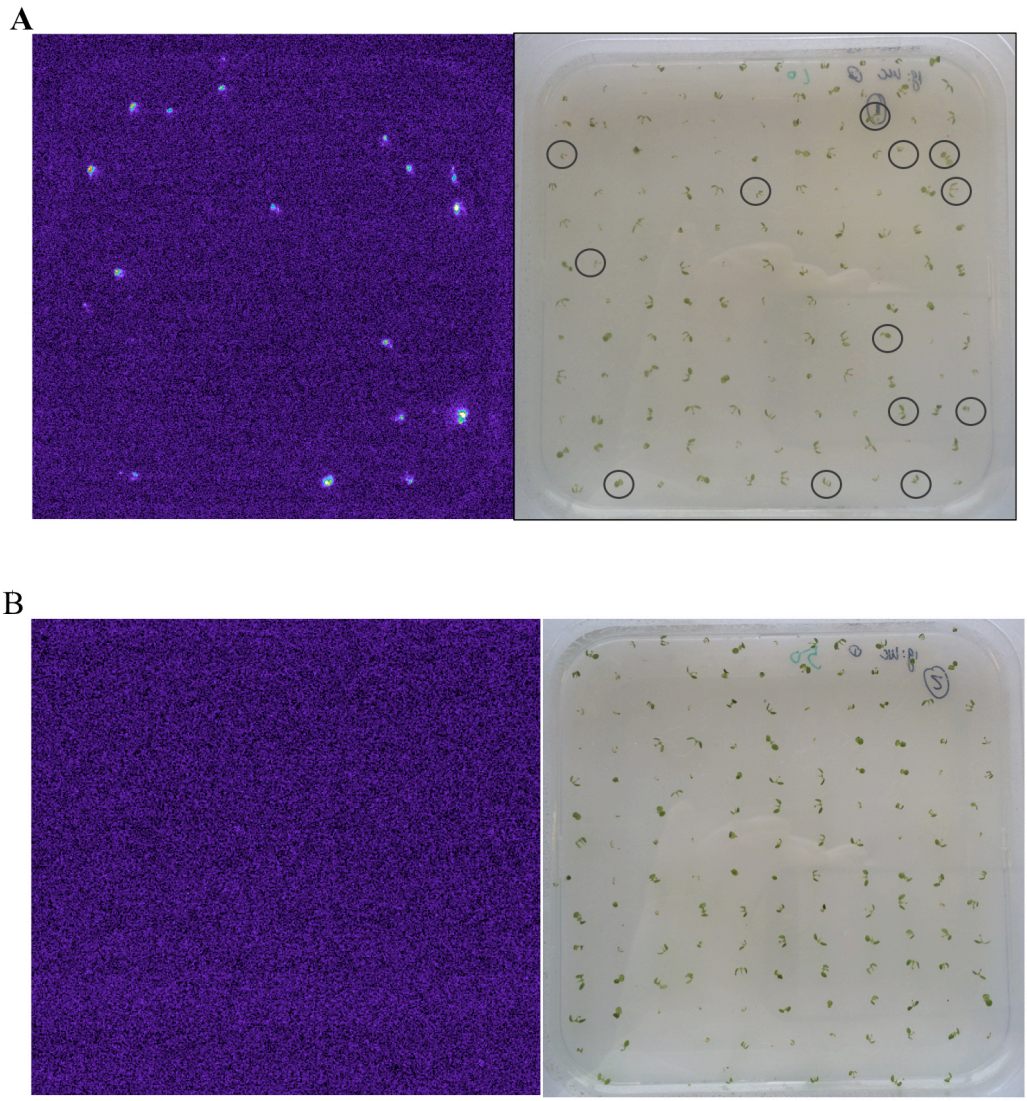

Figure 5-4 Luciferase activity in *P-1G: LUC* plants.

A. *P-1G: LUC* transgenic plants were sprayed with 10 mM GSNO solution to induce luciferase activity, and luciferase activity was imaged with CCD camera. Seedlings with successful induced luciferase expression were circled. **B.** *P-1G: LUC* plants without GSNO treatment as control group.

5.3 Discussion

To aid functional dissection of the NO signalling network, NO-reporter plants were developed that faithfully report (S)NOs accumulation in real time. The NO-inducible marker genes were identified from published databases and verified by RT-PCR (Palmieri *et al.* 2008, Ahlfors *et al.* 2009). *At3g28740* and *At1g76600* were deemed to be NO marker genes. The promoter regions were used to make promoter-reporter cassettes.

When blasting the upstream sequence against known promoter motif database, such as plant promoter database (PPDB) and *Arabidopsis* Gene Regulatory Information Server (AGRIS). A number of putative regulatory motifs were found in the promoter regions of *At3g28740* and *At1g76600*, including G-box, MYB, MYCL and OCSE. These motifs might be involved in plant response to change in NO context (Chen *et al.* 2002, Palmieri *et al.* 2008).

For instance, MYCL motif is recognised by MYC TF family, which is implicated in defence response (Boter *et al.* 2004). It also frequently occurs in the promoter region of NO-regulated genes (Palmieri *et al.* 2008). Presently, *in vitro* study indicated that S-nitrosylation might regulate structures and binding activities of MYB30 TF and TGA1 TF (Mengel *et al.* 2013, Tavares *et al.* 2014). In addition, a G-box motif is known to bind with bZIP proteins and to be implicated in gene expression during pathogen attack (Kim *et al.* 1992). It is identified within first 500 bp upstream of *At3g28740* but different from that found in *At2g76600* promoter (-1075 bp upstream from TSS). Hence, the binding sites allow these two genes to be regulated by NO-influenced TF.

Interestingly, in addition to the motifs described above, the promoter region of *At1g76600* contains multiple putative WRKY binding sites, which has been found in promoters of many plants defence genes (Dong *et al.* 2003). This suggests that *At1g76600* might undertake a role in defence regulation that has access to NO signalling (Figure 5-2 B) (Palmieri *et al.* 2008). It could be the explanation that there are two different transcription profiles of two genes upon *Pst* DC3000 (*avrB*) infection (Figure 5-2). The expression of *At3g28740* is clearly S(NO)s-inducible

rather than pathogen-inducible. Oppositely, the transcript of At1g76600 is thought to be triggered by pathogen attack due to the existence of WRKY binding motifs. In addition, the presence of OCSE motifs enables interaction with SA-mediated TFs, but might be in an opposite manner (Figure 5-2). To confirm these hypothesise, subsequent analysis of transgenic plants will be required, which are transformed with deletions and/or mutations of the promoters fused to luciferase.

Currently, 19 individual putative *P-1G: LUC* transgenic lines and 15 of *P-3G: LUC* transgenic plants have been isolated through BASTA resistance, and SNO-induced luciferase activity has been confirmed in one of *P-1G: LUC* candidate. However, the homozygous genotype of reporter gene transgenic lines will be required for subsequent analysis, especially *P-3G: LUC* transgenic plants. In addition, the in-house microarray data reflected the different expression pattern of *At3g28740* and *At1g76600* in response to *Pst* DC3000 (*avrB*) infection (Figure 5-2). The resulting analysis of these lines might uncover the role of NO in these pathogen-inducible transcripts elevation.

Chapter 6 NO-inducible Zinc Finger Proteins

6.1 Introduction

While identifying the NO-inducible marker genes (Chapter 5) from both publically available and in-house microarray databases, a number of C2H2 type zinc finer proteins (ZFPs) were found to be inducible by NO donors (Palmieri *et al.* 2008, Ahlfors *et al.* 2009). ZFPs constitute one of the largest families of transcriptional regulators (TRs). The ZF domains enable interaction with DNA, RNA, or proteins (Iuchi 2001, Ciftci-Yilmaz and Mittler 2008). In *Arabidopsis*, 176 members of C2H2-type ZFPs were identified, which are mostly plant specific and predicted to bind DNA (Englbrecht *et al.* 2004). Several studies have suggested that C2H2 ZFPs could function as key TRs involved in regulating stress responses of plants (Rizhsky *et al.* 2004, Mittler *et al.* 2006, Eulgem and Somssich 2007, Qureshi *et al.* 2013)

Transcriptional reprogramming is an important event of signal transduction in plants. In this context, transcription factors (TFs) and their cofactors are crucial to ensure initiate gene expression at the right time and place, which allows plants to respond to different stimuli (Yu *et al.* 2001). Additionally, *in vitro* study revealed that S-nitrosylation of TGA1 might be required for its DNA-binding activity, which might lead to an impact in plant disease resistance (Lindermayr *et al.* 2010).

To investigate the role of NO-inducible ZFPs and their possible role in defence response of plants, several approaches were performed: (1) phenotypes of loss-of function mutants were characterised to explore the potential role of these proteins in plant disease resistance. (2) Transgenic *Arabidopsis* lines expressing green fluorescent protein (GFP)-tagged ZFPs were generated for visualisation of *in vivo* localisation.

In this chapter, the NO-inducible C2H2 ZFPs and their T-DNA insertion knockout (KO) mutants are identified. Furthermore, due to their genetic tandem duplication, RNA interference (RNAi) was employed to generate double knockdown *Arabidopsis*

lines. Thus, the phenotypes of loss-of-function mutants implied that ZFPs might function as part of an NO regulatory network that contributes to basal resistance.

In addition to the study of loss of function mutants, the computational model of these NO-inducible C2H2 ZFPs structures were established, which revealed conserved putative functional domains. These *in silico* analysis suggested that the DNA-binding activity of these proteins might be regulated by S-nitrosylation, and they might function as repressors involved in the regulation of defence-related transcriptional reprogramming. To verify such hypothesis, *GFP-ZAT8* cassette was engineered for subsequent plant transformation. Such transgenic plants might be utilised for studying protein trans-localisation in transcriptional reprogramming.

6.2 Results

6.2.1 Identification of NO-inducible C2H2 ZFPs

Following analysis of the microarray data generated by (Palmieri *et al.* 2008, Ahlfors *et al.* 2009), we identified *ZAT8* (*At3g46080*), *ZAT7* (*At3g46090*) and *ZAT12* (*At5g59820*) as induced by NO donors. Based on analysis of zinc finger position, sequence and number of fingers, they were classified into the subclass of C2H2 type ZFPs (Englbrecht *et al.* 2004, Ciftci-Yilmaz and Mittler 2008). Hence, these NO-inducible C2H2 type ZFPs were selected for subsequent experiments. In addition, *ZAT16* (*At3g46070*), the tandem duplication of *ZAT8* and *ZAT7*, was also included due to potential functional redundancy.

Current studies suggested that ZAT12 is implicated in multiple stress responses and required for the expression of several abiotic stress-related genes (Rizhsky *et al.* 2004, Davletova *et al.* 2005). Alongside, ZAT7 (a distant relative of Zat12) has been reported to be involved in oxidative stress and salinity tolerance (Rizhsky *et al.* 2004). In contrast, there is no direct evidence regarding the role of ZAT8 in stress responses of plants (Obulareddy *et al.* 2013). These studies emphasized the importance of C2H2 ZFPs in stress responses in plants, but the role of these ZFPs in plant defence response remains unknown, which promotes researches performed with C2H2 type ZFPs. Our findings reveal not only the function of these proteins in defence response pathways, but also the mechanisms that regulate their role in signal transduction.

6.2.2 Impact of NO-inducible ZFPs in plant disease resistance

6.2.2.1 Identification of loss-of-function mutants

The T-DNA insertion lines of *ZAT7, ZAT8, ZAT16* and *ZAT12* were found in the TAIR (Table 6-1). SAIL_434_G05 (*zat7*), SM_3_1198 (*zat8*) and GABI_348H06 (*zat12*) lines were selected, as the insertions are located in their exons. However, the insertion site of T-DNA line of *ZAT7*, SAIL_404_G03, is located at its five prime untranslated region (5' UTR). They were acquired from Nottingham *Arabidopsis* Stock Centre (NASC) and genotyped to be homozygous.

The selected T-DNA lines were genotyped by PCR with T-DNA verification primers and the genomic primers. A large size PCR product (~1000 bp) was amplified with Col-0 genomic DNA, whereas a small-sized band (~500 bp) was produced with DNA from homozygous plants and both bands were found in PCR products from heterozygous plants (Figure 6-1). In addition, the insertion of *zat7* has a short repeat at 5' end. As a result, two bands (509 bp and 809 bp) were determined in genotyping in comparison with Col-0 (Figure 6-1C).

In order to experimentally confirm that selected *ZFPs* are knockouts, RT-PCR was performed to compare the basal expression of targeted genes in T-DNA mutants and Col-0 (Figure 6-2). Three determined homozygous plants (*) were selected for from each line for RT-PCT (Figure 6-2). As a result, the knockout plants were selected that showed no bands of any targets genes.

Table 6-1 T-DNA insertion lines of zinc finger proteins.

Gene ID	T-DNA lines	Loci of insertion	Genotype	Basal expression
At3g46070	SAIL_434_G05 *zat16*	Exon	Homozygous	No
At3g46080	SM_3_1198 *zat8*	Exon	Homozygous	No
At3g46090	SAIL_404_G03 *zat7*	300_UTR5	Homozygous	No
At5g59820	GABI_348H06 *zat12*	Exon	Homozygous	No

The insertion of *zat16, zat8* and *zat12* were located in the exon of targeted genes. However, there is no exon insertion mutant available for *zat7*. Thus, the mutant with insertion located at 300 bp upstream of untranslated region (UTR) has been ordered. All ordered mutants were confirmed to be homozygous and no basal expression level of target genes in comparison with Col-0.

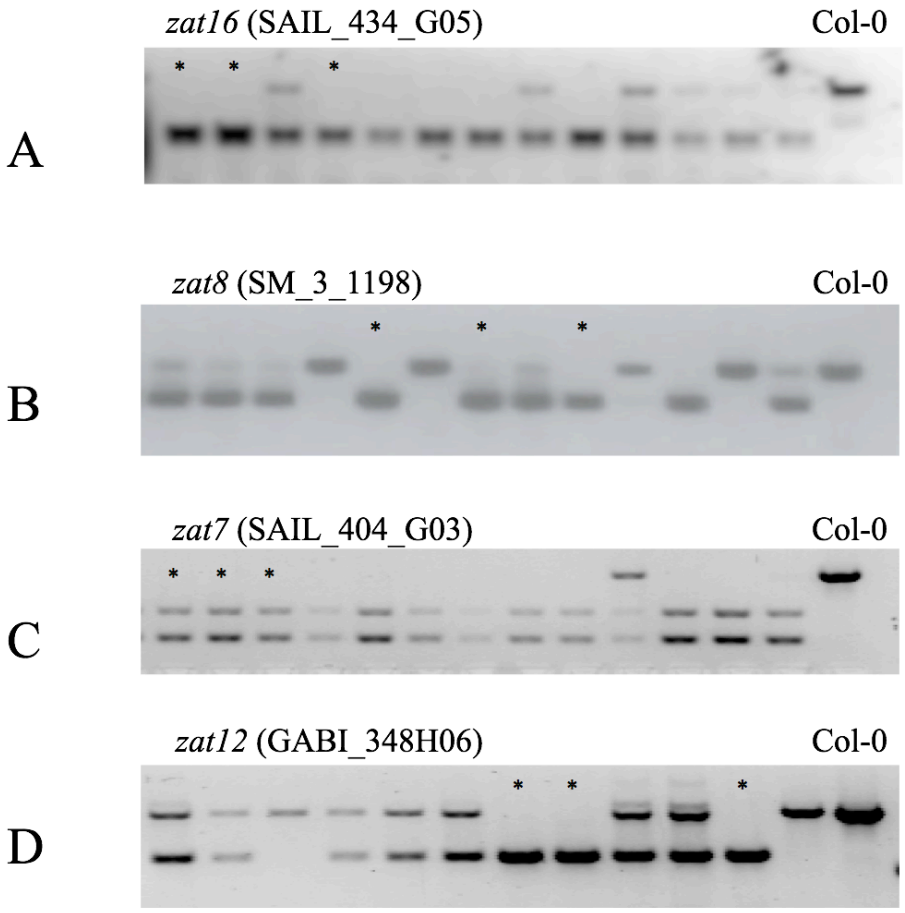

Figure 6-1 Genotyping of *zat7, zat8, zat16* and *zat12*.

The genotyping PCR was carried out with three primers. The gene specific genomic primers pair is only functioning in Col-0 and heterozygous. The T-DNA left border primer reveals the genotype of heterozygous or homozygous. Homozygous (*) plants were selected for RT-PCR.

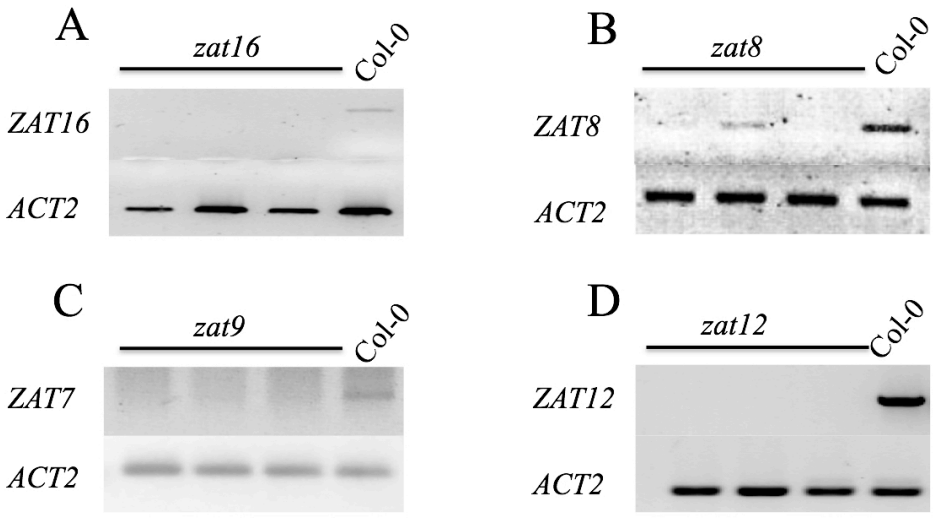

Figure 6-2 Confirmation of knockout mutants by RT-PCR

A. Expression levels of *ZAT16* transcripts in *zat16* mutant in comparison with Col-0. **B.** *ZAT8* transcript level in *zat8* plants relative to Col-0. **C.** Expression level of *ZAT7* in *zat7* mutant relative to Col-0. **D.** Expression levels of *ZAT12* in *zat12* mutant and Col-0. *ACT2* was used as a loading control. The RT-PCR was optimized for 22 cycles.

6.2.2.2 Generation of *zat7zat8* double knockdown mutant

Recent study of C2H2 ZFP family suggested that *zat7* and *zat8* might be the result of recent gene duplication (Ciftci-Yilmaz and Mittler 2008). Hence, *zat7 zat8* double mutant was engineered because of potential functional redundancy. In consideration of their tandem location, it would be difficult to generate a double mutant by crossing the T-DNA insertion mutants. As a result, a double knockdown mutant *zat7zat8* was established by RNAi. The sense and anti-sense fragments were therefore designed to 100% matched with both *ZAT7* and *ZAT8* so that RNAi would disrupt translation of both genes.

The CDS of *ZAT8* and *ZAT77* were obtained from TAIR. By aligning two CDS, a 100 bp sequence of *ZAT8* was selected as the sense fragment, which is also found in *ZAT7* with 98% sequence similarity. The complementary sequence was amplified to be antisense fragments, and additional 200 bp downstream region was selected as hairpin intron (Figure 6-3). The RNAi construct was established as described as in

2.1.1.2. By employing *Agrobacterium* floral dipping, the RNAi construct was delivered and integrated into Col-0 genome. The harvested seeds were then sowed on agar plates with Kan selection. The seeds were collected from each F1 individual candidate and grown into F2 progeny plants, which were then further verified by RT-PCR (Figure 6-4).

It has been known that expression of *ZAT7* and *ZAT8* is promoted by NO donor (Ahlfors *et al.* 2009). In Figure 6-4, *rnai* candidates and Col-0 were infiltrated with 0.5mM GSNO as a NO donor. The leaf samples were collected at 0 and 3 hpi for RT-PCR. In comparison with Col-0, there are no visible basal transcriptions of *ZAT8* in all candidate plants; after GSNO-induction, there are no visible bands of *ZAT8* transcript in tested lines except *rnai-1* plant. Meanwhile, both basal and GSNO-inducible transcripts of *ZAT7* were reduced in *rnai-3* plants. Therefore, *rnai-3* line was deemed to be *zat7 zat8* double knockdown mutant and selected for subsequent susceptibility test.

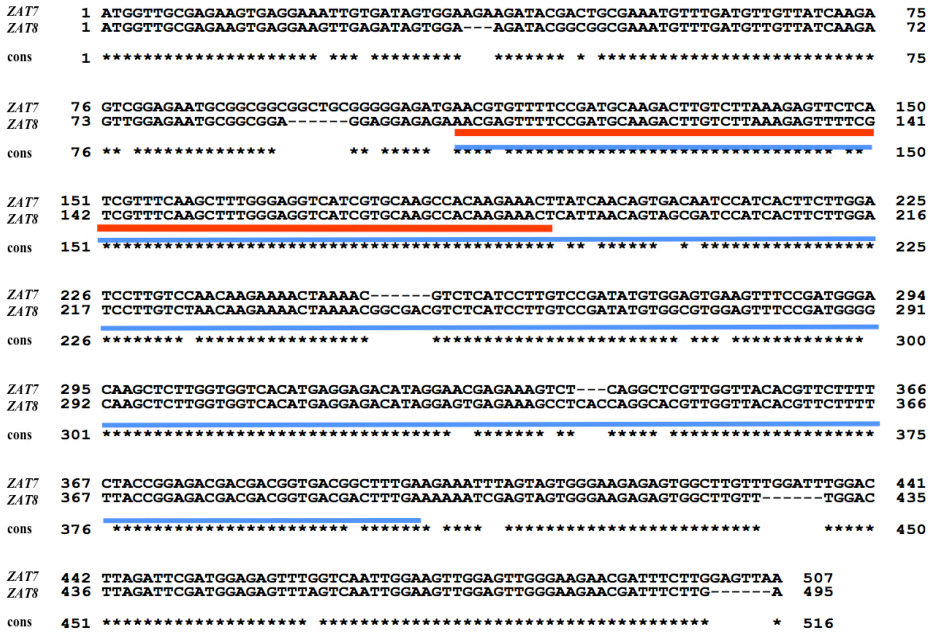

Figure 6-3 CDS alignment of *zat7* and *zat8*.

The alignment was carried out by clustarX, and the consensus was indicated as *. The sequence that underlined in red was selected to be the sense fragment. The underlined sequence in blue was selected to be antisense fragment (complementary sequence of sense fragment) and hairpin intron.

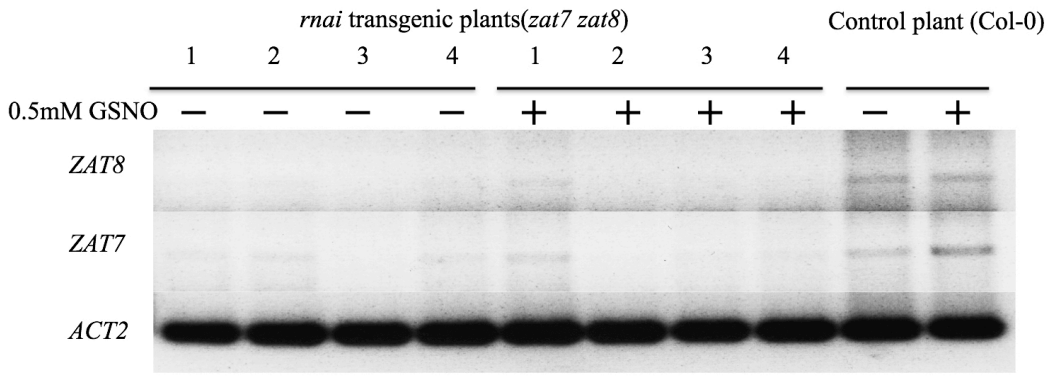

Figure 6-4 Confirmation of *zat7 zat8* double knockdown mutants.

The basal and GSNO-induced accumulations of *ZAT8* and *ZAT7* transcripts were determined by RT-PCR in 4 tested individual *rnai* lines and Col-0. *ACT2* was used as a loading control. The RT-PCR was optimized for 22 cycles.

6.2.2.3 ZAT8 might be required for tolerance of nitrosative stress

In order to study the role of ZAT8 in NO signalling, *zat8* plants were grown in agar plates with the supplement of NO donor. The Col-0 and *atgsnor1-3* seeds were used as positive and negative controls, respectively. There were 30 seeds of each line sowed on each LB agar plate containing 1.5 mM GSNO, and three plates for each line (Figure 6-5). While 96% of Col-0 seeds germinated, less than half seeds of *zat8* germinated with GSNO supplement.

S-Nitroso-cysteine (Cys-NO) is the product of reaction between Cysteine (Cys) and GSNO and is used as an NO donor as an alternative to GSNO. The experiment procedure was repeated on plates supplied with 2 mM Cys-NO (Figure 6-5). The germination frequency of *zat8* was reduced to half when compared to Col-0. Consequently, the results demonstrated that Zat8 might function in the response against nitrosative stress.

Interestingly, the germination frequencies of *atgsnor1-3* and *zat8* plants are very similar on GSNO, which is 43% of *zat8* compared to 33% for *atgsnor1-3* mutant and no statistical difference (P, 0.248). Although, the germination frequencies are also similar on Cys-NO plates, 50% (*zat8*) compared to 38% (*atgsnor1-3*), statistical

analysis indicated that the difference is significant at P, 0.0365. Thus increased nitrosative susceptibility in *zat8* plants might be due to the impaired GSNOR activity.

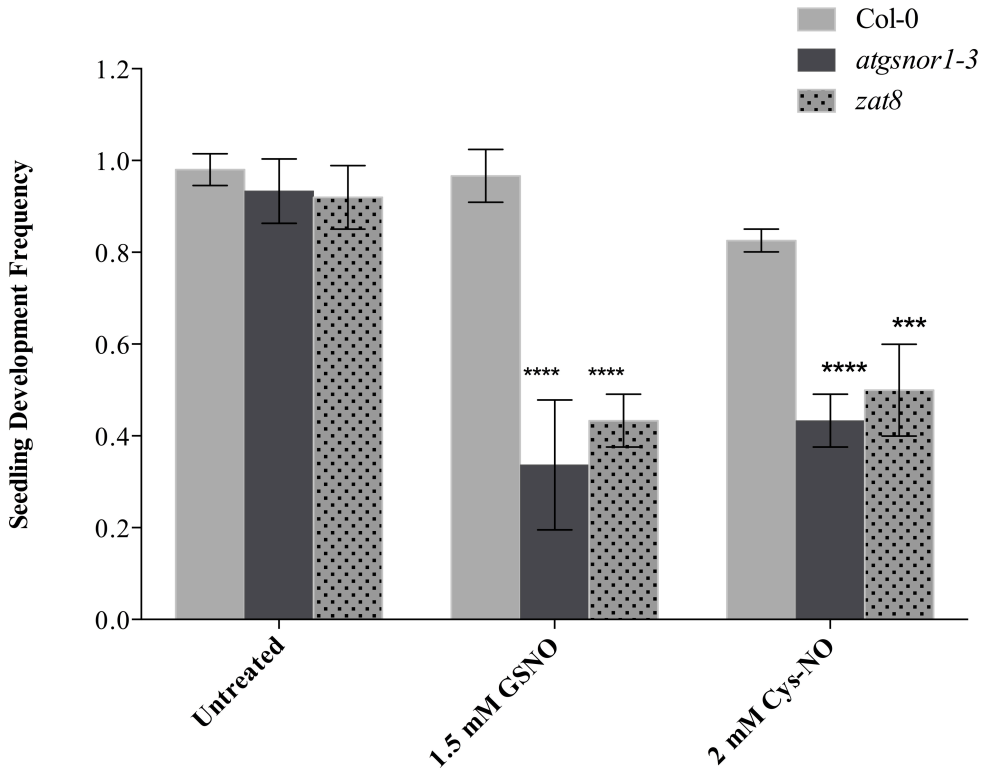

Two-Way ANOVA	Tukey's multiple comparisons test					
	Un treated		1.5 mM GSNO		2 mM Cyc-NO	
	Significant	P-value	Significant	P-value	Significant	P-value
Col-0 & *atgsnor1-3*	ns	0.7234	****	< 0.0001	****	< 0.0001
Col-0 & *zat8*	ns	0.5893	****	< 0.0001	***	0.0001
atgsnor1-3 & *zat8*	ns	0.9734	ns	0.248	*	0.0365

P-values above are multiplicity adjusted P values. The threshold of family-wise significant is set at 0.05.

Figure 6-5 Seedling development frequency of stated lines +/- NO donor.

Percentage germination of Col-0, *atgsnor1-3* and *zat8* after 6 days on LB agar plates supplemented with 1.5 mM GSNO and 2 mM Cys-NO. The plates were maintained in a dark room at 22 °C for 6 days.

6.2.2.4 NO-inducible ZFPs might be required for basal resistance

To study the possible impact of these zinc fingers in defence regulation, *Pst* DC3000 suspensions were inoculated in 4-weeks old Col-0, *atgsnor1-3, zat7, zat8, zat16,* and *zat12* plants, as well as the *zat7 za8* double mutant. Leaf extracts were collected at 5 dpi. The extracts were then spread on agar plates for quantification of bacterial growth in the stated lines. The number of bacterial colonies were recorded after 3 days. Pathogen susceptibilities of *Arabidopsis* genotypes were present in Figure 6-6, there is no significant difference between two genotypes labelled with same letter.

Although the protein function analysis suggested that these NO-induced ZFPs might function redundantly, *zat8* showed enhanced susceptibility relative to *zat7* and the difference was statistically significant (P, 0.0001). A similar result was determined between *zat8* and *zat16*. In addition, statistical analysis demonstrated no significant difference among *zat7, zat16* and Col-0 (P, 0.078). Furthermore, *zat7 zat8* double transgenic plants exhibited similar level of bacterial titre relative to *zat8*, which showed no statistical difference (P, 0.772) in between. The findings suggested that *ZAT 7* and *ZAT16* might be function redundant; however, *ZAT8* might be epistatic to *ZAT7* and *ZAT16* to regulate defence response.

The increased bacterial growth was identified in *zat12* plants relative to Col-0, and difference in between is statistically significant (P, 0.0001). Interestingly, there is no significant difference (P, 0.095) detected between *zat12* and *zat7*. The same result was also demonstrated between *zat12* and *zat16*. In addition, *zat12* exhibited similar susceptibility compared to *zat8* (P, 0.518). Therefore, one possible hypothesis is that *Zat8* is epistatic to *ZAT12*, which is subsequently epistatic to *ZAT7* and *ZAT16* in basal resistance.

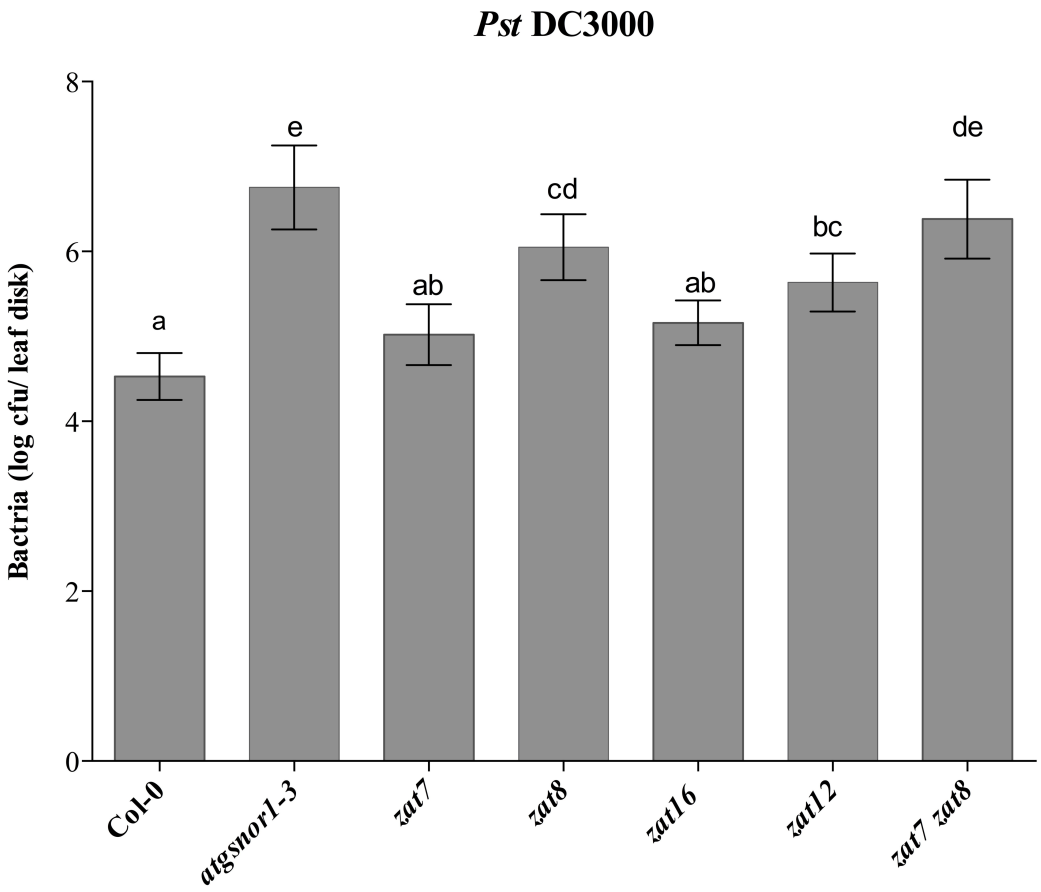

P-values above are multiplicity adjusted P values. The threshold of family-wise significant is set at 0.05.

ANOVA	Tukey's multiple comparisons test				
Significant	ns	ns	ns	ns	ns
P- value	0.078	0.095	0.518	0.772	0.653
Col-0	a				
zat7	a	b			
zat16	a	b			
zat12		b	c		
zat8			c	d	
zat7 zat8				d	e
atgsnor1-3					e

Figure 6-6 Pathogenicity test in stated lines upon treatment of *Pst* DC3000.

Number of colonies recorded upon 5 dpi towards *Pst* DC3000 at 1 × 10^5 cfu/ml. Col-0 and *atgsnor1-3* are WT resistant and susceptible controls, respectively. The Data represented the average of 3 replicates ± S.E.

6.2.3 Functional characterisation of NO-inducible ZFPs

6.2.3.1 Sequence alignment and conserved domains

In order to identify the potential functional domains, the amino acid sequence of these ZFPs was aligned using ClustalX (Figure 6-7). It revealed a high consensus sequence among these 4 ZFPs. Multiple invariant sequences were also determined in two zinc fingers. The specific DNA binding sequence [QALGGH] has been found in both first and second finger of these selected proteins (Kubo *et al.* 1998). A conserved domain $LD^{L}/_{F}DLN$ was revealed at the C terminus of these ZFPs. This conserved domain has been identified to be the core sequence of the EAR motif (Ciftci-Yilmaz *et al.* 2007). Furthermore, there are 6 Cys residuals found in the conserved domains with 4 of them found in the finger sequence, one in an invariant sequence at the N terminus, and another within the EAR motif at the C terminus. Therefore, the function of these NO-induced ZFPs might be regulated by S-nitrosylation. In addition, they might also function as transcription repressors through EAR motif.

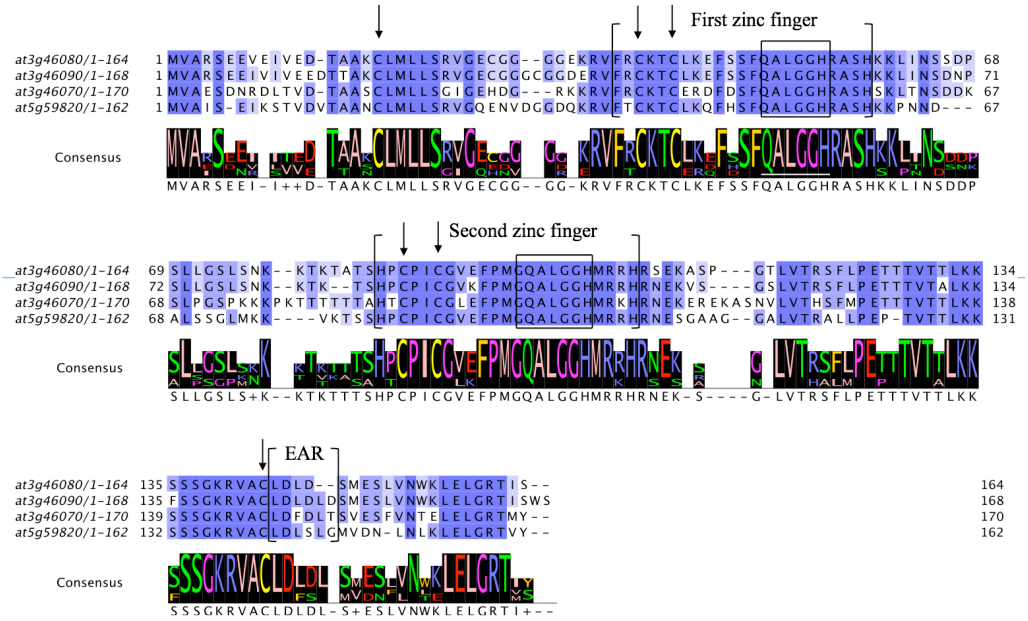

Figure 6-7 Alignments of protein sequences of ZAT8, ZAT7, ZAT16 and ZAT12.

Consensus sequence was found among 4 selected ZFPs. The colour represents the degree of conservation. Conserved sequences and invariant specific DNA binding sequences (QALGGH) are located in two zinc finger domains. The core sequence of EAR motif [$^{L}/_{F}$DLN$^{L}/_{F}$ (x)] is found at the C terminus.

6.2.3.2 Secondary structures of ZFPs

The secondary structures of ZAT8, ZAT7, ZAT12 and ZAT16 were predicted in I-TASSER online server of protein structure and function predictions, which the 3D models were built on multiple threading alignments and iterative template fragment stimulations (Roy *et al.* 2010). The secondary structure of ZAT8 contains a helix loop (Figure 6-8A and B). The DNA binding sequences present on the fingers is found at the inner surface of the helix (Figure 6-8A). In contrast, the Cys residuals on the fingers are exposed outside of the helix (Figure 6-8B). The EAR domain is located at the end of C-terminal (Figure 6-8B). However, the Cys at the head of EAR domain is only found at the inner side of the helix. The similar features are also determined in secondary structures of ZAT7, ZAT12 and ZAT16. This model suggested that these ZFPs might function in transcriptional regulation as the helix

structure might facilitate the contact with DNA double helix. Moreover, the Cys residuals that located on two fingers and EAR domain might interfere the DNA-binding activity and repression activity through S-nitrosylation.

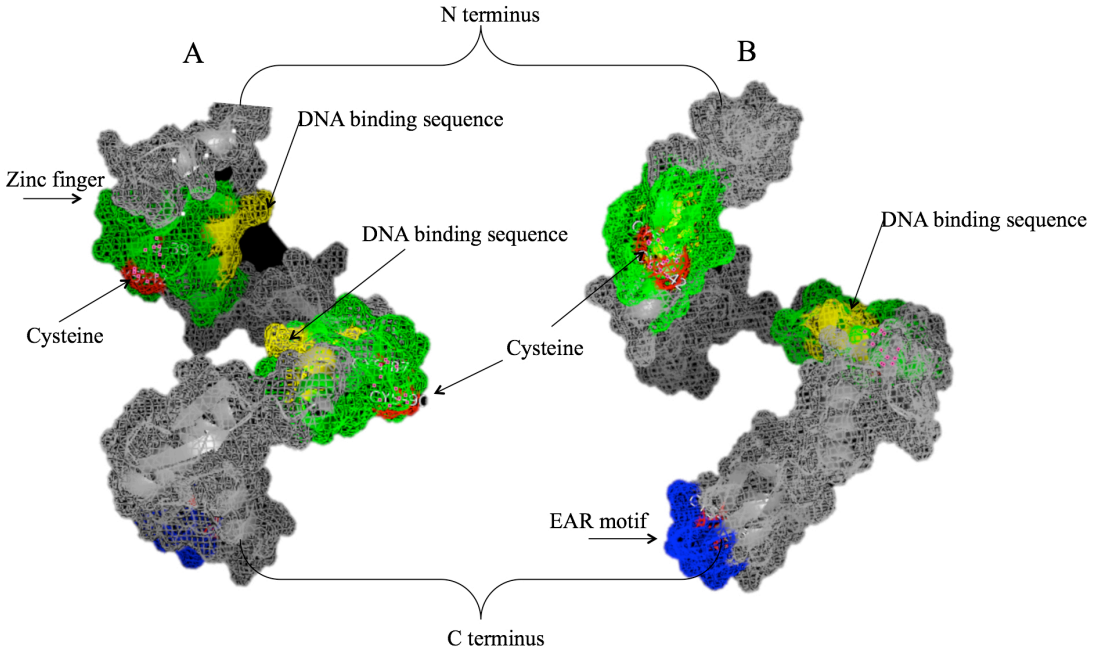

Figure 6-8 Predicted secondary structure of ZAT8.

A. Specific DNA binding sequence is located at the inner surface of Zinc finger domains. **B.** Location of EAR motif. Zinc finger domains are highlighted in green. The specific DNA binding sequences are labelled in yellow. Red indicates the location of Cysteine residues. The EAR motif core sequence is coloured in dark blue.

6.2.3.3 Localization assay of ZAT8

As shown above, ZAT8 might function as a transcription repressor. Hence, the subcellular localization of ZAT might be in the nucleus. GFP is a convenient marker used to visualize the *in vivo* localization of target proteins. It emits bright green fluorescence when exposed under the light with wavelength between blue and ultraviolet range (Sheen *et al.* 1995). Hence, a GFP coding sequence was fused with *ZAT8* and transiently expressed in tobacco leaves. Expectedly, GFP-ZAT8 located in the nucleus (Figure 6-9).

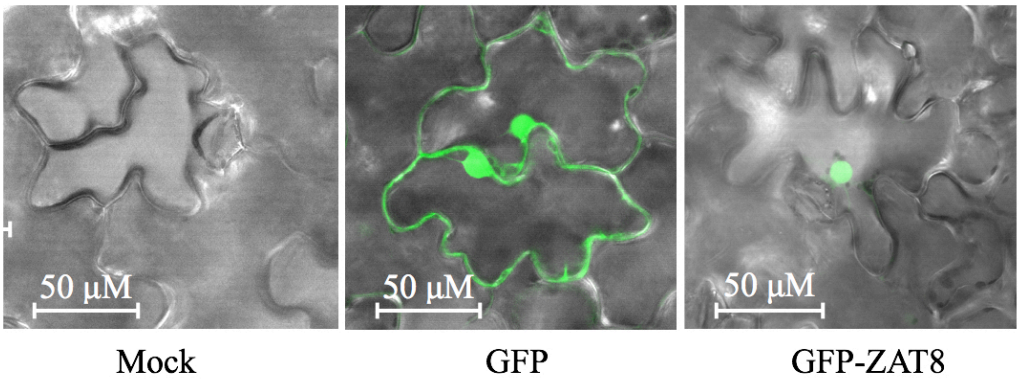

Figure 6-9 Localization of GFP-Zat8 in tobacco leaves after 4 days infiltration

GFP (middle) indicated expression of 35S: GFP in cell wall and nucleus. GFP (right) showed localization of GFP-ZAT8 in nucleus.

6.3 Discussion

The recent evidence has implied a C2H2 Zinc finger TF (Fzf1) as a regulator of nitrosative stress in *S. cerevisiae* (Sarver and DeRisi 2005). In addition, a yeast specific zinc cluster protein, CTA4, has been shown to control the responses to NO in *C. albicans* (Chiranand *et al.* 2008). The NO sensitivity test indicated that *ZAT8* might be required for tolerance of nitrosative stress in *Arabidopsis*. Interestingly, *zat8* mutant exhibits nitrosative susceptibility relative to Col-0, to a level similar to that of *atgsnor1-3* plants (Figure 6-5). To investigate whether enhanced nitrosative susceptibility in *zat8* plants is GSNOR-related, the transcripts level and activity of GSNOR could be examined in a *zat8* mutant background. In addition, the expression level of *ZAT8* would be examined in the *atgsnor1-3* mutant.

In response to *Pst* DC3000, loss of function *Arabidopsis* plants exhibited enhanced susceptibilities in comparison with Col-0 (Figure 6-6). ZAT7 and ZAT12 positively regulate cytosolic ascorbate peroxidase 1 (Apx1) expression, a key H_2O_2 removal enzyme, during oxidative stress (Rizhsky *et al.* 2004). Moreover, the expression of luciferase, which is driven by *ZAT12* native promoter, was largely delayed and repressed in an *rbohD* mutant compared to Col-0 in response to a wound-induced ROS signal (Miller *et al.* 2009). This suggests that the *rbohD*-produced ROS might trigger the expression of ZAT12. Hence, it is possible that ZAT12 might be required to limit the ROS-potentiated cell death. Therefore, it is possible that these T-DNA insertion mutants are susceptible to *Pst* DC3000 due to the extended ROS induction. However, to confirm this hypothesis and further understand the role of ZFPs in defence response, full characterisation of mutant plants will be required, including ROS accumulation, HR development, SA accumulation, *R*-gene related disease resistance and disease-related gene transcription.

The protein sequence alignment and secondary structure of ZAT7, ZAT8 and ZAT16 suggested that they might be functionally redundant (Englbrecht *et al.* 2004). However, the pathogenicity test result indicates that only ZAT7 and ZAT16 might be functionally redundant. Previous study proposed that ZAT12 might function upstream of ZAT7, which is a possible explanation to this phenomenon, because *zat7*

zat8 plants exhibited increased bacteria titre compared to *zat7, zat16* and *zat12* single mutants, but as similar to *zat8* plants. Thus, ZAT8 might be epistatic to ZAT12, subsequently epistatic to ZAT7 and ZAT16. It will be necessary to determine the expression pattern of other NO-induced ZFPs in *zat8* mutant. In addition, electrophoresis mobility shift assay (EMSA) could be employed to examine the binding activity of ZAT8 on promoter regions of *ZAT7, ZAT16 and ZAT12*.

In silico analysis indicated that ZAT7, ZAT8, ZAT16 and ZAT12 contain specific DNA-binding sequence "QALGGH" located on their C2H2 zinc fingers, which is the classic feature of TF IIIA type C2H2 ZFPs (Miller *et al.* 1985, Kubo *et al.* 1998). Therefore, these proteins could function as DNA binding proteins and are considered to be potential TFs, which might have an impact on NO-mediated transcriptional reprogramming. Moreover, the alignment of protein sequences revealed a core sequence of EAR motif located at C-terminal of ZFPs (Figure 6-7). The EAR motif is an active repression motif identified in a number of ZFPs with repression activity (Ohta *et al.* 2001).

Furthermore, the predicted protein structure implied that these NO-inducible ZFPs might function as repressors in transcriptional regulation. The helical structure of selected ZFPs mirrors the DNA double helix facilitates the contact with the DNA-binding sequences located at the inner surface of the two fingers (Figure 6-8). This putative structure suggested that these ZFPs might negatively regulate transcription initiation (HannaRose and Hansen 1996).

ZFPs are rich in Cys. In particular, two Cys residuals on the zinc fingers show a surface presentation in the protein residues model. This might promote S-nitrosylation, which leads to changes in structure and activity. Thus, the GST fusion protein *in vitro* expression system will be employed to express *GST-ZAT8* in *E. coli*. The purified recombinant Zat8 could be used in biotin-switch for protein S-nitrosylation assay. Alongside, the transgenic line expressing *GFP-ZAT8* was generated to visualise its localisation *in vivo*. As expected, GFP-ZAT8 was detected in nucleus, which suggested that function of *ZAT8* might be involved in transcriptional reprogramming. In addition, a recent study revealed that *ZAT8* transcripts were isolated in the transcriptome of guard cells by deep sequencing, and

might be involved in biotic stress (Obulareddy *et al.* 2013). Hence, ZAT8 might be also involved in regulation of stomata closure during response to pathogen attack.

The further analysis of these lines might identify a role as NO-modified transcriptional factors for these regulatory proteins, contributing to the understanding of NO-regulated transcriptional reprogramming during host-pathogen interaction.

Chapter 7 General discussion

In this concluding chapter, I aim to integrate the current understanding of *nox1* and *atgsnor1-3 nox1* mutants in disease resistance. In addition, the forward genetic strategy is presented using an NO-reporter system to identify the mutations, which disrupt NO perception. Finally, the implications of selected ZFPs in NO-induced transcriptional reprogramming can be hypothesised.

7.1 NO and GSNO function additively in the plant defence response

NO is a key signalling molecule implicated in plant development and defence responses (Delledonne *et al.* 1998, Durner *et al.* 1998, He *et al.* 2004, Zeidler *et al.* 2004). Because of the proposed diverse and abundant sources of NO in plants, it might be necessary to regulate the level and bioactivity of NO (Moreau *et al.* 2010, Yu *et al.* 2014). GSNO provides a reservoir of NO bioactivity that is central to NO signal transduction. Evidence indicated that GSNOR regulates GSNO and SNO level, and its activity is required for the defence response but this enzyme does not control NO levels in plants (Liu *et al.* 2001, Feechan *et al.* 2005). Thus, the defence-related phenotypes of *nox1* and *atgsnor1-3 nox1* mutants are the key interest in this study.

Our findings suggest that the *nox1* mutant exhibits compromised *R*-gene mediated resistance, including extend HR cell death and enhanced pathogen susceptibility in response to *Pst* DC3000 (*avrB*) and *Pst* DC3000 (*avrRPS4*). These phenotypes are also shown in *atgsnor1-3* plants. In addition, the intercellular SNO level was also increased in *nox1* plants in response to *Pst* DC3000 (*avrB*). Herein, it is reasonable to presume that the compromised *R*-gene mediated resistance in *nox1* plants is due to the increased GSNO production. Firstly, the activity of NADPH oxidase is supressed through S-nitrosylation in both *nox1* and *atgsnor1-3* plants (Yun *et al.* 2011). A NADPH-independent pathway promotes the HR development in both *nox1* and *atgsnor1-3* mutants. In addition, GSNOR is a metalloenzyme that binds zinc and

contains 15 Cys residues. It is possible that GSNOR activity is regulated by S-nitrosylation.

Moreover, *nox1* plants show repressed basal resistance, which has similar disease symptoms and growth level of *Pst* DC3000 as these found in *atgsnor1-3* plants. The NPR1 monomers are thought to be important for basal resistance, but the NPR1 monomerization shift in *nox1* plants is reduced in response to SA treatment compared to Col-0 (Yun and Loake, unpublished). Therefore, the reduced NPR1 monomerization might be associated with the enhanced susceptibility in *nox1* plants.

It is possible that the increased GSNO promotes disease susceptibilities in *nox1* plants. However, *atgsnor1-3 nox1* mutant shows greater HR development and pathogen susceptibility than its parental plants. Thus, NO and GSNO might additively function to manipulate the host defence, but GSNO plays a predominant role.

GSNOR is highly specific for the metabolism of GNSO that lacks the specificity to fine-turn the NO signalling. S-nitrosylation specifically targets protein metal or critical Cys residues. Therefore, in addition to GSNOR, an enzyme might function on specific S-nitrosylated Cys or metal residues (Foster *et al.* 2009). In summary, NO might use a distinct pathway to regulate the plant defence response.

7.2 Genetic screening for mutants integral NO recognition

NO signal transduction is well studied in mammals, which initiates cGMP dependent signalling pathway and an alternative pathway through S-nitrosylation (Foster *et al.* 2003, Yamasaki 2010). However, there are no genes identified to encode NOS in high plants (Foresi *et al.* 2010, Moreau *et al.* 2010). Furthermore, no NO-dependent sGC are identified to be responsible for cGMP production (Ludidi and Gehring 2003, Kwezi *et al.* 2007). Hence, identification of key genes involved in NO perception could uncover the molecular machinery underpinning NO signal transduction. For this purpose, forward genetic approaches have been employed in plants to genetically dissect S(NO) signalling.

Forward genetics could be used to identify genes integral to NO recognition. Herein, *At3g28740* and *At1g76600* were identified to be NO inducible, and transgenic lines containing the NO-reporter cassettes were established in this study. Further work is to induce heritable mutants of non-allelic suppressor and/or enhancer mutations by ethyl methane sulfonate (EMS) treatment. The seeds from NO-reporter lines will be subjected to mutagenesis, and subsequently two distinct genetic screens will be approached to isolate candidate plants that have abnormal NO recognition ability, including failure to respond to NO and constitutive expression of NO-marker genes in the absence of NO. Furthermore, the mutations will be identified by next generation sequencing to locate the mutation sites in the genome, which corresponds to the loss and gain of NO perception ability.

In mammalians, NOS/sGC/cGMP mediated NO production and signal transduction is intensively studied, which involves in metal nitration (Moreau *et al.* 2010, Yamasaki 2010). In plants, several possible resources, oxidative or reductive mechanisms, have been proposed responsible for NO production (Durner *et al.* 1998, Modolo *et al.* 2005, Rumer *et al.* 2009, Foresi *et al.* 2010). However, to date, the routes of NO biosynthesis in plants have not been well described. In addition, the enzyme that structurally related NOS has not been identified in higher plants. The earlier study suggests that an additional enzyme might regulate specific S-nitrosylated proteins, or protein metal-nitrosylation to fine-turn NO bioactivity.

Accordingly, genetic screens in *Arabidopsis* mutants integral NO recognition might be informative to understanding of NO generating mechanisms.

7.3 Potential key genes involved in NO signalling

Putative transcriptional factors (TFs) *ZAT7, ZAT8* and *ZAT12* might be involved in the regulatory mechanism of NO signalling in plants. Evidence indicated that the expression of these genes is up regulated by exogenous NO donor (Palmieri *et al.* 2008, Ahlfors *et al.* 2009) and considered as the result of gene duplication (Ciftci-Yilmaz and Mittler 2008). Moreover, both *ZAT7* and *ZAT12* have been potentially shown to be involved in oxidative response (Rizhsky *et al.* 2004).

Here, we report that growth of *zat8* plants is repressed by different NO donors. Thus, *ZAT8* might be important to protect against nitrosative stress. The zinc finger TF mediated induction of nitrosative stress response has been demonstrated in yeast (Chiranand *et al.* 2008). GSNOR is critical for establishment of resistance against nitrosative stress. Hence, the experiment of determining transcript level and activity of GSNOR will be carried out in *zat8* plants, which might ultimately influence the nitrosative response.

In this study, *zat7, zat8* and *zat12* plants show strong disease susceptibility to *Pst* DC3000, which implies that they might positively regulate NO-induced basal resistance. Following the analysis of protein secondary structures, EAR domain was found in ZAT7, ZAT8 and ZAT12. Several EAR motif-containing proteins have been reported to function as repressors (Kagale and Rozwadowski 2011). The EAR motif is required for interaction between ZAT7 and WRKY70, in which WRKY70 confers enhanced expression of SA-induced *PR1* to increase the resistance to virulent pathogen (Li *et al.* 2004, Ciftci-Yilmaz *et al.* 2007). It is possible that these ZFPs might interact with defence regulators to positively regulate host defence. In addition, *ZAT12*-deficient mutant failed to enhance the expression of *WRKY25* during oxidative stress (Rizhsky *et al.* 2004). Evidence suggested that WRKY25 is involved in both pathogen growth and disease symptom development and its induction can be altered by both SA treatment and pathogen infection in Col-0 plants (Rizhsky *et al.* 2004, Zheng *et al.* 2007). Therefore, it is reasonable to speculate that these ZFPs repress the transcriptional initiation of repressors of NO-related defence response.

Analysis of protein function and structure suggested that *ZAT7* and *ZAT8* might function redundantly. Surprisingly, both *zat7* and *zat8* single mutants showed enhanced pathogen growth in response to *Pst* DC3000, which repudiate the previous hypothesis. Because *ZAT7* has been reported to be involved in H_2O_2-induced oxidative stress (Rizhsky *et al.* 2004). Therefore, it is possible that *ZAT7* and *ZAT8* might function in *R-gene* mediated resistance and basal resistance, respectively. However, to verify this hypothesis, further characterisation of *zat7, zat8* and *zat7 zat8* plants against various pathogens will need to be carried out.

An *in vitro* study suggested that S-nitrosylation influences the structure and DNA binding activity of an *Arabidopsis* TF AtMYB30, which might subsequently regulate the defence responce (Tavares *et al.* 2014). Herein, it could be worth determining whether S-nitrosylation regulates the activity of these NO-induced ZFPs. In addition, *in silico* analysis suggests that *ZAT8* promoter region contains the binding sites of C_2H_2 ZFTF, it implies that expression of *ZAT8* might be autoregulatory. Moreover, there are several defence-related TFs are predicted to interact with promoters of these putative ZFTFs, such as WRKY 33, WRKY 18 and WRKY48. Hence, biotin-switch and electrophoresis mobility shift assay (EMSA) will help to understand the binding activity of ZAT8 and the effect by S-nitrosylation. In the meantime, characterisation of *zat7, zat8, zat12* and *zat7 zat8* double mutants is required. These data may provide evidence to elucidate the potential mechanisms for NO-mediated transcriptional reprogramming in the plant defence response.

7.4 Conclusion

S-nitrosylation is the major route of NO signal transduction, which has emerged as one of the most important post-translational modifications in plant defence responses. The results reported here show that high NO levels might compromise plant defence responses by promoting S-nitrosylation of proteins. This finding has supported the study of NO-mediated negative feedback loop that restricts HR development by inhibiting reactive oxygen species (ROS) production through NAPDH oxidase (RbohD) S-nitrosylation (Yun *et al.* 2011).

GSNO is thought to be an endogenous NO reservoir in plants that contributes to the equilibrium of protein S-nitrosylation and de-S-nitrosylation. In yeast, NO-dependent but GSNO-independent protein modification has been demonstrated previously (Foster *et al.* 2009). This project has shown a similar finding in plants that a NO-signalling pathway exists in addition to a GSNO-dependent pathway. Hence, NO and GSNO might have additive functions in disease resistance.

NO synthesis and associated signal transduction have been well described in mammals. However, a NOS-like enzyme for NO production remains elusive in plants. In addition, there is no current evidence for an NO-regulated, soluble guanyl cyclase (sGC). Hence, whether 3,5-cyclic guanosine monophosphate (cGMP) serves as secondary messenger of NO signal transduction in plants is questionable. In this study, generation of an NO-reporter *Arabidopsis* plants has provided a platform to identify genes that might involve in NO perception, which will help to understand the initial NO signalling pathway in plants.

S-nitrosylation of nuclear proteins might play a role in the regulation of transcription in plants. For example, the Zinc-finger (ZF) motif found in ZF transcriptional factors (ZnTFs) is rich in cysteines and is also sensitive to S-nitrosylation, which makes this TF class a target of redox-mediated regulation. In mammals, several ZnTFs that function in neuronal physiology are reported to be S-nitrosylated and participate in NO-mediated gene expression (Matthews *et al.* 1996, Riccio *et al.* 2006, Nott and Riccio 2009). This project has identified several putative ZnTFs in *Arabidopsis*

which are strongly induced by NO and might function in basal resistance in response to *Pst* DC3000. In-depth analysis of these NO-inducible ZnTFs in disease resistance may provide insights into the regulation of the plant immune system through NO-mediated transcriptional regulation.

Due to time constraints, some key experiments have not been undertaken. For instance, studies of dynamical changes in the SA-mediated defence pathway in *nox1* and *atgsnor1-3 nox1* double mutants will help to understand crosstalk of NO and SA signals in the modulation of the defence response. The study of transgenic plants expressing Flag-tagged ZnTFs will provide *in vivo* evidence to demonstrate the impacts of S-nitrosylation of TFs in the regulation of the defence response. In addition, mutant screen on NO-reporter lines and characterisation might lead to identification of proteins that regulate NO level.

In summary, a model of NO-signalling transduction in plant immunity is shown below. This project has provided a series of platforms to dissect the NO signalling network in the plants defence response. These findings might help discover additional NO signalling components and contribute to our understanding of how NO signalling is initiated, transduced and translated into downstream defence responses in plants.

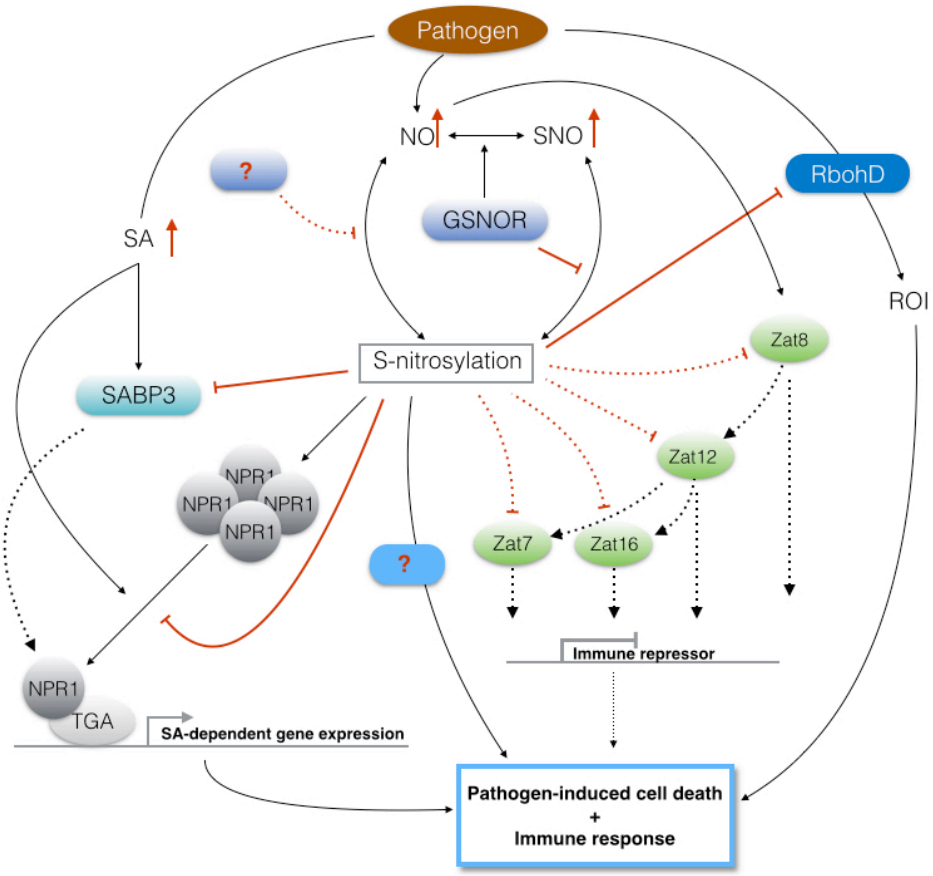

Figure 7-1 Model of NO-signalling in plant immunity.

Pathogen perception results in NO production. Its bioactivity is transduced through S-nitrosylation of rare highly reactive Cys residues of protein. The cellular S-nitrosylation levels are controlled by both GSNOR-dependent and GSNOR-independent pathways. ROI burst through RbohD leads to the development of cell death. S(NO) might block RboHD activity by S-nitrosylation and regulate cell death via an unknown pathway after reaching a critical threshold level. Pathogen recognition also triggers SA accumulation, resulting in activation of SABP3 and conversion of NPR1 monomeric from oligomeric. Monomeric NPR1 is translocated into nucleus and binds TGA1 to express SA-dependent defence genes, which enables immune response. However, S-nitrosylation negatively regulates SABP3 activity and promotes NPR1 oligomeric, which limits immune response. *ZAT8* expression is triggered by NO accumulation, and subsequently activates expression of *ZAT12, ZAT7* and *Zat16.* These proteins then repress the expression of immune repressors and result in pathogen-induced cell death and immune response. However, the activities of these proteins might be blunt by S-nitrosylation, which enables the expression of immune repressors.

Bibliography

Abbas, A.K., Lichtman, A.H., 2009. Basic immunology: Functions and disorders of the immune system. Philadelphia, Pa. : Saunders/Elsevier, [2009], ©2009.

Aboul-Soud, M.A., Aboul-Enein, A.M., Loake, G.J., 2009. Nitric oxide triggers specific and dose-dependent cytosolic calcium transients in *Arabidopsis*. Plant Signaling & Behavior 4 (3), 191-196.

Aboul-Soud, M.a.M., Cook, K., Loake, G.J., 2004. Measurement of salicylic acid by a high-performance liquid chromatography procedure based on ion-exchange. Chromatographia 59 (1-2), 129-133.

Aharoni, A., Dixit, S., Jetter, R., Thoenes, E., Van Arkel, G., Pereira, A., 2004. The SHINE Clade of AP2 domain transcription factors activates wax biosynthesis, alters cuticle properties, and confers drought tolerance when overexpressed in *Arabidopsis*. Plant Cell 16 (9), 2463-2480.

Ahern, G.P., Klyachko, V.A., Jackson, M.B., 2002. cGMP and S-nitrosylation: Two routes for modulation of neuronal excitability by NO. Trends in Neurosciences 25 (10), 510-517.

Ahlfors, R., Brosche, M., Kollist, H., Kangasjarvi, J., 2009. Nitric oxide modulates ozone-induced cell death, hormone biosynthesis and gene expression in *Arabidopsis thaliana*. Plant Journal 58 (1), 1-12.

Ali, R., Ma, W., Lemtiri-Chlieh, F., Tsaltas, D., Leng, Q., Von Bodman, S., Berkowitz, G.A., 2007. Death don't have NO mercy and neither does calcium: *Arabidopsis* Cyclic Nucleotide Gated Channel 2 and innate immunity. Plant Cell 19 (3), 1081-1095.

Amicucci, E., Gaschler, K., Ward, J.M., 1999. NADPH oxidase genes from tomato (*Lycopersicon esculentum*) and curly-leaf pondweed (*Potamogeton crispus*). Plant Biology 1 (5), 524-528.

Anand, B., Surana, P., Prakash, B., 2010. Deciphering the catalytic machinery in 30s Ribosome assembly GTPase YqeH. PloS one 5 (4), e9944.

Appleby, C.A., 1984. Leghemoglobin and *rhizobium* respiration. Annual Review of Plant Physiology and Plant Molecular Biology 35, 443-478.

Arasimowicz, M., Floryszak-Wieczorek, J., 2007. Nitric oxide as a bioactive signalling molecule in plant stress responses. Plant Science 172 (5), 876-887.

Asai, T., Tena, G., Plotnikova, J., Willmann, M.R., Chiu, W.L., Gomez-Gomez, L., Boller, T., Ausubel, F.M., Sheen, J., 2002. MAP kinase signalling cascade in *Arabidopsis* innate immunity. Nature 415 (6875), 977-983.

Astier, J., Besson-Bard, A., Wawer, I., Parent, C., Rasul, S., Jeandroz, S., Dat, J. And Wendehenne, D., 2010. Nitric oxide signalling in plants: Crosstalk with Ca^{2+}, protein kinases and reactive oxygen species. Annual Plant Reviews 42: Nitrogen Metabolism in Plants in the Post-Genomic Era, Wiley-Blackwell, 147-170, 2010.

Atkinson, M.M., Midland, S.L., Sims, J.J., Keen, N.T., 1996. Syringolide 1 triggers Ca^{2+} influx, K^{+} efflux, and extracellular alkalization in soybean cells carrying the disease-resistance gene *Rpg4*. Plant Physiology 112 (1), 297-302.

Ausubel, F., 2005. Are innate immune signaling pathways in plants and animals conserved? Nature Immunology 6 (10), 973-979.

Avram, D., Leid, M., Bakalinsky, A.T., 1999. Fzf1p of *Saccharomyces cerevisiae* is a positive regulator of *SSU1* transcription and its first zinc finger region is required for DNA binding. Yeast 15 (6), 473-480.

Bailey, B., Dean, J., Anderson, J., 1990. An ethylene biosynthesis-inducing endoxylanase elicits electrolyte leakage and necrosis in *Nicotiana tabacum* cv Xanthi leaves. Plant physiology 94 (4), 1849-1854.

Beck, K.F., Eberhardt, W., Frank, S., Huwiler, A., Messmer, U.K., Muhl, H., Pfeilschifter, J., 1999. Inducible no synthase: Role in cellular signalling. Journal of Experimental Biology 202 (6), 645-653.

Belenghi, B., Romero-Puertas, M.C., Vercammen, D., Brackenier, A., Inze, D., Delledonne, M., Van Breusegem, F., 2007. Metacaspase activity of *Arabidopsis thaliana* is regulated by S-nitrosylation of a critical cysteine residue. Journal of Biological Chemistry 282 (2), 1352-1358.

Berg, J.M., Shi, Y.G., 1996. The galvanization of biology: A growing appreciation for the roles of zinc. Science 271 (5252), 1081-1085.

Berrocal-Lobo, M., Stone, S., Yang, X., Antico, J., Callis, J., Ramonell, K.M., Somerville, S., 2010. ATL9, a RING zinc finger protein with E3 ubiquitin ligase activity implicated in chitin- and NADPH oxidase-mediated defense responses. PloS One 5 (12), e14426.

Besson-Bard, A., Pugin, A., Wendehenne, D., 2008. New insights into nitric oxide signaling in plants. Annual Review of Plant Biology 59, 21-39.

Bethke, P.C., Badger, M.R., Jones, R.L., 2004. Apoplastic synthesis of nitric oxide by plant tissues. Plant Cell 16 (2), 332-341.

Boller, T., Felix, G., 2009. A renaissance of elicitors: Perception of microbe-associated molecular patterns and danger signals by pattern-recognition receptors. Annual Review of Plant Biology 60, 379-406.

Boller, T., He, S.Y., 2009. Innate immunity in plants: An arms race between pattern recognition receptors in plants and effectors in microbial pathogens. Science 324 (5928), 742-744.

Bolwell, G.P., Bindschedler, L.V., Blee, K.A., Butt, V.S., Davies, D.R., Gardner, S.L., Gerrish, C., Minibayeva, F., 2002. The apoplastic oxidative burst in response to biotic stress in plants: A three-component system. Journal of Experimental Botany 53 (372), 1367-1376.

Bolwell, G.P., Wojtaszek, P., 1997. Mechanisms for the generation of reactive oxygen species in plant defence - a broad perspective. Physiological and Molecular Plant Pathology 51 (6), 347-366.

Bonfoco, E., Krainc, D., Ankarcrona, M., Nicotera, P., Lipton, S.A., 1995. Apoptosis and necrosis: two distinct events induced, respectively, by mild and intense insults with N-methyl-D-aspartate or nitric-oxide/superoxide in cortical cell-cultures. Proceedings of the National Academy of Sciences of the United States of America 92 (16), 7162-7166.

Boter, M., Ruiz-Rivero, O., Abdeen, A., Prat, S., 2004. Conserved MYC transcription factors play a key role in jasmonate signaling both in tomato and *Arabidopsis*. Genes & Development 18 (13), 1577-1591.

Bradley, D.J., Kjellbom, P., Lamb, C.J., 1992. Elicitor-induced and wound-induced oxidative cross-linking of a proline-rich plant-cell wall protein: a novel, rapid defense response. Cell 70 (1), 21-30.

Brandwagt, B.F., Mesbah, L.A., Takken, F.L.W., Laurent, P.L., Kneppers, T.J.A., Hille, J., Nijkamp, H.J.J., 2000. A longevity assurance gene homolog of tomato mediates resistance to *Alternaria alternata* f. Sp *lycopersici* toxins and fumonisin B_1. Proceedings of the National Academy of Sciences of the United States of America 97 (9), 4961-4966.

Bright, J., Desikan, R., Hancock, J.T., Weir, I.S., Neill, S.J., 2006. ABA-induced NO generation and stomatal closure in *Arabidopsis* are dependent on H_2O_2 synthesis. Plant Journal 45 (1), 113-122.

Calabrese, V., Mancuso, C., Calvani, M., Rizzarelli, E., Butterfield, D.A., Stella, A.M., 2007. Nitric oxide in the central nervous system: Neuroprotection versus neurotoxicity. Nature Reviews Neuroscience 8 (10), 766-775.

Canonne, J., Marino, D., Jauneau, A., Pouzet, C., Briere, C., Roby, D., Rivas, S., 2011. The *Xanthomonas* type III effector XopD targets the *Arabidopsis* transcription factor MYB30 to suppress plant defense. Plant Cell 23 (9), 3498-3511.

Cao, H., Bowling, S.A., Gordon, A.S., Dong, X.N., 1994. Characterization of an *Arabidopsis* mutant that is nonresponsive to inducers of systemic acquired-resistance. Plant Cell 6 (11), 1583-1592.

Chanda, B., Xia, Y., Mandal, M., Yu, K., Sekine, K.-T., Gao, Q.-M., Selote, D., Hu, Y., Stromberg, A., Navarre, D., Kachroo, A., Kachroo, P., 2011. Glycerol-3-phosphate is a critical mobile inducer of systemic immunity in plants. Nature Genetics 43 (5), 421-427.

Chandok, M.R., Ytterberg, A.J., Van Wijk, K.J., Klessig, D.F., 2003. The pathogen-inducible nitric oxide synthase (iNOS) in plants is a variant of the P protein of the glycine decarboxylase complex. Cell 113 (4), 469-482.

Chassot, C., Nawrath, C., Metraux, J.P., 2007. Cuticular defects lead to full immunity to a major plant pathogen. Plant Journal 49 (6), 972-980.

Chen, S.R., Dickman, M.B., 2004. Bcl-2 family members localize to tobacco chloroplasts and inhibit programmed cell death induced by chloroplast-targeted herbicides. Journal of Experimental Botany 55 (408), 2617-2623.

Chen, W.Q., Provart, N.J., Glazebrook, J., Katagiri, F., Chang, H.S., Eulgem, T., Mauch, F., Luan, S., Zou, G.Z., Whitham, S.A., Budworth, P.R., Tao, Y., Xie, Z.Y., Chen, X., Lam, S., Kreps, J.A., Harper, J.F., Si-Ammour, A., Mauch-Mani, B., Heinlein, M., Kobayashi, K., Hohn, T., Dangl, J.L., Wang, X., Zhu, T., 2002. Expression profile matrix of *Arabidopsis* transcription factor genes suggests their putative functions in response to environmental stresses. Plant Cell 14 (3), 559-574.

Cheval, C., Aldon, D., Galaud, J.P., Ranty, B., 2013. Calcium/calmodulin-mediated regulation of plant immunity. Biochimica et Biophysica Acta (BBA) - Molecular Cell Research 1833 (7), 1766-1771.

Chinchilla, D., Zipfel, C., Robatzek, S., Kemmerling, B., Nurnberger, T., Jones, J.D., Felix, G., Boller, T., 2007. A flagellin-induced complex of the receptor FLS2 and BAK1 initiates plant defence. Nature 448 (7152), 497-500.

Chini, A., Grant, J.J., Seki, M., Shinozaki, K., Loake, G.J., 2004. Drought tolerance established by enhanced expression of the CC-NBS-LRR gene, *ADR1*, requires salicylic acid, EDS1 and ABI1. Plant Journal 38 (5), 810-822.

Chiranand, W., Mcleod, I., Zhou, H.J., Lynn, J.J., Vega, L.A., Myers, H., Yates, J.R., Lorenz, M.C., Gustin, M.C., 2008. *CTA4* transcription factor mediates induction of nitrosative stress response in *Candida albicans*. Eukaryotic Cell 7 (2), 268-278.

Chisholm, S.T., Coaker, G., Day, B., Staskawicz, B.J., 2006. Host-microbe interactions: Shaping the evolution of the plant immune response. Cell 124 (4), 803-814.

Ciftci-Yilmaz, S., Mittler, R., 2008. The zinc finger network of plants. Cellular and Molecular Life Sciences 65 (7-8), 1150-1160.

Ciftci-Yilmaz, S., Morsy, M.R., Song, L.H., Coutu, A., Krizek, B.A., Lewis, M.W., Warren, D., Cushman, J., Connolly, E.L., Mittler, R., 2007. The EAR-motif of the Cys2/His2-type zinc finger protein ZAT7 plays a key role in the defense response of *Arabidopsis* to salinity stress. Journal of Biological Chemistry 282 (12), 9260-9268.

Clementi, E., 1998. Role of nitric oxide and its intracellular signalling pathways in the control of Ca^{2+} homeostasis. Biochemical Pharmacology 55 (6), 713-718.

Clough, S.J., Bent, A.F., 1998. Floral dip: A simplified method for *Agrobacterium*-mediated transformation of *Arabidopsis thaliana*. Plant Journal 16 (6), 735-743.

Clough, S.J., Fengler, K.A., Yu, I.C., Lippok, B., Smith, R.K., Jr., Bent, A.F., 2000. The Arabidopsis *dnd1* "defense, no death" gene encodes a mutated cyclic nucleotide-gated ion channel. Proceedings of the National Academy of Sciences of the United States of America 97 (16), 9323-9328.

Coll, N.S., Vercammen, D., Smidler, A., Clover, C., Van Breusegem, F., Dangl, J.L., Epple, P., 2010. *Arabidopsis* type I metacaspases control cell death. Science 330 (6009), 1393-1397.

Corpas, F.J., Palma, J.M., Del Rio, L.A., Barroso, J.B., 2009. Evidence supporting the existence of L-arginine-dependent nitric oxide synthase activity in plants. New Phytologist 184 (1), 9-14.

Crane, B.R., Sudhamsu, J., Patel, B.A., 2010. Bacterial nitric oxide synthases. Annual Review of Biochemistry 79, 445-470.

Crawford, N.M., Galli, M., Tischner, R., Heimer, Y.M., Okamoto, M., Mack, A., 2006. Response to Zemojtel *et al*: Plant nitric oxide synthase: back to square one. Trends in Plant Science 11 (11), 526-527.

Cueto, M., Hernandezperera, O., Martin, R., Bentura, M.L., Rodrigo, J., Lamas, S., Golvano, M.P., 1996. Presence of nitric oxide synthase activity in roots and nodules of *Lupinus albus*. FEBS Letters 398 (2-3), 159-164.

Dangl, J.L., Jones, J.D.G., 2001. Plant pathogens and integrated defence responses to infection. Nature 411 (6839), 826-833.

Danna, C.H., Millet, Y.A., Koller, T., Han, S.W., Bent, A.F., Ronald, P.C., Ausubel, F.M., 2011. The *Arabidopsis* flagellin receptor FLS2 mediates the perception of *Xanthomonas* Ax21 secreted peptides. Proceedings of the National Academy of Sciences of the United States of America 108 (22), 9286-9291.

Darvill, A., Albersheim, P., 1984. Phytoalexins and their elicitors-a defense against microbial infection in plants. Annual Review of Plant Physiology 35, 243-275.

Davletova, S., Schlauch, K., Coutu, J., Mittler, R., 2005. The zinc-finger protein ZAT12 plays a central role in reactive oxygen and abiotic stress signaling in *Arabidopsis*. Plant Physiology 139 (2), 847-856.

De Guzman, R.N., Liu, H.Y., Martinez-Yamout, M., Dyson, H.J., Wright, P.E., 2000. Solution structure of the TAZ2 (CH3) domain of the transcriptional adaptor protein CBP. Journal of Molecular Biology 303 (2), 243-253.

Delaney, T., Uknes, S., Vernooij, B., Friedrich, L., Weymann, K., Negrotto, D., Gaffney, T., Gut-Rella, M., Kessmann, H., Ward, E., Ryals, J., 1994. A central role of salicylic acid in plant disease resistance. Science 266 (5188), 1247-1250.

Dellagi, A., Brisset, M.N., Paulin, J.P., Expert, D., 1998. Dual role of desferrioxamine in *Erwinia amylovora* pathogenicity. Molecular Plant-Microbe Interactions 11 (8), 734-742.

Delledonne, M., Murgia, I., Ederle, D., Sbicego, P.F., Biondani, A., Polverari, A., Lamb, C., 2002. Reactive oxygen intermediates modulate nitric oxide signaling in the plant hypersensitive disease-resistance response. Plant Physiology and Biochemistry 40 (6-8), 605-610.

Delledonne, M., Xia, Y., Dixon, R.A., Lamb, C., 1998. Nitric oxide functions as a signal in plant disease resistance. Nature 394 (6693), 585-8.

Delledonne, M., Zeier, J., Marocco, A., Lamb, C., 2001. Signal interactions between nitric oxide and reactive oxygen intermediates in the plant hypersensitive disease resistance response. Proceedings of the National Academy of Sciences of the United States of America 98 (23), 13454-13459.

Deng, H.Q., Liu, H.B., Li, X.H., Xiao, J.H., Wang, S.P., 2012. A CCCH-type zinc finger nucleic acid-binding protein quantitatively confers resistance against rice bacterial blight disease. Plant Physiology 158 (2), 876-889.

Derelle, E., Ferraz, C., Rombauts, S., Rouze, P., Worden, A.Z., Robbens, S., Partensky, F., Degroeve, S., Echeynie, S., Cooke, R., Saeys, Y., Wuyts, J., Jabbari, K., Bowler, C., Panaud, O., Piegu, B., Ball, S.G., Ral, J.P., Bouget, F.Y., Piganeau, G., De Baets, B., Picard, A., Delseny, M., Demaille, J., Van De Peer, Y., Moreau, H., 2006. Genome analysis of the smallest free-living eukaryote *Ostreococcus tauri* unveils many unique features. Proceedings of the National Academy of Sciences of the United States of America 103 (31), 11647-11652.

Desikan, R., Griffiths, R., Hancock, J., Neill, S., 2002. A new role for an old enzyme: Nitrate reductase-mediated nitric oxide generation is required for abscisic acid-induced stomatal closure in *Arabidopsis thaliana*. Proceedings of the National Academy of Sciences of the United States of America 99 (25), 16314-16318.

Deslandes, L., Olivier, J., Peeters, N., Feng, D.X., Khounlotham, M., Boucher, C., Somssich, I., Genin, S., Marco, Y., 2003. Physical interaction between RRS1-R, a protein conferring resistance to bacterial wilt, and PopP2, a type III effector targeted to the plant nucleus. Proceedings of the National Academy of Sciences of the United States of America 100 (13), 8024-8029.

Dixon, R.A., 2001. Natural products and plant disease resistance. Nature 411 (6839), 843-847.

Dodds, P.N., Rathjen, J.P., 2010. Plant immunity: Towards an integrated view of plant-pathogen interactions. Nature Reviews Genetics 11 (8), 539-548.

Doke, N., Miura, Y., Sanchez, L.M., Park, H.J., Noritake, T., Yoshioka, H., Kawakita, K., 1996. The oxidative burst protects plants against pathogen attack: Mechanism and role as an emergency signal for plant bio-defence - a review. Gene 179 (1), 45-51.

Donaldson, L., Ludidi, N., Knight, M.R., Gehring, C., Denby, K., 2004. Salt and osmotic stress cause rapid increases in *Arabidopsis thaliana* cGMP levels. FEBS Letters 569 (1-3), 317-320.

Dong, J.X., Chen, C.H., Chen, Z.X., 2003. Expression profiles of the *Arabidopsis* WRKY gene superfamily during plant defense response. Plant Molecular Biology 51 (1), 21-37.

Dordas, C., Rivoal, J., Hill, R.D., 2003. Plant haemoglobins, nitric oxide and hypoxic stress. Annals of Botany 91 (2), 173-178.

Dorey, S., Kopp, M., Geoffroy, P., Fritig, B., Kauffmann, S., 1999. Hydrogen peroxide from the oxidative burst is neither necessary nor sufficient for hypersensitive cell death induction, phenylalanine ammonia lyase stimulation, salicylic acid accumulation, or scopoletin consumption in cultured tobacco cells treated with elicitin. Plant Physiology 121 (1), 163-172.

Dudler, R., 2013. Manipulation of host proteasomes as a virulence mechanism of plant pathogens. Annual Review of Phytopathology, Vol 51 51, 521-542.

Durner, J., Wendehenne, D., Klessig, D.F., 1998. Defense gene induction in tobacco by nitric oxide, cyclic GMP, and cyclic ADP-ribose. Proceedings of the National Academy of Sciences of the United States of America 95 (17), 10328-10333.

Ellis, J., Jones, D., 1998. Structure and function of proteins controlling strain-specific pathogen resistance in plants. Current Opinion in Plant Biology 1 (4), 288-293.

Englbrecht, C.C., Schoof, H., Bohm, S., 2004. Conservation, diversification and expansion of C2H2 zinc finger proteins in the *Arabidopsis thaliana* genome. BMC Genomics 5 (1), 39.

Epple, P., Mack, A.A., Morris, V.R.F., Dangl, J.L., 2003. Antagonistic control of oxidative stress-induced cell death in *Arabidopsis* by two related, plant-specific zinc finger proteins. Proceedings of the National Academy of Sciences of the United States of America 100 (11), 6831-6836.

Erbs, G., Silipo, A., Aslam, S., De Castro, C., Liparoti, V., Flagiello, A., Pucci, P., Lanzetta, R., Parrilli, M., Molinaro, A., Newman, M.-A., Cooper, R., 2008. Peptidoglycan and Muropeptides from pathogens *Agrobacterium* and *Xanthomonas* elicit plant innate immunity: Structure and activity. Chemistry & biology 15 (5), 438-448.

Eulgem, T., Somssich, I.E., 2007. Networks of WRKY transcription factors in defense signaling. Current Opinion in Plant Biology 10 (4), 366-371.

Faulkner, C., Robatzek, S., 2012. Plants and pathogens: Putting infection strategies and defence mechanisms on the map. Current Opinion in Plant Biology 15 (6), 699-707.

Feechan, A., Kwon, E., Yun, B.W., Wang, Y., Pallas, J.A., Loake, G.J., 2005. A central role for S-nitrosothiols in plant disease resistance. Proceedings of the National Academy of Sciences of the United States of America 102 (22), 8054-8059.

Felix, G., Boller, T., 2003. Molecular sensing of bacteria in plants. The highly conserved RNA-binding motif RNP-1 of bacterial cold shock proteins is recognized as an elicitor signal in tobacco. The Journal of biological chemistry 278 (8), 6201-6208.

Felix, G., Duran, J.D., Volko, S., Boller, T., 1999. Plants have a sensitive perception system for the most conserved domain of bacterial flagellin. Plant Journal 18 (3), 265-276.

Felix, G., Regenass, M., Boller, T., 1993. Specific perception of subnanomolar concentrations of chitin fragments by tomato cells: Induction of extracellular alkalinization, changes in protein phosphorylation. Plant Journal 4 (2), 307-316.

Feys, B.J., Parker, J.E., 2000. Interplay of signaling pathways in plant disease resistance. Trends in Genetics 16 (10), 449-455.

Foissner, I., Wendehenne, D., Langebartels, C., Durner, J., 2000. In vivo imaging of an elicitor-induced nitric oxide burst in tobacco. Plant Journal 23 (6), 817-824.

Foresi, N., Correa-Aragunde, N., Parisi, G., Calo, G., Salerno, G., Lamattina, L., 2010. Characterization of a nitric oxide synthase from the plant kingdom: No generation from the green alga *Ostreococcus tauri* is light irradiance and growth phase dependent. Plant Cell 22 (11), 3816-3830.

Foster, M.W., Liu, L., Zeng, M., Hess, D.T., Stamler, J.S., 2009. A genetic analysis of nitrosative stress. Biochemistry 48 (4), 792-799.

Foster, M.W., Mcmahon, T.J., Stamler, J.S., 2003. S-nitrosylation in health and disease. Trends in Molecular Medicine 9 (4), 160-168.

Foster, M.W., Stamler, J.S., 2004. New insights into protein S-nitrosylation - mitochondria as a model system. Journal of Biological Chemistry 279 (24), 25891-25897.

Fox, A.H., Liew, C., Holmes, M., Kowalski, K., Mackay, J., Crossley, M., 1999. Transcriptional cofactors of the FOG family interact with GATA proteins by means of multiple zinc fingers. EMBO Journal 18 (10), 2812-2822.

Foyer, C.H., Noctor, G., 2013. Redox signaling in plants. Antioxidants & Redox Signaling 18 (16), 2087-2090.

Fu, Z., Dong, X., 2013. Systemic acquired resistance: Turning local infection into global defense. Annual review of plant biology 64, 839-863.

Fu, Z.Q., Yan, S.P., Saleh, A., Wang, W., Ruble, J., Oka, N., Mohan, R., Spoel, S.H., Tada, Y., Zheng, N., Dong, X.N., 2012. NPR3 and NPR4 are receptors for the immune signal salicylic acid in plants. Nature 486 (7402), 228-232.

Gaffney, T., Friedrich, L., Vernooij, B., Negrotto, D., Nye, G., Uknes, S., Ward, E., Kessmann, H., Ryals, J., 1993. Requirement of salicylic acid for the induction of systemic acquired resistance. Science 261 (5122), 754-756.

Garcia-Mata, C., Lamattina, L., 2002. Nitric oxide and Abscisic acid cross talk in guard cells. Plant Physiology 128 (3), 790-792.

Gardner, P.R., Gardner, A.M., Martin, L.A., Salzman, A.L., 1998. Nitric oxide dioxygenase: An enzymic function for flavohemoglobin. Proceedings of the National Academy of Sciences of the United States of America 95 (18), 10378-10383.

Gassmann, W., Hinsch, M.E., Staskawicz, B.J., 1999. The *Arabidopsis RPS4* bacterial-resistance gene is a member of the TIR-NBS-LRR family of disease-resistance genes. Plant Journal 20 (3), 265-277.

Gaulin, E., Dramé, N., Lafitte, C., Torto-Alalibo, T., Martinez, Y., Ameline-Torregrosa, C., Khatib, M., Mazarguil, H., Villalba-Mateos, F., Kamoun, S., Mazars, C., Dumas, B., Bottin, A., Esquerré-Tugayé, M.-T., Rickauer, M., 2006. Cellulose binding domains of a *Phytophthora* cell wall protein are novel pathogen-associated molecular patterns. Plant cell 18 (7), 1766-1777.

Gaupels, F., Furch, A.C.U., Will, T., Mur, L.a.J., Kogel, K.H., Van Bel, A.J.E., 2008. Nitric oxide generation in *Vicia faba* phloem cells reveals them to be sensitive detectors as well as possible systemic transducers of stress signals. New Phytologist 178 (3), 634-646.

Geilfus, C.M., Muhling, K.H., Kaiser, H., Plieth, C., 2014. Bacterially produced *Pt*-GFP as ratiometric dual-excitation sensor for *in planta* mapping of leaf apoplastic pH in intact *Avena sativa* and *Vicia faba*. Plant Methods 10 (1), 31.

Glazebrook, J., Rogers, E.E., Ausubel, F.M., 1996. Isolation of *Arabidopsis* mutants with enhanced disease susceptibility by direct screening. Genetics 143 (2), 973-982.

Glowacki, S., Macioszek, V.K., Kononowicz, A.K., 2011. R proteins as fundamentals of plant innate immunity. Cellular & Molecular Biology Letters 16 (1), 1-24.

Gomez-Gomez, L., Bauer, Z., Boller, T., 2001. Both the extracellular leucine-rich repeat domain and the kinase activity of FLS2 are required for flagellin binding and signaling in *Arabidopsis*. Plant Cell 13 (5), 1155-1163.

Gomez-Gomez, L., Felix, G., Boller, T., 1999. A single locus determines sensitivity to bacterial flagellin in *Arabidopsis thaliana*. Plant Journal 18 (3), 277-284.

Gow, A.J., Buerk, D.G., Ischiropoulos, H., 1997. A novel reaction mechanism for the formation of S-nitrosothiol *in vivo*. Journal of Biological Chemistry 272 (5), 2841-2845.

Grant, J.J., Chini, A., Basu, D., Loake, G.J., 2003. Targeted activation tagging of the *Arabidopsis NBS-LRR* gene, *ADR1*, conveys resistance to virulent pathogens. Molecular Plant-Microbe Interactions 16 (8), 669-680.

Grant, J.J., Yun, B.W., Loake, G.J., 2000a. Oxidative burst and cognate redox signalling reported by luciferase imaging: Identification of a signal network that functions independently of ethylene, SA and Me-JA but is dependent on MAPKK activity. Plant Journal 24 (5), 569-582.

Grant, M., Brown, I., Adams, S., Knight, M., Ainslie, A., Mansfield, J., 2000b. The *RPM1* plant disease resistance gene facilitates a rapid and sustained increase in cytosolic calcium that is necessary for the oxidative burst and hypersensitive cell death. Plant Journal 23 (4), 441-450.

Greenberg, J.T., Ausubel, F.M., 1993. *Arabidopsis* mutants compromised for the control of cellular damage during pathogenesis and aging. Plant Journal 4 (2), 327-341.

Greenberg, J.T., Guo, A., Klessig, D.F., Ausubel, F.M., 1994. Programmed cell death in plants: A pathogen-triggered response activated coordinately with multiple defense functions. Cell 77 (4), 551-563.

Groom, Q.J., Torres, M.A., Fordhamskelton, A.P., Hammondkosack, K.E., Robinson, N.J., Jones, J.D.G., 1996. *RbohA* a rice homologue of the mammalian *gp91*^{phox} respiratory burst oxidase gene. Plant Journal 10 (3), 515-522.

Guillaume, T., Marie, B., Jen, S., 2011. Protein kinase signaling networks in plant innate immunity. Current Opinion in Plant Biology 14 (5), 519-529.

Gupta, K.J., Stoimenova, M., Kaiser, W.M., 2005. In higher plants, only root mitochondria, but not leaf mitochondria reduce nitrite to NO, *in vitro* and *in situ*. Journal of Experimental Botany 56 (420), 2601-2609.

Gust, A., Biswas, R., Lenz, H., Rauhut, T., Ranf, S., Kemmerling, B., Götz, F., Glawischnig, E., Lee, J., Felix, G., Nürnberger, T., 2007. Bacteria-derived peptidoglycans

constitute pathogen-associated molecular patterns triggering innate immunity in *Arabidopsis*. The Journal of biological chemistry 282 (44), 32338-32348.

Hammond-Kosack, K.E., Silverman, P., Raskin, I., Jones, J., 1996. Race-specific elicitors of *Cladosporium fulvum* induce changes in cell morphology and the synthesis of ethylene and salicylic acid in tomato plants carrying the corresponding Cf disease resistance gene. Plant Physiology 110 (4), 1381-1394.

Hannarose, W., Hansen, U., 1996. Active repression mechanisms of eukaryotic transcription repressors. Trends in Genetics 12 (6), 229-234.

Hara, M.R., Agrawal, N., Kim, S.F., Cascio, M.B., Fujimuro, M., Ozeki, Y., Takahashi, M., Cheah, J.H., Tankou, S.K., Hester, L.D., Ferris, C.D., Hayward, S.D., Snyder, S.H., Sawa, A., 2005. S-nitrosylated GAPDH initiates apoptotic cell death by nuclear translocation following siah1 binding. Nature Cell Biology 7 (7), 665-674.

He, Y., Tang, R.H., Hao, Y., Stevens, R.D., Cook, C.W., Ahn, S.M., Jing, L., Yang, Z., Chen, L., Guo, F., Fiorani, F., Jackson, R.B., Crawford, N.M., Pei, Z.M., 2004. Nitric oxide represses the *Arabidopsis* floral transition. Science 305 (5692), 1968-1971.

Heazlewood, J.L., Tonti-Filippini, J., Verboom, R.E., Millar, A.H., 2005. Combining experimental and predicted datasets for determination of the subcellular location of proteins in *Arabidopsis*. Plant Physiology 139 (2), 598-609.

Hellens, R.P., Edwards, E.A., Leyland, N.R., Bean, S., Mullineaux, P.M., 2000. pGreen: A versatile and flexible binary Ti vector for *Agrobacterium*-mediated plant transformation. Plant Molecular Biology 42 (6), 819-832.

Hess, D.T., Matsumoto, A., Kim, S.O., Marshall, H.E., Stamler, J.S., 2005. Protein S-nitrosylation: Purview and parameters. Nature Reviews Molecular Cell Biology 6 (2), 150-166.

Holtgrefe, S., Gohlke, J., Starmann, J., Druce, S., Klocke, S., Altmann, B., Wojtera, J., Lindermayr, C., Scheibe, R., 2008. Regulation of plant cytosolic glyceraldehyde 3-phosphate dehydrogenase isoforms by thiol modifications. Physiologia Plantarum 133 (2), 211-228.

Huang, X., Von Rad, U., Durner, J., 2002. Nitric oxide induces transcriptional activation of the nitric oxide-tolerant alternative oxidase in *Arabidopsis* suspension cells. Planta 215 (6), 914-923.

Huffaker, A., Pearce, G., Ryan, C., 2006. An endogenous peptide signal in *Arabidopsis* activates components of the innate immune response. Proceedings of the National Academy of Sciences of the United States of America 103 (26), 10098-10103.

Ichimori, K., Stuehr, D.J., Atkinson, R.N., King, S.B., 1999. Synthesis and evaluation of new sulfur-containing L-arginine-derived inhibitors of nitric oxide synthase. Journal of Medicinal Chemistry 42 (10), 1842-1848.

Ingelman, M., Bianchi, V., Eklund, H., 1997. The three-dimensional structure of flavodoxin reductase from *Escherichia coli* at 1.7 å resolution. Journal of Molecular Biology 268 (1), 147-157.

Ingle, R.A., Carstens, M., Denby, K.J., 2006. PAMP recognition and the plant-pathogen arms race. Bioessays 28 (9), 880-889.

Ishiguro, S., Nakamura, K., 1994. Characterization of a cDNA encoding a novel DNA-binding protein, SPF1, that recognizes SP8 sequences in the 5' upstream regions of

genes coding for sporamin and beta-amylase from sweet potato. Molecular and General Genetics 244 (6), 563-571.

Iuchi, S., 2001. Three classes of C2H2 zinc finger proteins. Cellular and Molecular Life Sciences 58 (4), 625-635.

Jasid, S., Simontacchi, M., Bartoli, C.G., Puntarulo, S., 2006. Chloroplasts as a nitric oxide cellular source. Effect of reactive nitrogen species on chloroplastic lipids and proteins. Plant Physiology 142 (3), 1246-1255.

Jones, J.D.G., Dangl, J.L., 2006. The plant immune system. Nature 444 (7117), 323-329.

Jung, H.W., Tschaplinski, T.J., Wang, L., Glazebrook, J., Greenberg, J.T., 2009. Priming in systemic plant immunity. Science 324 (5923), 89-91.

Jurkowski, G.I., Smith, R.K., Jr., Yu, I.C., Ham, J.H., Sharma, S.B., Klessig, D.F., Fengler, K.A., Bent, A.F., 2004. *Arabidopsis DND2*, a second cyclic nucleotide-gated ion channel gene for which mutation causes the "defense, no death" phenotype. Molecular Plant-Microbe Interactions 17 (5), 511-520.

Kagale, S., Rozwadowski, K., 2011. EAR motif-mediated transcriptional repression in plants an underlying mechanism for epigenetic regulation of gene expression. Epigenetics 6 (2), 141-146.

Kaku, H., Nishizawa, Y., Ishii-Minami, N., Akimoto-Tomiyama, C., Dohmae, N., Takio, K., Minami, E., Shibuya, N., 2006. Plant cells recognize chitin fragments for defense signaling through a plasma membrane receptor. Proceedings of the National Academy of Sciences of the United States of America 103 (29), 11086-11091.

Karimi, M., Inze, D., Depicker, A., 2002. Gateway vectors for *Agrobacterium*-mediated plant transformation. Trends Plant Sci 7 (5), 193-195.

Kato, H., Asai, S., Yamamoto-Katou, A., Yoshioka, H., Doke, N., Kawakita, K., 2008. Involvement of NbNOA1 in NO production and defense responses in INF1-treated *Nicotiana benthamiana*. Journal of General Plant Pathology 74 (1), 15-23.

Kauss, Fauth, Merten, Jeblick, 1999. Cucumber hypocotyls respond to cutin monomers via both an inducible and a constitutive H_2O_2-generating system. Plant physiology 120 (4), 1175-1182.

Kazan, K., 2006. Negative regulation of defence and stress genes by EAR-motif-containing repressors. Trends in Plant Science 11 (3), 109-112.

Keller, T., Damude, H.G., Werner, D., Doerner, P., Dixon, R.A., Lamb, C., 1998. A plant homolog of the neutrophil NADPH oxidase $gp91^{phox}$ subunit gene encodes a plasma membrane protein with Ca^{2+} binding motifs. Plant Cell 10 (2), 255-266.

Kim, H.S., Delaney, T.P., 2002. Over-expression of *TGA5*, which encodes a bZIP transcription factor that interacts with NIM1/NPR1, confers SAR-independent resistance in *Arabidopsis thaliana* to *Peronospora parasitica*. Plant Journal 32 (2), 151-163.

Kim, S.R., Choi, J.L., Costa, M.A., An, G.H., 1992. Identification of G-box sequence as an essential element for methyl jasmonate response of potato proteinase inhibitor II promoter. Plant Physiology 99 (2), 627-631.

Kinkema, M., Fan, W.H., Dong, X.N., 2000. Nuclear localization of NPR1 is required for activation of *PR* gene expression. Plant Cell 12 (12), 2339-2350.

Klok, E.J., Wilson, I.W., Wilson, D., Chapman, S.C., Ewing, R.M., Somerville, S.C., Peacock, W.J., Dolferus, R., Dennis, E.S., 2002. Expression profile analysis of the low-oxygen response in *Arabidopsis* root cultures. Plant Cell 14 (10), 2481-2494.

Knepper, C., Day, B., 2010. From perception to activation: The molecular-genetic and biochemical landscape of disease resistance signaling in plants. *Arabidopsis* Book 8, e012.

Knowles, R.G., Moncada, S., 1994. Nitric oxide synthases in mammals. Biochem Journal 298 (Pt 2), 249-58.

Kobayashi, A., Sakamoto, A., Kubo, K., Rybka, Z., Kanno, Y., Takatsuji, H., 1998. Seven zinc-finger transcription factors are expressed sequentially during the development of anthers in petunia. Plant Journal 13 (4), 571-576.

Kohler, A., Rinaldi, C., Duplessis, S., Baucher, M., Geelen, D., Duchaussoy, F., Meyers, B.C., Boerjan, W., Martin, F., 2008. Genome-wide identification of *NBS* resistance genes in *Populus trichocarpa*. Plant Molecular Biology 66 (6), 619-636.

Kornberg, M.D., Sen, N., Hara, M.R., Juluri, K.R., Nguyen, J.V., Snowman, A.M., Law, L., Hester, L.D., Snyder, S.H., 2010. GAPDH mediates nitrosylation of nuclear proteins. Nature Cell Biology 12 (11), 1094-1100.

Krause, M., Durner, J., 2004. Harpin inactivates mitochondria in *Arabidopsis* suspension cells. Molecular Plant-Microbe Interactions 17 (2), 131-139.

Krol, E., Mentzel, T., Chinchilla, D., Boller, T., Felix, G., Kemmerling, B., Postel, S., Arents, M., Jeworutzki, E., Al-Rasheid, K.A., Becker, D., Hedrich, R., 2010. Perception of the *Arabidopsis* Danger Signal Peptide 1 involves the pattern recognition receptor *At*PEPR1 and its close homologue *At*PEPR2. Journal of Biological Chemistry 285 (18), 13471-13479.

Kubo, K., Sakamoto, A., Kobayashi, A., Rybka, Z., Kanno, Y., Nakagawa, H., Takatsuji, H., 1998. Cys_2/His_2 zinc-finger protein family of petunia: Evolution and general mechanism of target-sequence recognition. Nucleic Acids Research 26 (2), 608-615.

Kunze, G., Zipfel, C., Robatzek, S., Niehaus, K., Boller, T., Felix, G., 2004. The N terminus of bacterial Elongation Factor Tu elicits innate immunity in *Arabidopsis* plants. Plant Cell 16 (12), 3496-3507.

Kutateladze, T.G., Ogburn, K.D., Watson, W.T., De Beer, T., Emr, S.D., Burd, C.G., Overduin, M., 1999. Phosphatidylinositol 3-phosphate recognition by the FYVE domain. Molecular Cell 3 (6), 805-811.

Kwezi, L., Meier, S., Mungur, L., Ruzvidzo, O., Irving, H., Gehring, C., 2007. The *Arabidopsis* thaliana Brassinosteroid Receptor (*AtBRI1*) contains a domain that functions as a Guanylyl Cyclase *in vitro*. PloS One 2 (5), e449.

Kwon, E., Feechan, A., Yun, B.W., Hwang, B.H., Pallas, J.A., Kang, J.G., Loake, G.J., 2012. *AtGSNOR1* function is required for multiple developmental programs in *Arabidopsis*. Planta 236 (3), 887-900.

Laity, J.H., Lee, B.M., Wright, P.E., 2001. Zinc finger proteins: New insights into structural and functional diversity. Current Opinion in Structural Biology 11 (1), 39-46.

Lamb, C., Dixon, R.A., 1997. The oxidative burst in plant disease resistance. Annual Review of Plant Physiology and Plant Molecular Biology 48, 251-275.

Lamotte, O., Gould, K., Lecourieux, D., Sequeira-Legrand, A., Lebrun-Garcia, A., Durner, J., Pugin, A., Wendehenne, D., 2004. Analysis of nitric oxide signaling functions in

tobacco cells challenged by the elicitor cryptogein. Plant Physiology 135 (1), 516-529.

Lebel, E., Heifetz, P., Thorne, L., Uknes, S., Ryals, J., Ward, E., 1998. Functional analysis of regulatory sequences controlling *PR1* gene expression in *Arabidopsis*. Plant Journal 16 (2), 223-233.

Lee, S.-W., Han, S.-W., Sririyanum, M., Park, C.-J., Seo, Y.-S., Ronald, P., 2009. A type I-secreted, sulfated peptide triggers XA21-mediated innate immunity. Science 326 (5954), 850-853.

Leterrier, M., Chaki, M., Airaki, M., Valderrama, R., Palma, J.M., Barroso, J.B., Corpas, F.J., 2011. Function of S-nitrosoglutathione reductase (GSNOR) in plant development and under biotic/abiotic stress. Plant Signaling and Behavior 6 (6), 789-793.

Levine, A., Pennell, R.I., Alvarez, M.E., Palmer, R., Lamb, C., 1996. Calcium-mediated apoptosis in a plant hypersensitive disease resistance response. Current Biology 6 (4), 427-437.

Li, J., Brader, G., Palva, E.T., 2004. The WRKY70 transcription factor: A node of convergence for jasmonate-mediated and salicylate-mediated signals in plant defense. Plant Cell 16 (2), 319-331.

Lima, B., Forrester, M.T., Hess, D.T., Stamler, J.S., 2010. S-nitrosylation in cardiovascular signaling. Circulation Research 106 (4), 633-646.

Lindermayr, C., Saalbach, G., Durner, J., 2005. Proteomic identification of S-nitrosylated proteins in *Arabidopsis thaliana.* Comparative Biochemistry and Physiology a-Molecular & Integrative Physiology 141 (3), S241-S241.

Lindermayr, C., Sell, S., Muller, B., Leister, D., Durner, J., 2010. Redox regulation of the NPR1-TGA1 system of *Arabidopsis thaliana* by nitric oxide. Plant Cell 22 (8), 2894-2907.

Liu, J., Elmore, J.M., Fuglsang, A.T., Palmgren, M.G., Staskawicz, B.J., Coaker, G., 2009. RIN4 functions with plasma membrane H^+-ATPases to regulate stomatal apertures during pathogen attack. Plos Biology 7 (6), e1000139.

Liu, J., Hughes, T., Sessa, W., 1997. the first 35 amino acids and fatty acylation sites determine the molecular targeting of endothelial nitric oxide synthase into the Golgi region of cells: A green fluorescent protein. Journal of Cell Biology 137 (7), 1525-1535.

Liu, L., Hausladen, A., Zeng, M., Que, L., Heitman, J., Stamler, J.S., 2001. A metabolic enzyme for S-nitrosothiol conserved from bacteria to humans. Nature 410 (6827), 490-494.

Liu, L., Zeng, M., Hausladen, A., Heitman, J., Stamler, J.S., 2000. Protection from nitrosative stress by yeast flavohemoglobin. Proceedings of the National Academy of Sciences of the United States of America 97 (9), 4672-4676.

Liu, L.M., Yan, Y., Zeng, M., Zhang, J., Hanes, M.A., Ahearn, G., Mcmahon, T.J., Dickfeld, T., Marshall, H.E., Que, L.G., Stamler, J.S., 2004. Essential roles of S-nitrosothiols in vascular homeostasis and endotoxic shock. Nitric Oxide-Biology and Chemistry 11 (1), 39-39.

Liu, Y., Schiff, M., Czymmek, K., Talloczy, Z., Levine, B., Dinesh-Kumar, S.P., 2005. Autophagy regulates programmed cell death during the plant innate immune response. Cell 121 (4), 567-577.

Liu, Y., Wu, R., Wan, Q., Xie, G., Bi, Y., 2007. Glucose-6-phosphate dehydrogenase plays a pivotal role in nitric oxide-involved defense against oxidative stress under salt stress in red kidney bean roots. Plant & Cell Physiology 48 (3), 511-522.

Loake, G., Feechan, A., Yuri, W., Wang, Y., 2007. Uncovering the roles of S-nitrosothiols in plant disease resistance. Comparative Biochemistry and Physiology a-Molecular & Integrative Physiology 146 (4), S256-S256.

Lorrain, S., Vailleau, F., Balague, C., Roby, D., 2003. Lesion mimic mutants: Keys for deciphering cell death and defense pathways in plants? Trends in Plant Science 8 (6), 263-271.

Lu, D., Wu, S., Gao, X., Zhang, Y., Shan, L., He, P., 2010. A receptor-like cytoplasmic kinase, BIK1, associates with a flagellin receptor complex to initiate plant innate immunity. Proceedings of the National Academy of Sciences of the United States of America 107 (1), 496-501.

Ludidi, N., Gehring, C., 2003. Identification of a novel protein with guanylyl cyclase activity in *Arabidopsis thaliana*. Journal of Biological Chemistry 278 (8), 6490-6494.

Lukowitz, W., Gillmor, C.S., Scheible, W.R., 2000. Positional cloning in *Arabidopsi*s. Why it feels good to have a genome initiative working for you. Plant Physiology 123 (3), 795-805.

Lydyard, P.M., Whelan, A., Fanger, M.W., Lydyard, P.M., 2004. Immunology London : BIOS Scientific [2004], ©2004. Second edition.

Mach, J.M., Castillo, A.R., Hoogstraten, R., Greenberg, J.T., 2001. The *Arabidopsis*-accelerated cell death gene *ACD2* encodes red chlorophyll catabolite reductase and suppresses the spread of disease symptoms. Proceedings of the National Academy of Sciences of the United States of America 98 (2), 771-776.

Macho, A.P., Zipfel, C., 2014. Plant PRRs and the activation of innate immune signaling. Molecular Cell 54 (2), 263-272.

Mackey, D., Holt, B.F., Wiig, A., Dangl, J.L., 2002. RIN4 interacts with *Pseudomonas syringae* type III effector molecules and is required for *RPM1*-mediated resistance in *Arabidopsi*s. Cell 108 (6), 743-754.

Maldonado, A., Doerner, P., Dixon, R., Lamb, C., Cameron, R., 2002. A putative lipid transfer protein involved in systemic resistance signalling in *Arabidopsi*s. Nature 419 (6905), 399-403.

Mallick, N., Mohn, F.H., Rai, L.C., Soeder, C.J., 2000. Evidence for the non-involvement of nitric oxide synthase in nitric oxide production by the green alga *Scenedesmus obliquus*. Journal of Plant Physiology 156 (3), 423-426.

Mallick, N., Rai, L.C., Mohn, F.H., Soeder, C.J., 1999. Studies on nitric oxide (NO) formation by the green alga *Scenedesmus obliquus* and the diazotrophic cyanobacterium *Anabaena doliolum*. Chemosphere 39 (10), 1601-1610.

Manning, V.A., Hamilton, S.M., Karplus, P.A., Ciuffetti, L.M., 2008. The ARG-GLY-ASP-containing, solvent-exposed loop of Ptr ToxA is required for internalization. Molecular Plant-Microbe Interactions 21 (3), 315-325.

Mateos, F., Rickauer, M., Esquerré-Tugayé, M., 1997. Cloning and characterization of a cDNA encoding an elicitor of *Phytophthora parasitica* var. *nicotianae* that shows cellulose-binding and lectin-like activities. Molecular plant-microbe interactions 10 (9), 1045-1053.

Matthews, J.R., Botting, C.H., Panico, M., Morris, H.R., Hay, R.T., 1996. Inhibition of NF-kappaB DNA binding by nitric oxide. Nucleic Acids Research 24 (12), 2236-2242.

Maud, B., Jeffrey, G.E., Peter, N.D., 2011. New insights in plant immunity signaling activation. Current Opinion in Plant Biology 14 (5), 512-518.

Mccormack, E., Tsai, Y.C., Braam, J., 2005. Handling calcium signaling: *Arabidopsis* CaMs and CMLs. Trends in Plant Science 10 (8), 383-389.

Mcdowell, J.M., Woffenden, B.J., 2003. Plant disease resistance genes: Recent insights and potential applications. Trends in Biotechnology 21 (4), 178-183.

Melotto, M., Underwood, W., He, S.Y., 2008. Role of stomata in plant innate immunity and foliar bacterial diseases. Annual Review of Phytopathology 46, 101-122.

Mengel, A., Chaki, M., Shekariesfahlan, A., Lindermayr, C., 2013. Effect of nitric oxide on gene transcription - S-nitrosylation of nuclear proteins. Frontier in Plant Science 4, 293.

Meyers, B.C., Kozik, A., Griego, A., Kuang, H.H., Michelmore, R.W., 2003. Genome-wide analysis of *NBS-LRR*-encoding genes in *Arabidopsis*. Plant Cell 15 (7), 1683-1683.

Miller, G., Schlauch, K., Tam, R., Cortes, D., Torres, M.A., Shulaev, V., Dangl, J.L., Mittler, R., 2009. The plant NADPH oxidase RbohD mediates rapid systemic signaling in response to diverse stimuli. Science Signaling 2 (84), ra45.

Miller, J., Mclachlan, A.D., Klug, A., 1985. Repetitive zinc-binding domains in the protein transcription factor IIIA from Xenopus oocytes. EMBO Journal 4 (6), 1609-1614.

Mittler, R., Kim, Y., Song, L., Coutu, J., Coutu, A., Ciftci-Yilmaz, S., Lee, H., Stevenson, B., Zhu, J.K., 2006. Gain- and loss-of-function mutations in *ZAT10* enhance the tolerance of plants to abiotic stress. FEBS Letters 580 (28-29), 6537-6542.

Miya, A., Albert, P., Shinya, T., Desaki, Y., Ichimura, K., Shirasu, K., Narusaka, Y., Kawakami, N., Kaku, H., Shibuya, N., 2007. CERK1, a LysM receptor kinase, is essential for chitin elicitor signaling in *Arabidopsis*. Proceedings of the National Academy of Sciences of the United States of America 104 (49), 19613-19618.

Modolo, L.V., Augusto, O., Almeida, I.M.G., Magalhaes, J.R., Salgado, I., 2005. Nitrite as the major source of nitric oxide production by *Arabidopsis thaliana* in response to *Pseudomonas syringae*. FEBS Letters 579 (17), 3814-3820.

Monaghan, J., Zipfel, C., 2012. Plant pattern recognition receptor complexes at the plasma membrane. Current Opinion in Plant Biology 15 (4), 349-357.

Moreau, M., Lindermayr, C., Durner, J., Klessig, D.F., 2010. NO synthesis and signaling in plants - where do we stand? Physiologia Plantarum 138 (4), 372-383.

Moreau, S., Peron, C., Pitt, K.A., Connolly, R.M., Lee, S.Y., Meziane, T., 2008. Opportunistic predation by small fishes on epibiota of jetty pilings in urban waterways. Journal of Fish Biology 72 (1), 205-217.

Mou, Z., Fan, W.H., Dong, X.N., 2003. Inducers of plant systemic acquired resistance regulate NPR1 function through redox changes. Cell 113 (7), 935-944.

Mungrue, I.N., Husain, M., Stewart, D.J., 2002. The role of NOS in heart failure: Lessons from murine genetic models. Heart Failure Reviews 7 (4), 407-422.

Murray, S.L., Thomson, C., Chini, A., Read, N.D., Loake, G.J., 2002. Characterization of a novel, defense-related *Arabidopsis* mutant, *cir1*, isolated by luciferase imaging. Molecular Plant-Microbe Interactions 15 (6), 557-566.

Nandi, A., Welti, R., Shah, J., 2004. The *Arabidopsis thaliana* dihydroxyacetone phosphate reductase gene suppresssor of fatty acid desaturase deficiency 1 is required for glycerolipid metabolism and for the activation of systemic acquired resistance. Plant cell 16 (2), 465-477.

Nathan, C., Xie, Q.W., 1994. Regulation of biosynthesis of nitric-oxide. Journal of Biological Chemistry 269 (19), 13725-13728.

Navarova, H., Bernsdorff, F., Doring, A.C., Zeier, J., 2012. Pipecolic acid, an endogenous mediator of defense amplification and priming, is a critical regulator of inducible plant immunity. Plant Cell 24 (12), 5123-5141.

Nawrath, C., 2006. Unraveling the complex network of cuticular structure and function. Current Opinion in Plant Biology 9 (3), 281-287.

Nawrath, C., Metraux, J.P., 1999. Salicylic acid induction-deficient mutants of *Arabidopsis* express *PR-2* and *PR-5* and accumulate high levels of camalexin after pathogen inoculation. Plant Cell 11 (8), 1393-1404.

Nelson, D.R., 2011. Progress in tracing the evolutionary paths of cytochrome p450. Biochimica et Biophysica Acta (BBA) - Molecular Cell Research 1814 (1), 14-18.

Newman, M., Daniels, M., Dow, J., 1995. Lipopolysaccharide from *Xanthomonas campestris* induces defense-related gene expression in *Brassica campestris*. Molecular plant-microbe interactions : MPMI 8 (5), 778-780.

Newman, M.A., Sundelin, T., Nielsen, J.T., Erbs, G., 2013. MAMP (microbe-associated molecular pattern) triggered immunity in plants. Frontier in Plant Science 4, 139.

Nicaise, V., Roux, M., Zipfel, C., 2009. Recent advances in PAMP-triggered immunity against bacteria: Pattern recognition receptors watch over and raise the alarm. Plant Physiology 150 (4), 1638-1647.

Nomura, K., Debroy, S., Lee, Y., Pumplin, N., Jones, J., He, S., 2006. A bacterial virulence protein suppresses host innate immunity to cause plant disease. Science 313 (5784), 220-223.

Nomura, K., Mecey, C., Lee, Y.N., Imboden, L.A., Chang, J.H., He, S.Y., 2011. Effector-triggered immunity blocks pathogen degradation of an immunity-associated vesicle traffic regulator in *Arabidopsis*. Proceedings of the National Academy of Sciences of the United States of America 108 (26), 10774–10779.

Nott, A., Riccio, A., 2009. Nitric oxide-mediated epigenetic mechanisms in developing neurons. Cell Cycle 8 (5), 725-730.

Nürnberger, T., Nennstiel, D., Jabs, T., Sacks, W., Hahlbrock, K., Scheel, D., 1994. High affinity binding of a fungal oligopeptide elicitor to parsley plasma membranes triggers multiple defense responses. Cell 78 (3), 449-460.

Obulareddy, N., Panchal, S., Melotto, M., 2013. Guard cell purification and RNA isolation suitable for high-throughput transcriptional analysis of cell-type responses to biotic stresses. Molecular Plant-Microbe Interactions 26 (8), 844-849.

Ohta, M., Matsui, K., Hiratsu, K., Shinshi, H., Ohme-Takagi, M., 2001. Repression domains of class II ERF transcriptional repressors share an essential motif for active repression. Plant Cell 13 (8), 1959-1968.

Omichinski, J.G., Clore, G.M., Schaad, O., Felsenfeld, G., Trainor, C., Appella, E., Stahl, S.J., Gronenborn, A.M., 1993. NMR structure of a specific DNA complex of Zn-containing DNA binding domain of GATA-1. Science 261 (5120), 438-446.

Pagnussat, G.C., Simontacchi, M., Puntarulo, S., Lamattina, L., 2002. Nitric oxide is required for root organogenesis. Plant Physiology 129 (3), 954-956.

Palmieri, M.C., Sell, S., Huang, X., Scherf, M., Werner, T., Durner, J., Lindermayr, C., 2008. Nitric oxide-responsive genes and promoters in *Arabidopsis thaliana*: A bioinformatics approach. Journal of Experimental Botany 59 (2), 177-186.

Park, H., Bakalinsky, A.T., 2000. *SSU1* mediates sulphite efflux in *Saccharomyces cerevisiae*. Yeast 16 (10), 881-888.

Park, S.W., Kaimoyo, E., Kumar, D., Mosher, S., Klessig, D.F., 2007. Methyl salicylate is a critical mobile signal for plant systemic acquired resistance. Science 318 (5847), 113-116.

Pattanayak, G.K., Venkataramani, S., Hortensteiner, S., Kunz, L., Christ, B., Moulin, M., Smith, A.G., Okamoto, Y., Tamiaki, H., Sugishima, M., Greenberg, J.T., 2012. Accelerated cell death 2 suppresses mitochondrial oxidative bursts and modulates cell death in *Arabidopsis*. Plant Journal 69 (4), 589-600.

Penson, S.P., Schuurink, R.C., Fath, A., Gubler, F., Jacobsen, J.V., Jones, R.L., 1996. cGMP is required for gibberellic acid-induced gene expression in barley aleurone. Plant Cell 8 (12), 2325-2333.

Perazzolli, M., Dominici, P., Romero-Puertas, M.C., Zago, E., Zeier, A., Sonoda, M., Lamb, C., Delledonne, M., 2004. *Arabidopsis* nonsymbiotic hemoglobin AHb1 modulates nitric oxide bioactivity. Plant Cell 16 (10), 2785-2794.

Petre, B., Kamoun, S., 2014. How do filamentous pathogens deliver effector proteins into plant cells? Plos Biology 12 (2), e1001801.

Pfeiffer, S., Janistyn, B., Jessner, G., Pichorner, H., Ebermann, R., 1994. Gaseous nitric-oxide stimulates guanosine-3',5'-cyclic monophosphate (cGMP) formation in spruce needles. Phytochemistry 36 (2), 259-262.

Pnueli, L., Liang, H., Rozenberg, M., Mittler, R., 2003. Growth suppression, altered stomatal responses, and augmented induction of heat shock proteins in cytosolic ascorbate peroxidase (*Apx1*)-deficient *Arabidopsis* plants. Plant Journal 34 (2), 185-201.

Polverari, A., Molesini, B., Pezzotti, M., Buonaurio, R., Marte, M., Delledonne, M., 2003. Nitric oxide-mediated transcriptional changes in *Arabidopsis thaliana*. Molecular Plant-Microbe Interactions 16 (12), 1094-1105.

Porter, B.W., Paidi, M., Ming, R., Alam, M., Nishijima, W.T., Zhu, Y.J., 2009. Genome-wide analysis of *Carica papaya* reveals a small *NBS* resistance gene family. Molecular Genetics and Genomics 281 (6), 609-626.

Qiao, W.H., Xiao, S.H., Yu, L., Fan, L.M., 2009. Expression of a rice gene *OsNOA1* re-establishes nitric oxide synthesis and stress-related gene expression for salt tolerance in *Arabidopsis* nitric oxide-associated 1 mutant *Atnoa1*. Environmental and Experimental Botany 65 (1), 90-98.

Qureshi, M.K., Sujeeth, N., Gechev, T.S., Hille, J., 2013. The zinc finger protein ZAT11 modulates paraquat-induced programmed cell death in *Arabidopsis thaliana*. Acta Physiologiae Plantarum 35 (6), 1863-1871.

Radwan, O., Gandhi, S., Heesacker, A., Whitaker, B., Taylor, C., Plocik, A., Kesseli, R., Kozik, A., Michelmore, R.W., Knapp, S.J., 2008. Genetic diversity and genomic distribution of homologs encoding NBS-LRR disease resistance proteins in sunflower. Molecular Genetics and Genomics 280 (2), 111-125.

Rasmussen, J., Hammerschmidt, R., Zook, M., 1991. Systemic induction of salicylic acid accumulation in cucumber after inoculation with *Pseudomonas syringae* pv *syringae*. Plant physiology 97 (4), 1342-1347.

Riccio, A., Alvania, R.S., Lonze, B.E., Ramanan, N., Kim, T., Huang, Y., Dawson, T.M., Snyder, S.H., Ginty, D.D., 2006. A nitric oxide signaling pathway controls CREB-mediated gene expression in neurons. Molecular Cell 21 (2), 283-294.

Rivas, S., Rougon-Cardoso, A., Smoker, M., Schauser, L., Yoshioka, H., Jones, J.D.G., 2004. CITRX thioredoxin interacts with the tomato Cf-9 resistance protein and negatively regulates defence. EMBO Journal 23 (10), 2156-2165.

Rizhsky, L., Davletova, S., Liang, H., Mittler, R., 2004. The zinc finger protein ZAT12 is required for cytosolic ascorbate peroxidase 1 expression during oxidative stress in *Arabidopsis*. Journal of Biological Chemistry 279 (12), 11736-11743.

Robatzek, S., Chinchilla, D., Boller, T., 2006. Ligand-induced endocytosis of the pattern recognition receptor FLS2 in *Arabidopsis*. Genes & Development 20 (5), 537-542.

Rockel, P., Strube, F., Rockel, A., Wildt, J., Kaiser, W.M., 2002. Regulation of nitric oxide (NO) production by plant nitrate reductase *in vivo* and *in vitro*. Journal of Experimental Botany 53 (366), 103-110.

Romero-Puertas, M., Laxa, M., Mattè, A., Zaninotto, F., Finkemeier, I., Jones, A., Perazzolli, M., Vandelle, E., Dietz, K.-J., Delledonne, M., 2007. S-nitrosylation of peroxiredoxin II E promotes peroxynitrite-mediated tyrosine nitration. Plant cell 19 (12), 4120-4130.

Ron, M., Avni, A., 2004. The receptor for the fungal elicitor ethylene-inducing xylanase is a member of a resistance-like gene family in tomato. Plant Cell 16 (6), 1604-1615.

Roy, A., Kucukural, A., Zhang, Y., 2010. I-tasser: A unified platform for automated protein structure and function prediction. Nature Protocols 5 (4), 725-738.

Rubbo, H., Freeman, B.A., 1996. Nitric oxide regulation of lipid oxidation reactions: Formation and analysis of nitrogen-containing oxidized lipid derivatives. Methods in Enzymology 269, 385-394.

Rumer, S., Gupta, K.J., Kaiser, W.M., 2009. Plant cells oxidize hydroxylamines to NO. Journal of Experimental Botany 60 (7), 2065-2072.

Ryals, J., Neuenschwander, U., Willits, M., Molina, A., Steiner, H., Hunt, M., 1996. Systemic acquired resistance. Plant cell 8 (10), 1809-1819.

Sakamoto, A., Sakurao, S., Fukunaga, K., Matsubara, T., Ueda-Hashimoto, M., Tsukamoto, S., Takahashi, M., Morikawa, H., 2004. Three distinct *Arabidopsis* hemoglobins exhibit peroxidase-like activity and differentially mediate nitrite-dependent protein nitration. FEBS Letters 572 (1-3), 27-32.

Sanchez-Garcia, I., Rabbitts, T.H., 1994. The LIM domain: A new structural motif found in zinc-finger-like proteins. Trends in Genetics 10 (9), 315-320.

Sang, J., Jiang, M., Lin, F., Xu, S., Zhang, A., Tan, M., 2008. Nitric oxide reduces hydrogen peroxide accumulation involved in water stress-induced subcellular anti-oxidant defense in maize plants. Journal of Integrative Plant Biology 50 (2), 231-243.

Saraste, M., Sibbald, P.R., Wittinghofer, A., 1990. The P-loop--a common motif in ATP- and GTP-binding proteins. Trends in Biochemical Sciences 15 (11), 430-434.

Sarver, A., Derisi, J., 2005. Fzf1p regulates an inducible response to nitrosative stress in *Saccharomyces cerevisiae*. Molecular Biology of the Cell 16 (10), 4781-4791.

Savvides, S.N., Scheiwein, M., Bohme, C.C., Arteel, G.E., Karplus, P.A., Becker, K., Schirmer, R.H., 2002. Crystal structure of the antioxidant enzyme glutathione reductase inactivated by peroxynitrite. Journal of Biological Chemistry 277 (4), 2779-2784.

Schindler, U., Beckmann, H., Cashmore, A.R., 1993. HAT3.1, a novel *Arabidopsis* homeodomain protein containing a conserved cysteine-rich region. Plant Journal 4 (1), 137-150.

Schopfer, F.J., Baker, P.R.S., Freeman, B.A., 2003. NO-dependent protein nitration: A cell signaling event or an oxidative inflammatory response? Trends in Biochemical Sciences 28 (12), 646-654.

Schweizer, P., Felix, G., Buchala, A., Müller, C., 1996. Perception of free cutin monomers by plant cells. Plant Journal 10 (2), 331-341.

Schwessinger, B., Roux, M., Kadota, Y., Ntoukakis, V., Sklenar, J., Jones, A., Zipfel, C., 2011. Phosphorylation-dependent differential regulation of plant growth, cell death, and innate immunity by the regulatory receptor-like kinase BAK1. PLoS Genetics 7 (4), e1002046.

Scofield, S.R., Tobias, C.M., Rathjen, J.P., Chang, J.H., Lavelle, D.T., Michelmore, R.W., Staskawicz, B.J., 1996. Molecular basis of gene-for-gene specificity in bacterial speck disease of tomato. Science 274 (5295), 2063-2065.

Segonzac, C., Zipfel, C., 2011. Activation of plant pattern-recognition receptors by bacteria. Current Opinion in Microbiology 14 (1), 54-61.

Séjalon-Delmas, N., Mateos, F., Bottin, A., Rickauer, M., Dargent, R., Esquerré-Tugayé, M., 1997. Purification, elicitor activity, and cell wall localization of a glycoprotein from *Phytophthora parasitica* var. *Nicotianae*, a fungal pathogen of tobacco. Phytopathology 87 (9), 899-909.

Senthil-Kumar, M., Mysore, K.S., 2013. Nonhost resistance against bacterial pathogens: Retrospectives and prospects. Annual Review of Phytopathology, 51, 407-427.

Sheen, J., Hwang, S.B., Niwa, Y., Kobayashi, H., Galbraith, D.W., 1995. Green-fluorescent protein as a new vital marker in plant-cells. Plant Journal 8 (5), 777-784.

Shimizu, T., Nakano, T., Takamizawa, D., Desaki, Y., Ishii-Minami, N., Nishizawa, Y., Minami, E., Okada, K., Yamane, H., Kaku, H., Shibuya, N., 2010. Two LysM receptor molecules, CEBiP and OsCERK1, cooperatively regulate chitin elicitor signaling in rice. Plant Journal 64 (2), 204-214.

Shirasu, K., Nakajima, H., Rajasekhar, V.K., Dixon, R.A., Lamb, C., 1997. Salicylic acid potentiates an agonist-dependent gain control that amplifies pathogen signals in the activation of defense mechanisms. Plant Cell 9 (2), 261-270.

Sirova, J., Sedlarova, M., Piterkova, J., Luhova, L., Petrivalsky, M., 2011. The role of nitric oxide in the germination of plant seeds and pollen. Plant Science 181 (5), 560-572.

Song, W., Wang, G., Chen, L., Kim, H., Pi, L., Holsten, T., Gardner, J., Wang, B., Zhai, W., Zhu, L., Fauquet, C., Ronald, P., 1995. A receptor kinase-like protein encoded by the rice disease resistance gene, *Xa21*. Science 270 (5243), 1804-1806.

Souza, J.M., Peluffo, G., Radi, R., 2008. Protein tyrosine nitration - functional alteration or just a biomarker? Free Radical Biology and Medicine 45 (4), 357-366.

Spoel, S.H., Dong, X.N., 2012. How do plants achieve immunity? Defence without specialized immune cells. Nature Reviews Immunology 12 (2), 89-100.

Spoel, S.H., Loake, G.J., 2011. Redox-based protein modifications: The missing link in plant immune signalling. Current Opinion in Plant Biology 14 (4), 358-364.

Srivastava, N., Gonugunta, V.K., Puli, M.R., Raghavendra, A.S., 2009. Nitric oxide production occurs downstream of reactive oxygen species in guard cells during stomatal closure induced by chitosan in abaxial epidermis of *Pisum sativum*. Planta 229 (4), 757-765.

Stakman, E.C., 1915. Relation between *Puccinia graminis* and plants highly resistant to its attack. Journal of Agricultural Research 4, 193-199.

Stamler, J.S., 1994. Redox signaling - nitrosylation and related target interactions of nitric-oxide. Cell 78 (6), 931-936.

Stone, S.L., Hauksdottir, H., Troy, A., Herschleb, J., Kraft, E., Callis, J., 2005. Functional analysis of the ring-type ubiquitin ligase family of *Arabidopsis*. Plant Physiology 137 (1), 13-30.

Streatfield, S.J., Weber, A., Kinsman, E.A., Hausler, R.E., Li, J., Post-Beittenmiller, D., Kaiser, W.M., Pyke, K.A., Flugge, U.I., Chory, J., 1999. The phosphoenolpyruvate/phosphate translocator is required for phenolic metabolism, palisade cell development, and plastid-dependent nuclear gene expression. Plant Cell 11 (9), 1609-1622.

Stuehr, D.J., 1999. Mammalian nitric oxide synthases. Biochimica et Biophysica Acta (BBA) - Molecular Cell Research 1411 (2-3), 217-230.

Tada, Y., Mori, T., Shinogi, T., Yao, N., Takahashi, S., Betsuyaku, S., Sakamoto, M., Park, P., Nakayashiki, H., Tosa, Y., Mayama, S., 2004. Nitric oxide and reactive oxygen species do not elicit hypersensitive cell death but induce apoptosis in the adjacent cells during the defense response of oat. Molecular Plant-Microbe Interactions 17 (3), 245-253.

Tada, Y., Spoel, S., Pajerowska-Mukhtar, K., Mou, Z., Song, J., Wang, C., Zuo, J., Dong, X., 2008. Plant immunity requires conformational changes of NPR1 via s-nitrosylation and thioredoxins. Science 321 (5891), 952-956.

Takatsuji, H., 1998. Zinc-finger transcription factors in plants. Cellular and Molecular Life Sciences 54 (6), 582-596.

Tameling, W., Vossen, J., Albrecht, M., Lengauer, T., Berden, J., Haring, M., Cornelissen, B., Takken, F., 2006. Mutations in the NB-ARC domain of I-2 that impair ATP hydrolysis cause autoactivation. Plant physiology 140 (4), 1233-1245.

Tang, X.Y., Frederick, R.D., Zhou, J.M., Halterman, D.A., Jia, Y.L., Martin, G.B., 1996. Initiation of plant disease resistance by physical interaction of AvrPto and Pto kinase. Science 274 (5295), 2060-2063.

Tanou, G., Filippou, P., Belghazi, M., Job, D., Diamantidis, G., Fotopoulos, V., Molassiotis, A., 2012. Oxidative and nitrosative-based signaling and associated post-translational modifications orchestrate the acclimation of citrus plants to salinity stress. Plant Journal 72 (4), 585-599.

Tavares, C.P., Vernal, J., Delena, R.A., Lamattina, L., Cassia, R., Terenzi, H., 2014. S-nitrosylation influences the structure and DNA binding activity of AtMYB30 transcription factor from *Arabidopsis thaliana.* Biochimica et Biophysica Acta (BBA) - Molecular Cell Research 1844 (4), 810-817.

Torres, M.A., Dangl, J.L., 2005. Functions of the respiratory burst oxidase in biotic interactions, abiotic stress and development. Current Opinion in Plant Biology 8 (4), 397-403.

Torres, M.A., Dangl, J.L., Jones, J.D., 2002. *Arabidopsis gp91^{phox}* homologues *AtrbohD* and *AtrbohF* are required for accumulation of reactive oxygen intermediates in the plant defense response. Proceedings of the National Academy of Sciences of the United States of America 99 (1), 517-522.

Torres, M.A., Onouchi, H., Hamada, S., Machida, C., Hammond-Kosack, K.E., Jones, J.D.G., 1998. Six *Arabidopsis thaliana* homologues of the human respiratory burst oxidase (*gp91^{phox}*). Plant Journal 14 (3), 365-370.

Truman, W., De Zabala, M.T., Grant, M., 2006. Type III effectors orchestrate a complex interplay between transcriptional networks to modify basal defence responses during pathogenesis and resistance. Plant Journal 46 (1), 14-33.

Uknes, S., Mauchmani, B., Moyer, M., Potter, S., Williams, S., Dincher, S., Chandler, D., Slusarenko, A., Ward, E., Ryals, J., 1992. Acquired-resistance in *Arabidopsis*. Plant Cell 4 (6), 645-656.

Umemoto, N., Kakitani, M., Iwamatsu, A., Yoshikawa, M., Yamaoka, N., Ishida, I., 1997. The structure and function of a soybean beta-glucan-elicitor-binding protein. Proceedings of the National Academy of Sciences of the United States of America 94 (3), 1029-1034.

Uren, A.G., O'rourke, K., Aravind, L., Pisabarro, M.T., Seshagiri, S., Koonin, E.V., Dixit, V.M., 2000. Identification of paracaspases and metacaspases: Two ancient families of caspase-like proteins, one of which plays a key role in malt lymphoma. Molecular Cell 6 (4), 961-967.

Vandelle, E., Delledonne, M., 2011. Peroxynitrite formation and function in plants. Plant science 181 (5), 534-539.

Vandervliet, A., Eiserich, J.P., Kaur, H., Cross, C.E., Halliwell, B., 1996. Nitrotyrosine as biomarker for reactive nitrogen species. Methods in Enzymology 269, 175-184.

Vernooij, B., Friedrich, L., Morse, A., Reist, R., Kolditz-Jawhar, R., Ward, E., Uknes, S., Kessmann, H., Ryals, J., 1994. Salicylic acid is not the translocated signal responsible for inducing systemic acquired resistance but is required in signal transduction. Plant cell 6 (7), 959-965.

Vierstra, R.D., 2003. The ubiquitin/26s proteasome pathway, the complex last chapter in the life of many plant proteins. Trends in Plant Science 8 (3), 135-142.

Voinnet, O., Rivas, S., Mestre, P., Baulcombe, D., 2003. An enhanced transient expression system in plants based on suppression of gene silencing by the p19 protein of tomato bushy stunt virus. Plant Journal 33 (5), 949-956.

Voll, L., Hausler, R.E., Hecker, R., Weber, A., Weissenbock, G., Fiene, G., Waffenschmidt, S., Flugge, U.I., 2003. The phenotype of the *Arabidopsis cue1* mutant is not simply caused by a general restriction of the shikimate pathway. Plant Journal 36 (3), 301-317.

Vonarnim, A.G., Deng, X.W., 1993. RING finger motif of *Arabidopsis thaliana* COP1 defines a new class of zinc-binding domain. Journal of Biological Chemistry 268 (26), 19626-19631.

Wan, J.R., Zhang, X.C., Neece, D., Ramonell, K.M., Clough, S., Kim, S.Y., Stacey, M.G., Stacey, G., 2008. A LysM receptor-like kinase plays a critical role in chitin signaling and fungal resistance in *Arabidopsis*. Plant Cell 20 (2), 471-481.

Wang, G., Ruan, D., Song, W., Sideris, S., Chen, L., Pi, L., Zhang, S., Zhang, Z., Fauquet, C., Gaut, B., Whalen, M., Ronald, P., 1998. *Xa21D* encodes a receptor-like molecule with a leucine-rich repeat domain that determines race-specific recognition and is subject to adaptive evolution. Plant cell 10 (5), 765-779.

Wang, J., Bayles, K.W., 2013. Programmed cell death in plants: Lessons from bacteria? Trends in Plant Sciences 18 (3), 133-139.

Wang, Y., Loake, G.J., Chu, C., 2013. Crosstalk of nitric oxide and reactive oxygen species in plant programed cell death. Frontier in Plant Science 4, 314.

Wang, Y.-Q., Feechan, A., Yun, B.-W., Shafiei, R., Hofmann, A., Taylor, P., Xue, P., Yang, F.-Q., Xie, Z.-S., Pallas, J., Chu, C.-C., Loake, G., 2009. S-nitrosylation of AtSABP3 antagonizes the expression of plant immunity. The Journal of biological chemistry 284 (4), 2131-2137.

Watt, S., Tellström, V., Patschkowski, T., Niehaus, K., 2006. Identification of the bacterial superoxide dismutase (SodM) as plant-inducible elicitor of an oxidative burst reaction in tobacco cell suspension cultures. Journal of biotechnology 126 (1), 78-86.

Watts, R.A., Hunt, P.W., Hvitved, A.N., Hargrove, M.S., Peacock, W.J., Dennis, E.S., 2001. A hemoglobin from plants homologous to truncated hemoglobins of microorganisms. Proceedings of the National Academy of Sciences of the United States of America 98 (18), 10119-10124.

Werck-Reichhart D, B.S., Paquette S 2002. Cytochromes p450. In: Somerville Cr, M.E.E.R. ed. The *Arabidopsis* book. American Society of Plant Biologists

Whalen, M.C., Innes, R.W., Bent, A.F., Staskawicz, B.J., 1991. Identification of *Pseudomonas syringae* pathogens of *Arabidopsis* and a bacterial locus determining avirulence on both *Arabidopsis* and Soybean. Plant Cell 3 (1), 49-59.

Whisson, S.C., Boevink, P.C., Moleleki, L., Avrova, A.O., Morales, J.G., Gilroy, E.M., Armstrong, M.R., Grouffaud, S., Van West, P., Chapman, S., Hein, I., Toth, I.K., Pritchard, L., Birch, P.R.J., 2007. A translocation signal for delivery of oomycete effector proteins into host plant cells. Nature 450 (7166), 115-118.

Willmann, R., Lajunen, H., Erbs, G., Newman, M.-A., Kolb, D., Tsuda, K., Katagiri, F., Fliegmann, J., Bono, J.-J., Cullimore, J., Jehle, A., Götz, F., Kulik, A., Molinaro, A., Lipka, V., Gust, A., Nürnberger, T., 2011. *Arabidopsis* lysin-motif proteins LyM1 LyM3 CERK1 mediate bacterial peptidoglycan sensing and immunity to bacterial infection. Proceedings of the National Academy of Sciences of the United States of America 108 (49), 19824-19829.

Wink, D.A., Grisham, M.B., Mitchell, J.B., Ford, P.C., 1996. Direct and indirect effects of nitric oxide in chemical reactions relevant to biology. Methods in Enzymology 268, 12-31.

Xu, H., Heath, M.C., 1998. Role of calcium in signal transduction during the hypersensitive response caused by basidiospore-derived infection of the cowpea rust fungus. Plant Cell 10 (4), 585-598.

Yamaguchi, Y., Pearce, G., Ryan, C., 2006. The cell surface leucine-rich repeat receptor for AtPep1, an endogenous peptide elicitor in *Arabidopsis*, is functional in transgenic

tobacco cells. Proceedings of the National Academy of Sciences of the United States of America 103 (26), 10104-10109.

Yamasaki, H., 2000. Nitrite-dependent nitric oxide production pathway: Implications for involvement of active nitrogen species in photoinhibition *in vivo*. Philosophical Transactions of the Royal Society B-Biological Sciences 355 (1402), 1477-1488.

Yamasaki, H., Itoh, R. D., Bouchard, J. N., Dghim, A. A., Hossain, K. K., Gurung, S. And Cohen, M. F, 2010. Nitric oxide synthase-like activities in plants. Annual Plant Reviews 42: Nitrogen Metabolism in Plants in the Post-Genomic Era. Wiley-Blackwell, Oxford, UK.

Yamasaki, H., Sakihama, Y., 2000. Simultaneous production of nitric oxide and peroxynitrite by plant nitrate reductase: *In vitro* evidence for the NR-dependent formation of active nitrogen species. FEBS Letters 468 (1), 89-92.

Yanagisawa, S., 1996. A novel multigene family that the gene for a maize DNA-binding protein, MNB1a belongs to: Isolation of genomic clones from this family and some aspects of its molecular evolution. International Journal of Biochemistry and Molecular biology 38 (4), 665-673.

Yoshioka, H., Sugie, K., Park, H.J., Maeda, H., Tsuda, N., Kawakita, K., Doke, N., 2001. Induction of plant gp91 *phox* homolog by fungal cell wall, arachidonic acid, and salicylic acid in potato. Molecular Plant-Microbe Interactions 14 (6), 725-736.

Yu, D.Q., Chen, C.H., Chen, Z.X., 2001. Evidence for an important role of WRKY DNA binding proteins in the regulation of *NPR1* gene express ion. Plant Cell 13 (7), 1527-1539.

Yu, M., Lamattina, L., Spoel, S.H., Loake, G.J., 2014. Nitric oxide function in plant biology: A redox cue in deconvolution. New Phytologist 202 (4), 1142-1156.

Yu, M., Yun, B.W., Spoel, S.H., Loake, G.J., 2012. A sleigh ride through the SNO: Regulation of plant immune function by protein S-nitrosylation. Current Opinion in Plant Biology 15 (4), 424-430.

Yun, B.W., Atkinson, H.A., Gaborit, C., Greenland, A., Read, N.D., Pallas, J.A., Loake, G.J., 2003. Loss of actin cytoskeletal function and EDS1 activity, in combination, severely compromises non-host resistance in *Arabidopsis* against wheat powdery mildew. Plant Journal 34 (6), 768-777.

Yun, B.W., Feechan, A., Yin, M., Saidi, N.B., Le Bihan, T., Yu, M., Moore, J.W., Kang, J.G., Kwon, E., Spoel, S.H., Pallas, J.A., Loake, G.J., 2011. S-nitrosylation of NADPH oxidase regulates cell death in plant immunity. Nature 478 (7368), 264-268.

Zeidler, D., Zahringer, U., Gerber, I., Dubery, I., Hartung, T., Bors, W., Hutzler, P., Durner, J., 2004. Innate immunity in *Arabidopsis thaliana*: Lipopolysaccharides activate nitric oxide synthase (NOS) and induce defense genes. Proceedings of the National Academy of Sciences of the United States of America 101 (44), 15811-15816.

Zeng, W., Melotto, M., He, S.Y., 2010. Plant stomata: A checkpoint of host immunity and pathogen virulence. Current Opinion in Biotechnology 21 (5), 599-603.

Zhang, A., Jiang, M., Zhang, J., Ding, H., Xu, S., Hu, X., Tan, M., 2007. Nitric oxide induced by hydrogen peroxide mediates abscisic acid-induced activation of the mitogen-activated protein kinase cascade involved in antioxidant defense in maize leaves. New Phytologist 175 (1), 36-50.

Zhang, C., Czymmek, K.J., Shapiro, A.D., 2003. Nitric oxide does not trigger early programmed cell death events but may contribute to cell-to-cell signaling governing progression of the *Arabidopsi*s hypersensitive response. Molecular Plant-Microbe Interactions 16 (11), 962-972.

Zhang, J., Li, W., Xiang, T.T., Liu, Z.X., Laluk, K., Ding, X.J., Zou, Y., Gao, M.H., Zhang, X.J., Chen, S., Mengiste, T., Zhang, Y.L., Zhou, J.M., 2010. Receptor-like cytoplasmic kinases integrate signaling from multiple plant immune receptors and are targeted by a *Pseudomonas syringae* effector. Cell Host & Microbe 7 (4), 290-301.

Zhang, J., Zhou, J.M., 2010. Plant immunity triggered by microbial molecular signatures. Molecular Plant 3, 1-11.

Zhang, Y.L., Fan, W.H., Kinkema, M., Li, X., Dong, X.N., 1999. Interaction of NPR1 with basic leucine zipper protein transcription factors that bind sequences required for salicylic acid induction of the *PR1* gene. Proceedings of the National Academy of Sciences of the United States of America 96 (11), 6523-6528.

Zheng, Z., Mosher, S.L., Fan, B., Klessig, D.F., Chen, Z., 2007. Functional analysis of *Arabidopsis* WRKY25 transcription factor in plant defense against *Pseudomonas syringae*. BMC Plant Biology 7, 2.

Zhou, T., Wang, Y., Chen, J.Q., Araki, H., Jing, Z., Jiang, K., Shen, J., Tian, D., 2004. Genome-wide identification of NBS genes in *japonica* rice reveals significant expansion of divergent non-TIR NBS-LRR genes. Molecular Genetics and Genomics 271 (4), 402-415.

Zipfel, C., Kunze, G., Chinchilla, D., Caniard, A., Jones, J.D., Boller, T., Felix, G., 2006. Perception of the bacterial PAMP EF-Tu by the receptor ERF restricts *Agrobacterium*-mediated transformation. Cell 125 (4), 749-760.